

# AUTOREGULATION OF NFATc1 GENE

Dissertation

For the completion of Doctorate degree in Natural Sciences at the  
Bayerische Julius-Maximilians-Universität Würzburg



by **Dmitry Tyrsin**

Moscow, Russia

**Würzburg, 2008**

The hereby submitted thesis was completed from October 2000 until July 2004 at the Department of Molekulare Pathologie, Institute für Pathologie, Bayerische Julius-Maximilians Universität, Würzburg under the supervision of **Professor Dr. Edgar Serfling** (Faculty of Medicine).

Submitted on:

Members of the thesis committee:

**Chairman:**

**1.) Examiner: Professor Dr. E. Serfling**

**2.) Examiner: Professor Dr. R. Benavente**

Date of oral examination:

Certificate issued on:

## **DECLARATION**

I hereby declare that the submitted dissertation was completed by myself and no other. I have not used any sources or materials other than those enclosed.

Moreover I declare that the following dissertation has not been submitted further in this form or any other form, and has not been used to obtain any other equivalent qualifications or degree at any other organisation/institution.

Additionally, I have not applied for, nor will I attempt to apply for any other degree or qualification in relation to this work.

**Würzburg, den 02.08.2007**

**Dmitry Tyrsin**

## ACKNOWLEDGMENTS

First of all I would like to thank Prof. Dr. E. Serfling for inviting me to the Pathology Institute Wuerzburg, and giving me the chance to express myself as a young scientist doing research. Thank you for giving me the important lessons in conducting an independent and fruitful research and for the strong scientific guidance. Also I greatly appreciate the international atmosphere in our lab that helped all people to stay deeper in touch and know more about different cultures. I would also thank Prof. R. Benavente for accepting me to the Faculty of Biology and his support during my doctorate degree.

I am delighted to thank Sergey Chuvpilo – my scientific “Godfather” for many illuminating discussions and guiding me through the obscure labyrinths of molecular immunology. Very special thanks to Stefan, Alois and Andris for their strong intellectual and other supports throughout this work. Thanks to Rike, for her eagerness to help in Riboquant analysis. I am grateful to Askar, Denis, Nikolai and Oleg for their readiness to help every time. Many thanks to Mithilesh from whom I learnt lymphocyte preparation and enjoyed fruitful co-operation. I must thank Doris and Ilona for superb technical support. Thanks to Stefan for serious efforts in the translation of Summary into the Deutsch version. I would also like to express my thanks to my supportive colleagues: Nikola, Li, Chao, Jiming, Claudia, and Fabian.

It is difficult to express in a few sentences the gratitude for my family, for their love and support. The greatest acknowledgement I reserve for my lovely Lidia, supporting me every time either mentally or in reality, to whom I dedicate this dissertation.

## Table of Contents

1. INTRODUCTION.....	1
1.1 Evolution of NFAT signaling .....	2
1.2 Structure and localization of NFAT family members.....	2
<i>Expression pattern and chromosome localization</i> .....	3
<i>Structure of NFAT proteins</i> .....	3
1.3 Activation and function.....	4
<i>Cooperation with AP-1, NFAT activation</i> .....	5
1.3.1 Ca <sup>2+</sup> /Calcineurin - dependent TCR signaling pathway .....	5
<i>MAP/SAP kinases</i> .....	6
1.3.1.1 Nuclear transport of NFAT proteins.....	7
1.3.2 PKC/ IKK/ Ras/ MAPK costimulatory signaling pathways.....	8
<i>PKC<math>\theta</math> in ERK and JNK/SAPK activation</i> .....	8
<i>PKC<math>\theta</math> and NF-<math>\kappa</math>B activation</i> .....	9
1.4 NFAT partner proteins .....	10
1.4.1 Basic region-leucine zipper (bZIP) protein family.....	10
<i>p21SNFT</i> .....	10
<i>c-Maf</i> .....	11
<i>ICER</i> .....	11
1.4.2 Zinc finger proteins.....	12
<i>ERG</i> .....	12
<i>GATA</i> .....	12
1.4.3 Helix-turn-helix proteins.....	13
<i>IRF</i> .....	13
<i>NIP45</i> .....	13
<i>Octamer factors</i> .....	13
1.4.4 MADS-box proteins.....	14
<i>MEF-2</i> .....	14
1.5 NFAT target genes.....	14
1.6 Phenotypes of NFAT-deficient mice.....	15
<i>NFATc1 deficient mice</i> .....	15
<i>NFATc2 deficient mice</i> .....	15
<i>NFATc3 deficient mice</i> .....	16

## Table of Contents

<i>NFATc4</i> deficient mice .....	16
<i>NFATc1+c2</i> deficient mice .....	16
<i>NFATc2+c3</i> deficient mice .....	16
<i>NFATc3+c4</i> deficient mice .....	17
<i>NFATc2+c3+c4</i> deficient mice .....	17
<b>2. RESULTS</b> .....	18
2.1 Induction of NFATc1/ $\alpha$ A in T cells.....	18
2.2 Structure and organization of the chromosomal murine NFATc1 gene.....	19
2.3 Cell-specific utilization of the P1 and P2 promoters.....	21
2.4 Transcription initiation sites for the alternative mNFATc1 first exons.....	22
2.5 Characterization of the P1 core promoter.....	24
2.6 P1 promoter activation and NFATc1 regulation depends on well organized TF machinery.....	26
2.6.1 CREB contribution to P1 induction.....	26
2.6.2 NF- $\kappa$ B binds to P1 promoter.....	27
2.6.3 NFATs autoregulate P1 induction and enhance NFATc/ $\alpha$ A synthesis.....	28
2.7 Characterization of the P2 promoter.....	31
2.7.1 NFATs don't bind to the P2 promoter.....	32
2.8 Inducible alternative polyadenylation events contribute to the generation of NFATc/ $\alpha$ A.....	32
2.9 Quantification of RNA expression level of NFATc1 gene isoforms in Th cells.....	34
<b>3. DISCUSSION</b> .....	40
3.1 NFATc1: Control by two promoters, alternative splicing and two poly A sites.....	41
3.2 NFATc1: Autoregulation results in the predominant synthesis of NFATc1/ $\alpha$ A.....	43
3.3 T lymphocytes: NFATc1 autoregulation is a property of effector T helper cells.....	43
3.4 Conclusion.....	45
<b>4. SUMMARY</b> .....	46
<i>Zusammenfassung</i> .....	47

5. MATERIALS AND METHODS.....	48
5.1. Materials.....	48
5.1.1. Instruments.....	48
5.1.2. General materials.....	48
5.1.3. Chemical reagents.....	49
5.1.4. DNA size markers .....	50
5.1.4.1. Protein standards.....	50
5.1.5. Enzymes .....	50
5.1.6. Antibodies .....	50
5.1.7. Oligonucleotides and primers.....	50
5.1.8. Antibiotics .....	53
5.1.9. Solutions and buffers.....	53
5.1.10. DNA vectors .....	61
5.1.11. Growth media .....	61
5.1.11.1 Liquid medium and agar plates for bacterial culture .....	61
5.1.11.2. Mammalian cell culture media.....	61
5.2. Methods.....	63
5.2.1. Bacterial manipulation.....	63
5.2.1.1. Preparation of competent cells (CaCl <sub>2</sub> method) .....	63
5.2.1.2 Transformation of competent bacteria.....	64
5.2.1.3 Screening of transformants by colony hybridization .....	64
5.2.2 DNA methods.....	65
5.2.2.1. Electrophoresis of DNA on agarose gels.....	65
5.2.2.2. Isolation of plasmid DNA from agarose (QIAEX II agarose gel extraction protocol). .....	65
5.2.2.3. Purification of plasmid DNA (QIAquick PCR purification kit).....	66
5.2.2.4. Ligation of DNA fragments.....	66
5.2.2.5. Cohesive-end ligation.....	66
5.2.2.6. Mini-preparation of plasmid DNA.....	67
5.2.2.7. Maxi-preparation of plasmid DNA.....	67
5.2.2.8. Measurement of DNA concentration.....	67
5.2.2.9. DNA sequencing (Sanger Dideoxy Method) .....	67
5.2.2.10. DNA amplification by Polymerase Chain Reaction (PCR) .....	69
5.2.2.11. Southern blot.....	69

## Table of Contents

5.2.3 RNA Methods.....	69
5.2.3.1. Isolation of RNA from mammalian cells.....	69
5.2.3.2. Running RNA samples on denaturing gels.....	69
5.2.3.3. Ribonuclease protection assay.....	70
5.2.3.4. One step Real-Time PCR (QIAGEN QuantiTect SYBR Green RT-PCR Kit) .....	72
5.2.4 Protein Methods.....	73
5.2.4.1. Preparation of protein extracts.....	73
5.2.4.2. Measurement of protein concentration (Bio-Rad protein assay) .....	74
5.2.4.3. Immunodetection .....	74
5.2.4.4. DNA/Protein interaction assay.....	75
5.2.4.5. Radioactive labeling and purification of DNA probe.....	76
5.2.4.6. Electrophoretic Mobility Shift Assay (EMSA) .....	77
5.2.4.7 Chromatin Immunoprecipitation (ChIP) .....	77
5.2.5 Reporter Gene Analysis.....	78
5.2.5.1. Transfection of EL-4 cells .....	78
5.2.5.2. Luciferase Reporter Gene Assay.....	79
5.2.6 Cell culture techniques.....	80
5.2.6.1. Cell maintenance.....	80
5.2.6.2. Induction of cells.....	80
5.2.6.3. Preparation and activation of naïve CD4 <sup>+</sup> T lymphocytes .....	80
6. BIBLIOGRAPHY.....	83
7. CURRICULUM VITAE.....	91



## 1. INTRODUCTION

“Both the immune and nervous systems develop and function as a typical "supersystem." The prototype of the supersystem can be seen in embryogenesis and evolution. The concept of the supersystem can also be applied to the development of language, or a city, or other cultural phenomena that human beings have created as a result of their vital activities.”

Tomio Tada

Although best known for its role in inducible gene transcription in lymphoid system (Fig. 1.1), the calcineurin/nuclear factor of activated T cells (NFAT) signaling pathway is also known to be involved in a wide range of other biological processes, such as formation of a complex vascular system, a recombinational immune system, certain aspects of the nervous system, and complex adaptive responses characteristic of vertebrates. Receptor stimulation and calcium mobilization result in activation of many intracellular enzymes including the calcium- and calmodulin-dependent phosphatase calcineurin, a major upstream regulator of NFAT proteins [1, 2]. Activated cells inducibly transcribe a large array of potential NFAT- target genes coding

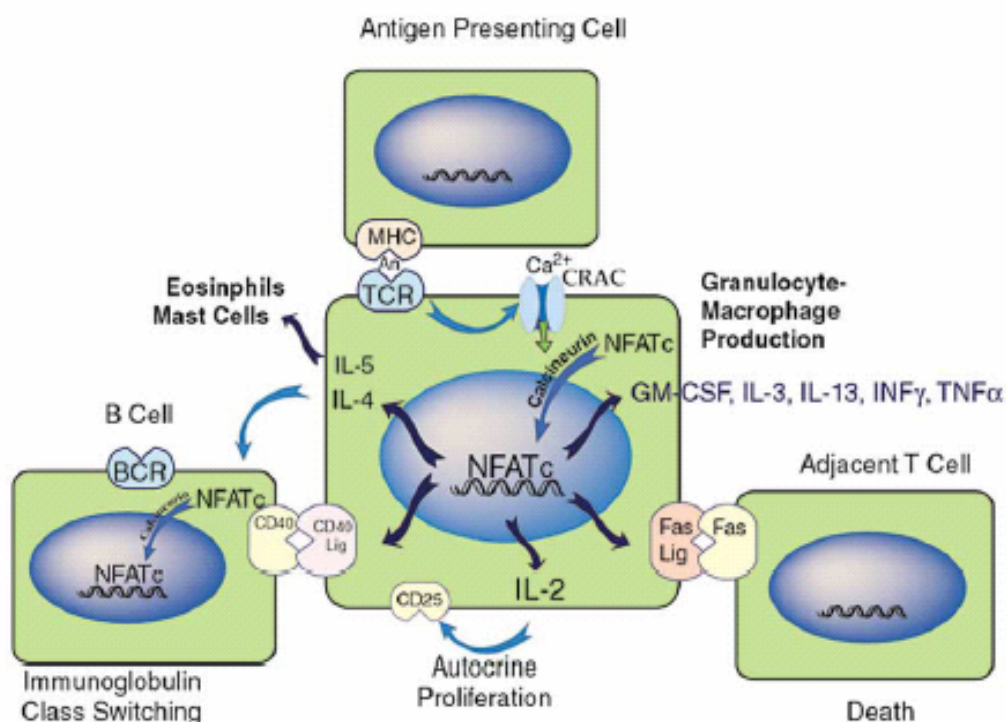


**Figure 1.1 NFAT signaling and lymphocyte cell-cell interactions [3].**

NFAT controls genes encoding proteins such as  $TNF\alpha$  that are secreted and appear in the plasma and cytokines such as IL-2, 4, and others that produce their effects by autocrine or paracrine mechanisms on nearby cells. T cell activation genes includes CD40 and Fas ligands. One role of CD40 ligand in conjunction with B cell receptor signals and IL-4 is to activate NFAT signaling in B cells leading to immunoglobulin class switching and the production of IgE. IgE activates NFATc1 translocation and function in mast cells, leading to the production of an array of cytokines and chemokines that in turn influence T cell function. Signaling in eosinophils also uses NFAT transcription complexes to activate cytokines and cell surface molecules.

transcription factors, signaling proteins, lymphokines, cell surface receptors and other effector molecules [4, 5]. As substrate for calcineurin, NFAT proteins can be inhibited by the immunosuppressive drugs cyclosporine A (CsA) and FK506 [6].

### ***1.1 Evolution of NFAT signaling***

The NFAT family of transcription factors consists of five evolutionarily conserved proteins, including the primordial NFAT5, that is the only NFAT member represented in the *Drosophila* genome [7, 8]. First, NFAT5 was described as an NFAT-related protein, which differs from the conventional NFAT proteins NFATc1-4 (Fig. 1.2) in its structure, DNA binding, and regulation. NFAT5 contains a NFAT-like Rel homology domain, bears the conserved DNA contact residues of NFATc1-4, and binds DNA sequences similar to those found in the regulatory regions of well-characterized NFAT-dependent genes. However, it lacks the majority of Fos/Jun contact residues and, therefore does not bind cooperatively with Fos and Jun to DNA [7]. Analysis of genes encoding proteins with rel domains demonstrates that the rel domain first appeared in invertebrates, such as in *Drosophila*, but apparently is absent in lower invertebrates, including the worm *Caenorhabditis elegans*. At the time of the appearance of vertebrates and clearly by the time of the appearance of bony fish, the NFATc1-4 family appeared probably by recombination of an exon encoding a  $\text{Ca}^{2+}$ / calcineurin-sensing domain with an exon encoding a rel domain. The NFATc1-4 family contains a rel domain similar to the TonEBP proteins found in insects but is otherwise distinct from the TonEBP proteins. These observations predict that the NFATc1-4 family will fulfill  $\text{Ca}^{2+}$ -dependent signaling functions specific to vertebrates [8], whereas in NFAT5 the  $\text{Ca}^{2+}$ /CN – dependent signaling domain is missing.

### ***1.2 Structure and localization of NFAT family members***

In humans, the NFATc1 (also designated as NFAT2 or NFATc) gene is located on chromosome 18q23, the NFATc2 gene (NFAT1 or NFATp) on chromosome 20q13.2-q13.3, the NFATc3 (NFAT4 or NFATx) gene on chromosome 16q22.2, NFATc4 (NFAT3) gene on chromosome 14q11.2 and the NFAT5 gene on chromosome 16q22.1. NFATc2 transcripts are ubiquitously expressed in mammalian cells, showing the highest constitutive expression level in peripheral lymphocytes [9, 10]. The three NFATc3 isoforms are found to be constitutively synthesized at a highest level in thymus [9, 11]. Whereas NFATc2 and c3 are constitutively expressed, transcription of the chromosomal NFATc1 gene is strongly induced upon activation of effector T cells [12].

NFATc1 is expressed in six isoforms. This is due to alternative splice/polyadenylation events and the use of two promoters P1 and P2 that lead to the predominant synthesis of four long isoforms ( $\alpha/\beta$  B and  $\alpha/\beta$  C) in naive T cells and the shorter NFATc1  $\alpha$  and  $\beta$  A isoform in effector T cells [13, 14]. Whereas the isoform NFATc1/A described previously [15] contains a relatively short C terminus, the longer isoforms, B and C, span extra C-terminal peptides of 128 and 246 aa, respectively. It was shown that in addition to the strong N-terminal trans-activation domain, TAD-A, NFATc/C contains a second trans-activation domain, TAD-B, in its C-terminal peptide [13]. It is also important to note the presence of an alternate N-terminal domain of shortest isoform (NFATc1/A), which differs from that of other NFAT isoforms in that it is not highly acidic. The structure of NFATc proteins are schematically presented in Fig. 1.2. All NFAT proteins share a comparable structure. They possess three conserved regions: the RSD (Rel/NF $\kappa$ B similarity domain), a TAD at the N-terminus and the regulatory domain. RSD harbors the DNA binding domain of approximately 300 amino acids (aa) and shares approximately 70% sequence homology among NFATc1-4 members. In all four NFATc proteins the regulatory domain is encoded in a single exon. This domain is phosphorylated in resting cells at two serin-rich regions (SRR) and in three repeated motifs termed the SP repeats (SPXXSPXXSPXXXXXD/ED/E). The SP1-3 and SRR motifs are substrates for

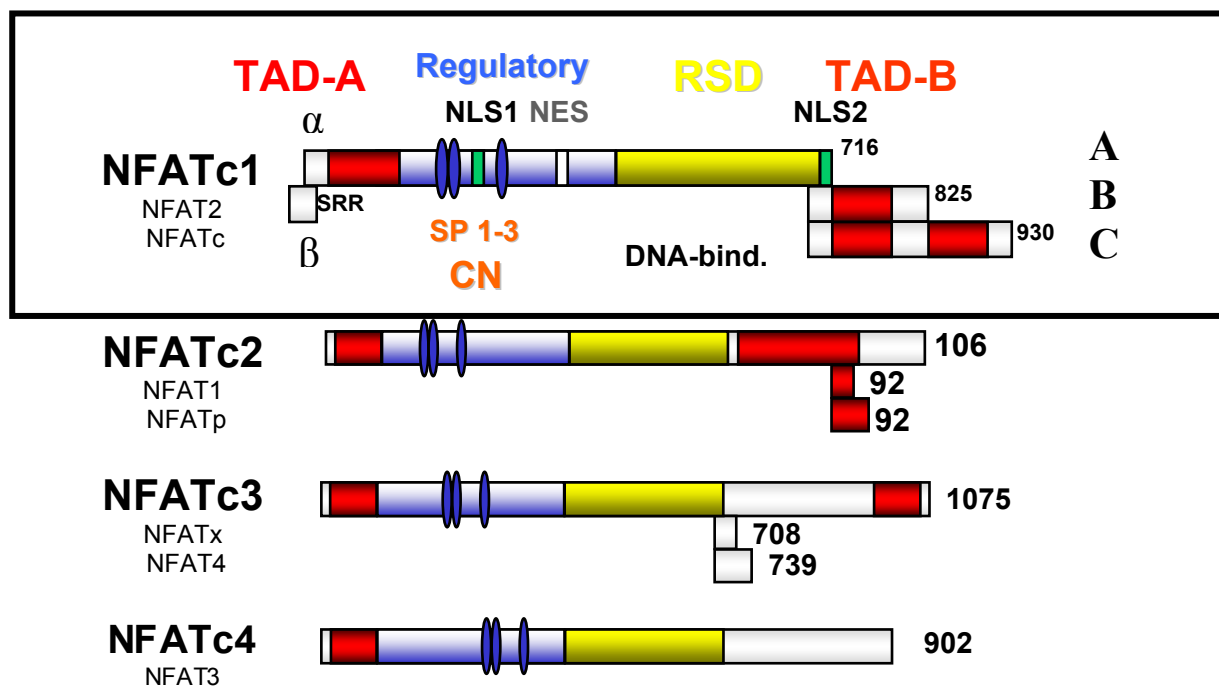


**Figure 1.2 Schematic structure of NFATc1-4 family members.**

The DNA binding regions of NFATs, the RSD, are shown as yellow boxes. The N- and C-terminal transactivation domains, TAD-A and TAD-B, are shown in red. Further sequence motifs are shown for NFATc1 only where TAD-B consists of two peptides which are separated by an inhibitory domain [13]. For the regulatory domain located between TAD-A and the RSD, the position of the SRR and SP motifs 1-3 are indicated. In addition, binding region for the calcineurin phosphatase as well as signals for nuclear localization (NLS) and nuclear export (NES) of NFATc1 are shown.

calcineurin and Ser/Thr protein kinases. Finally, the phosphorylation status of the regulatory domain specifies the DNA-binding affinity as well as relative exposure of nuclear localization signal (NLS) and nuclear export signal (NES), triggering active/inactive NFAT conformation mode [16].

### 1.3 NFAT activation and function

In cells of the immune system, NFAT proteins are activated by stimulation of receptors coupled to calcium mobilization and PKC/IKK/Ras/MAP kinase pathway activation, in particular the antigen receptors on T [17] and B [18] cells, the Fcε receptors on mast cells and basophiles [19] and the Fcγ receptors on macrophages and NK cells [20]. Combinatorial regulation is a powerful mechanism that enables a tight control of gene expression, via integration of multiple signaling pathways that induce different transcription factors required for enhanceosome assembly. In T cells, the four calcium-regulated transcription factors of the NFATc family act synergistically with AP-1 (Fos/Jun) proteins through composite DNA elements which contain adjacent NFAT and AP-1 binding sites of the classical structure

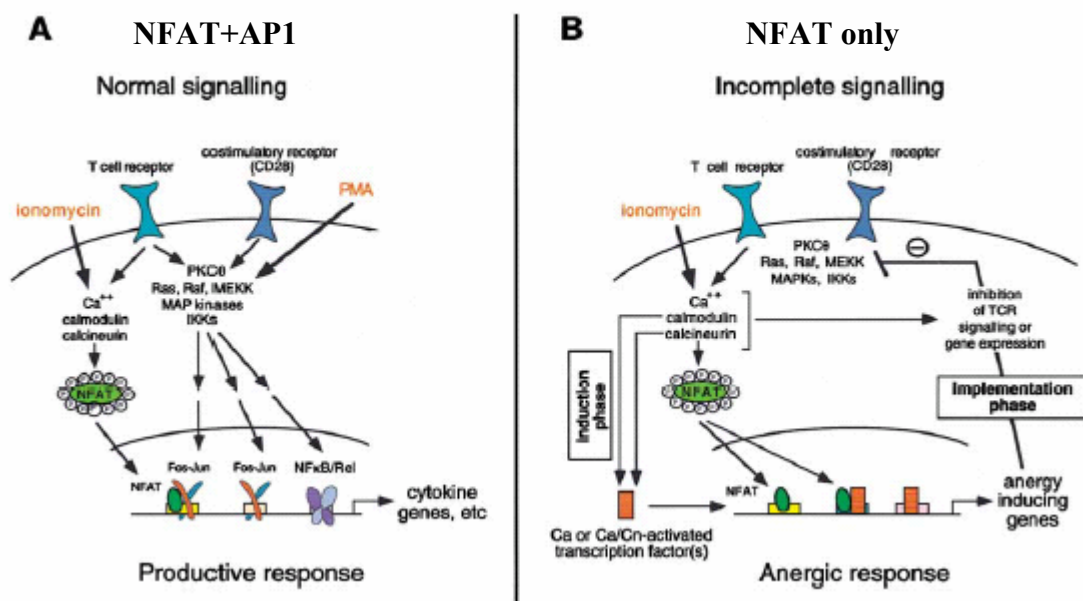


**Figure 1.3 NFAT plays a central role in productive activation as well as in lymphocyte tolerance [21].**

(A) Combined stimulation of TCR and costimulatory receptors (PKC/IKK/Ras/MAP kinase pathway) results in balanced activation of NFAT, AP-1, and NFκB; the cooperative NFAT: AP-1 complexes formed under these conditions are necessary for transcription of cytokine genes and other genes critical for the productive immune response.

(B) TCR stimulation without costimulation leads to unbalanced activation of NFAT relative to its cooperating transcription factor AP-1 (Fos/Jun), thus diverting NFAT toward transcription of an alternate set of anergy associated genes whose products together impose the tolerant state.

5'-caxwGGAAAawxxxg/aTGAC/GTCAG/tc-3' (where capital letters denote highly conserved nucleotides; w = A, or T; x = any nucleotide). The AP-1 transcription complex consists of Fos and Jun proteins that are encoded by families of genes including *c-jun*, *junB*, *junD*, as well as *c-fosB*, *fra1* and *fra2*. Transcription controlled by most AP-1 sites is insensitive to inhibition by CsA or FK506 [22]. These two factors form highly stable ternary complexes to regulate the expression of diverse inducible genes [23]. Concomitant induction of NFAT and AP-1 requires concerted activation of two different signaling pathways: calcium/calcineurin, which promotes NFAT dephosphorylation, nuclear translocation and, activation, and protein kinase C (PKC)/Ras pathways, which promotes the synthesis, phosphorylation and activation of members of the Fos and Jun families of transcription factors [9]. Recently, in context of different activation pathways a striking ability of NFATc1-4 proteins was shown to be involved in negative and positive regulation of immune responses. Briefly, in differentially stimulated T cells, NFAT associated with AP-1 regulates a very large set of activation-associated genes, classically associated with an ongoing immune response. It is formed through activation of both  $Ca^{2+}$  and PKC/MAP kinase signaling pathways (Fig. 1.3A). In contrast,  $Ca^{2+}$  signaling without PKC/MAP kinase signaling activates NFAT but not AP-1, inducing a much smaller set of genes that encode putative negative regulators involved in lymphocyte's tolerance or anergy (Fig. 1.3B) [21, 24]. In contrast to other NFAT members, NFAT5 controls the cellular response to osmotic stress by a mechanism that requires dimer formation which is independent of calcineurin or of interaction with AP-1 [7].

### ***1.3.1 $Ca^{2+}$ /Calcineurin - dependent TCR signaling pathway***

The  $Ca^{2+}$ , calcineurin/NFAT signaling pathway was defined about 15 years ago [25] and was one of the first signaling pathways to bridge the cell membrane with the nucleus. Although the pathway is relatively simple (Fig. 1.4), multiple levels of regulation impinge upon it, making it adaptable for many functions in a wide variety of cell types. A rise of intracellular free  $Ca^{2+}$  level depends on activation of phosphatidylinositol-specific phospholipase C (PLC)- $\gamma$ , $\beta$ . Immunoreceptors and receptor tyrosine kinases (RTKs) activate PLC- $\gamma$ , while G-protein-coupled receptors (GPCR) activate PLC- $\beta$ . Then, hydrolysis of phosphatidylinositol (PI)-4,5-bisphosphate (PIP2) by PLC results in generation of inositol-1,4,5-trisphosphate (IP3), which binds to IP3 receptors (IP3R) in the endoplasmic reticulum and promotes  $Ca^{2+}$  entry through  $Ca^{2+}$  release activated  $Ca^{2+}$  (CRAC) channels in the plasma membrane (Fig. 1.4).  $Ca^{2+}$  increases result in activation of many calmodulin (CaM)-dependent enzymes, including the phosphatase calcineurin and the multifunctional CaM-dependent kinases CaMKII and CaMKIV [26].

Calcineurin consists of two polypeptides: the large, catalytic subunit A and the smaller subunit B, and exert a number of cellular functions by binding to IP<sub>3</sub>, ryanoid and transforming growth factor- $\beta$  receptors [27]. Further important calcineurin targets are the NFAT factors. Many studies have shown that calcineurin dephosphorylates multiple phosphoserines on NFAT

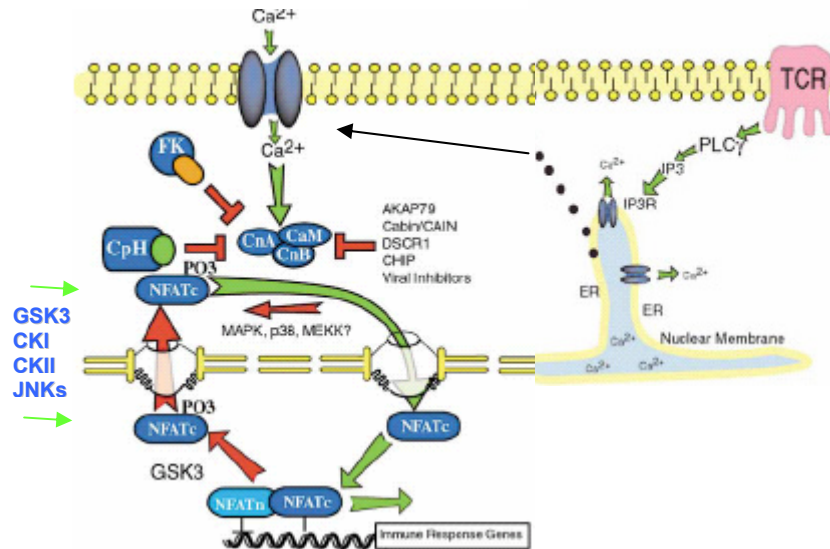


**Figure 1.4** The Ca<sup>2+</sup>/calcineurin/NFAT signaling pathway [3].

The components shown in blue appear to modulate NFAT signaling in many different cell types. Orange and green ovals represent FK506 and cyclosporin, respectively. Red arrows denote inhibitors and green arrows denote positive regulators of NFAT signaling. A simplified nuclear pore complex (NPC) is shown.

leading to its nuclear translocation and activation [9]. Calcineurin activity is inhibited by the immunosuppressive drugs cyclosporin A (CsA) and FK506, which act as complexes with their intracellular immunophilin receptors, cyclophilin and FKBP12, respectively [6]. In parallel, hydrolysis of PIP<sub>2</sub> by PLC results in production of diacylglycerols (DAG), which activate Ras and protein kinase C (PKC). Receptor activation is coupled to activation of protein tyrosine kinases (PTKs), Ras, MAP kinases (MAPK), and PI-3 kinase (PI3K). NFAT activation is initiated by dephosphorylation of the NFAT regulatory domain (Fig. 1.2). Efficient dephosphorylation requires a docking interaction between NFAT and calcineurin [28]. The major docking site for calcineurin is located near the N terminus of the NFAT regulatory domain, and has the consensus sequence PxIxIT (SPRIEIT in NFATc1). The individual NFAT proteins possess characteristic PxIxIT sequences with a low affinity for calcineurin (K<sub>d</sub> = 10–30  $\mu$ M), needed to maintain sensitivity to environmental signals and prevent constitutive activation of NFAT. Substitution of the SPRIEIT sequence of NFATC2 with VIVIT, a higher-affinity version obtained by peptide selection, increased the basal calcineurin sensitivity of the protein and resulted in partial nuclear localization [29]. Thus, NFAT proteins are bound by calcineurin, and upon dephosphorylation of SP repeats, the NFAT/calcineurin complexes are

translocated into the nucleus where they stimulate transcription [30]. The implication is that several constitutive kinases cooperate to maintain the inactive, phosphorylated state of NFAT in resting cells. Similarly, several inducible and/or constitutive kinases may act to rephosphorylate NFAT that has been dephosphorylated during cell activation. Glycogen synthase kinase-3 (GSK-3) and casein kinase I (CKI) are constitutive NFAT kinases that promote NFAT nuclear export [31, 32]. Phosphorylation by GSK3 requires prior phosphorylation by a priming kinase, such as protein kinase A (PKA) [33]. CKI was shown to play a role in controlling the phosphorylation and nuclear transport of NFATc3 [32]. This kinase is associated with aa 177-184 and phosphorylates the NFAT domain at additional phosphoacceptor sites located further downstream. Thus, the phosphorylation of Ser172 by MAP/SAP kinases and of next serine rich region (SRR) compose a perfect consensus phosphorylation site for CKI and CKII [34]. The MAP kinases p38 and JNK are inducible kinases that promote NFAT nuclear export, by selectively phosphorylating NFAT proteins at the SP sequences at the beginning of their SRR-1 regions: JNK1 phosphorylates NFATc1 and NFATc3, whereas p38 selectively targets NFATc2 and NFATc4 [35]. For JNK1, a proposed mechanism is that phosphorylation of the SPRIEIT calcineurin-docking site of NFATc1 blocks the interaction of NFATc1 with calcineurin [36].

### ***1.3.1.1 Nuclear transport of NFAT proteins***

Phosphoserines within SP-repeats and the serine-rich regions appear to mask nuclear localization sequences (NLS) [32]. Among the putative NLSs within NFATc1, two of them were detected, spanning the amino acid residues 263-271 and 681-685. Dephosphorylation exposes the NLS and leads to rapid nuclear import 5-10 min after T cell activation [37]. Surprisingly, the N-terminal  $\text{Ca}^{2+}$ /calcineurin - dependent translocation domain of NFATc1 was found not to be structured in solution, suggesting that it requires a second protein to mask the NLS and the nuclear export signal (NES) sequences [38]. A NES was identified in NFATc1 to be essential for export. Most likely, the export receptor is Crm1, which preferentially binds phosphorylated NFATc2 [16]. Crm1 was found to bind to the NES1 and NES2 motifs near the NFAT4 N-terminus, which are also bound by calcineurin. This phenomena led to suppose that the length of nuclear residence of NFATs can be controlled by competitive binding of Crm1 and calcineurin to NFAT [39]. Recent data showed that DYRK1A and DYRK2 were able to counter calcineurin mediated dephosphorylation of NFAT by directly phosphorylating NFAT's regulatory domain. Conversely, DYRK1A depletion by RNAi in HeLa cells led to NFAT activation further indicating that DYRKs are negative regulators of NFAT in vivo.

Interestingly, DYRKs were found to prime NFAT for further phosphorylation by GSK3 and CK1. Pre-phosphorylation by DYRK2 accelerated CK1-mediated phosphorylation by two-fold. However, unlike other 'priming kinases' DYRKs phosphorylate a distinct motif (SP-3) from those targeted by CK1 (the SRR-1 motif) or GSK3 (the SP-2 motif) [112].

### ***1.3.2 PKC/IKK/ Ras/ MAPK costimulatory signaling pathways***

The T cell surface molecule CD28 delivers costimulatory signals necessary for maximal activation through the TCR [40]. Enzymes of the PKC family are stimulated early in these signaling cascades by activation-induced lipid second messengers [41]. As a result, PKC proteins phosphorylate many cellular proteins, leading to modulation of surface antigens, activation of other Ser/Thr protein kinases, and subsequent induction of transcription factors [41]. Among several T cell-expressed protein kinase C (PKC) isoforms, only PKC $\theta$  was capable of stimulating AP-1 and JNK activity and synergizing with calcineurin to activate the IL-2 gene [42]. PKC $\theta$  is a Ca<sup>2+</sup>-independent member of the PKC family that is selectively expressed in skeletal muscle and T lymphocytes and plays an important role in T cell activation. Protein kinases activated by dual phosphorylation on Tyr and Thr within protein kinase subdomain VIII are called mitogen-activated protein kinases (MAPK), *e.g.* extracellular signal-regulated kinase (ERK), p38 and c-Jun N-terminal kinase (JNK) [also known as stress-activated protein kinase (SAPK)] [43].

### ***PKC $\theta$ in ERK and JNK/SAPK activation***

Importantly, the signal transduction pathways that lead to ERK and JNK/SAPK activation are biochemically and functionally distinct [44]. For example, the ERK group regulates multiple targets in response to growth factors via a PKC- $\alpha$ /Ras-dependent mechanism, and JNK/SAPK activates the transcription factors c-Jun, Elk-1 and ATF-2 in response to pro-inflammatory cytokines and exposure of cells to several forms of environmental stress via a Rac-dependent pathway (Fig.1.5) [45, 46]. This functional independence between these two signaling pathways is based on substrate specificities of multiple components of the upstream MAPK cascade recruited for distinct signal transduction pathways, allowing the integrated response of cells to different stimuli [43]. Once Ras is activated it is able to regulate diverse cellular processes in peripheral T cells by coupling to multiple biochemical effector signalling pathways including the Raf-1/MEK/ERK1,2 kinases and signalling pathways controlled by the Rac/Rho GTPases. The ERKs translocate to the nucleus when activated to regulate components of the AP-1 transcription factor complexes. JNK/SAPK activation is crucial during co-



stimulation of T lymphocytes [47]. It is known that JNK/SAPK binds to and phosphorylates the activation domain of their substrates, *e.g.* c-Jun and ATF-2 [48]. These transcription factors are members of the basic leucine zipper group that bind as homo- and heterodimeric complexes to AP-1 and AP-1-like sites in the promoters of many genes [24], including multiple cytokine genes such as those for IL-2 and TNF- $\alpha$ . Full activation of JNK/SAPK requires co-stimulation of T cells with either antibodies cross-linking TCR/CD3 and CD28 or PMA and Ca<sup>2+</sup> ionophore. Alone, each stimulus results in little or no activation. Hence, integration of signals that lead to T cell activation appears to occur at the level of JNK/SAPK activation [47]. Genetic evidence indicates that the JNK/SAPK signaling pathway is required for the normal regulation of AP-1 transcriptional activity [49].

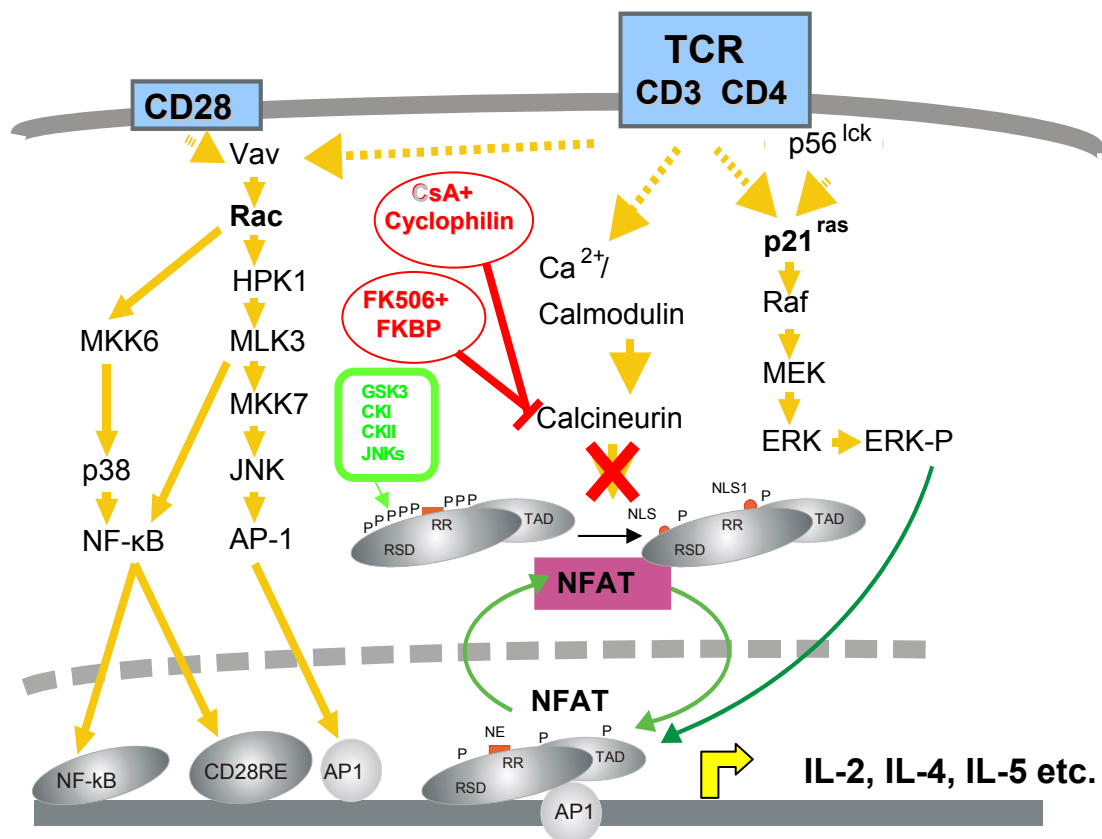


**Figure 1.5** The TCR/CD3 and CD28 signaling pathways in lymphokine gene regulation.

TCR stimulation leads to the rapid activation of PTKs, in particular of p56<sup>lck</sup>, a rise in free, intracellular Ca<sup>2+</sup> and, finally, activation of downstream kinase cascades, such as the Raf/MEK/Erk cascade. CD28 costimulatory signal stimulates enzymes of the PKC family, which, in turn, phosphorylate many cellular proteins, leading to modulation of surface antigens, activation of other Ser/Thr protein kinases, and subsequent induction of transcription factors [41].

### ***PKC $\theta$ and NF- $\kappa$ B activation***

Beside JNK, an additional important target for TCR/CD28 costimulation is represented by the NF- $\kappa$ B transcription factor complex and the CD28 response element (RE) in the IL-2 promoter

[50, 51], which cooperatively binds NF- $\kappa$ B and AP-1 [52]. The ability of phorbol esters to activate NF- $\kappa$ B, combined with the selective activation of JNK/AP-1 by PKC $\theta$  and the role of CD28 costimulation in JNK activation, raised the possibility that PKC $\theta$  plays a specialized role in activating the NF- $\kappa$ B cascade in T cells. Recently it was shown that PKC $\theta$ , but not other PKCs, mediates activation of the NF- $\kappa$ B complex induced by TCR/CD28 costimulation via selective activation of I $\kappa$ B kinase b (IKKb) [53]. This effect was T cell-specific since PKC $\theta$  was relatively inefficient in activating NF- $\kappa$ B in 293T cells [53]. Importantly, PKC $\theta$  appeared to replace neither the TCR nor the CD28 signal required for NF- $\kappa$ B activation, since enhanced activation of the CD28 RE mediated by transient overexpression of wild-type PKC $\theta$  was strictly dependent on TCR/CD28 costimulation [53]. This finding suggests that TCR/CD28 costimulation is essential for a 'productive' and optimal activation of PKC $\theta$ , which is necessary for NF- $\kappa$ B activation. This notion is supported by the findings that CD28 costimulation enhances and stabilizes the membrane translocation and enzymatic activation of PKC- $\theta$  [53] as well as its localization to membrane lipid rafts, when compared to TCR stimulation alone. The essential and selective role of PKC $\theta$  in NF- $\kappa$ B activation is also evident from the recent finding that T cells from PKC $\theta$  knockout mice display a severe defect in receptor-induced NF- $\kappa$ B activation [54].

### ***1.4 NFAT Partner Proteins***

The expression and induction levels of various transcription factors are cell and tissue type-dependent, leading to highly context-specific activities that are also coordinated by cooperativity between factors and sequence-specific DNA affinities. NFAT engages in direct protein-protein interactions and influences transcription synergistically with several families of transcription factors. Differential stimulation through the T cell receptor and various co-receptors leads to stimulus-dependent activation of factors, which selectively converge at promoter and enhancer elements to modulate transcription.

#### ***1.4.1 Basic region-leucine zipper (bZIP) protein family***

In addition to AP-1(Jun/Fos), the most prominent interaction partner of NFAT proteins in activated T cells, there are several other NFAT interplaying molecules.

#### ***p21SNFT***

p21SNFT (21-kDa small nuclear factor isolated from T cells) is a novel human protein of the bZIP family. Overexpression of p21SNFT leads to the significant and specific repression of

transcription from the IL-2 promoter as well as from several other AP-1-driven composite promoter elements [55]. p21SNFT has been shown to replace Fos in dimerization with Jun on a consensus AP-1 binding site (12-O-tetradecanolyphorbol-13-acetate response element (TRE)) and to interact with Jun and NFAT at the distal NFAT/AP-1 enhancer element [56]. Bower and colleagues demonstrated that a p21SNFT/Jun dimer binds a TRE and, like AP-1, binds cooperatively with NFAT to the NFAT/AP-1 composite element. However, Fos interacts significantly more efficiently than p21SNFT with Jun and NFAT, and the replacement of Fos by p21SNFT in the trimolecular complex drastically altered protein-DNA contacts. The data suggest that p21SNFT may repress transcriptional activity by inducing a unique conformation in the transcription factor complex [56].

### ***c-Maf***

c-Maf was identified as a transcriptional partner for NFAT in a yeast two-hybrid screen [57]. This factor is specifically expressed in Th2 but not Th1 cells. CD4<sup>+</sup> T cells and NK T cells from *c-maf*<sup>(-/-)</sup> mice were markedly deficient in IL-4 production. However, the mice produced normal levels of IL-13 and IgE, and, when differentiated in the presence of exogenous IL-4, *c-maf*<sup>(-/-)</sup> T cells produced approximately normal levels of other Th2 cytokines [58]. This finding support the view that c-Maf might control Th2 cell development and has a critical and selective function in IL-4 gene transcription in vivo.

### ***ICER***

Like p21SNFT, the inducible cAMP early repressor (ICER) is able to bind to NFAT and inhibit NFAT-dependent transcription [59]. The CD28-responsive element (CD28RE), a composite DNA binding element consisting of NFAT and cyclic AMP-responsive (CRE)-like motifs in position of -160 of IL-2 promoter has a high affinity for ICER binding as well as for NFAT/ICER complex formation. Moreover, CD28RE with adjacent DNA sequences was also shown to be essential for conferring anergy in T lymphocytes. Because ICER does not possess a transactivation domain required for the recruitment of CBP/p300, the binding of ICER to CD28RE and/or composite motifs containing CRE-like DNA motifs may lead to uncoupling of CBP/p300, thus extinguishing IL-2 expression as well as expression of numerous other cytokines and chemokines [59].

### **1.4.2 Zinc finger proteins**

#### ***ERG***

Early growth response-1 (EGR-1) factor and members of the NFAT protein family bind simultaneously to adjacent elements at positions –168 to –150 within the TNF $\alpha$  promoter. EGR-1 as well as EGR-4 functionally cooperate with NFAT proteins and induce the expression of IL-2 and TNF $\alpha$  cytokine genes. Using tagged NFATc1 and NFATc2 in glutathione S-transferase pull down assays interactions and physical complex formation was shown between each NFAT protein with recombinant as well as native EGR-1 and EGR-4 proteins. Thus, EGR-NFAT interaction and complex formation seems essential for cytokine expression, as adjacent ZIP and NFAT elements are conserved in the IL-2 and TNF $\alpha$  gene promoters. Binding of regulatory EGR and NFAT factors to these sites and the functional interaction and formation of stable heterodimeric complexes indicate an important role of these factors for gene transcription [60].

#### ***GATA***

Cooperation between NFAT and GATA family members has been observed in many systems, including Th2 cells, cardiomyocytes and IGF-1 - induced skeletal muscles. NFAT/GATA cooperation has been established by synergistic activation of reporter plasmids [61], [62], [63]. The Nemer laboratory showed that GATA5 and NFATc1, which are presently the only known transcription factors required for endocardial differentiation, synergistically activate endocardial transcription suggesting that they cooperate in endocardial differentiation [62]. Next, the strong cooperation was shown in coimmunoprecipitation experiments using a skeletal muscle cell line: GATA2 bound to NFATc1 but not to NFATc2 [64].

There is no overlap between NFAT/GATA and NFAT/AP-1 interaction surfaces, consistent with an involvement of RHR-C and RHR-N domains, respectively. An NFATc2 protein bearing mutations in three key Fos–Jun interacting residues that abrogated the ability of NFATc2 to cooperate with AP-1 was as effective, or even more effective than wild-type NFATc2 in its ability to synergize functionally with GATA3 in a transient reporter assay in T-cells [61].

Using immunoprecipitation and Western blotting, it was shown that NFATc1 interacted with GATA-6. NFATc1 further potentiated the GATA-6–mediated activation of smooth muscle–myosin heavy chain (Sm-MHC) transcription. In differentiated vascular smooth muscle cells (VSMCs), blockage of calcineurin down-regulated the amount of GATA-6-DNA binding as

well as the expression of Sm-MHC and its transcriptional activity. These findings demonstrate that the calcineurin pathway is associated with GATA-6 and is required for the maintenance of the differentiated phenotype in VSMCs [63].

### ***1.4.3 Helix-turn-helix proteins***

#### ***IRF***

Interferon regulatory factor 4 (IRF4) is predominantly expressed in the immune system and required for lymphocyte activation [65]. Recently, it was shown that IRF4 potently synergizes with NFATc2 to specifically enhance NFATc2-driven transcriptional activation of the IL-4 promoter. This function is dependent on the physical interaction of IRF4 with NFATc2. IRF4 synergizes with NFATc2 and the IL-4-inducing transcription factor, c-maf, to augment IL-4 promoter activity as well as to elicit significant levels of endogenous IL-4 production. Furthermore, naïve Th cells lacking IRF4 are unable to differentiate into IL-4-producing Th2 effector cells in vitro. Thus, NFATc2 and IRF4 are transcriptional partners that together regulate inducible IL-4 gene expression upon T cell activation [66].

#### ***NIP45***

It was demonstrated that NIP45 (NFAT-interacting protein) can force endogenous IL-4 production in non-producer cells. The addition of NIP45, in conjunction with c-maf and NFAT, to the same non-producing cell types results in appreciable levels of endogenous IL-4, i.e. in levels that approximate those produced by primary Th2 cells. Indeed, this synergy was so pronounced that cells transfected with NIP45 produced 50- to 200-fold more IL-4 than cells that did not receive NIP45 [67].

#### ***Octamer factors***

The T cell-specific IL-2, IL-3, and IL-4 promoters contain each Oct elements in addition to NFAT and AP-1 elements. A composite NFAT/AP-1 element from the widely active GM-CSF enhancer was active in numerous cell types that express NFAT, but NFAT/Oct enhancer activity was T cell specific even though Oct-1 is ubiquitously expressed [68]. By reconstituting the activities of both the IL-3 enhancer and its NFAT/Oct element in a variety of cell types, Cockerill and colleagues demonstrated that their T cell-specific activation required the lymphoid cofactors NIP45 and OCA-B in addition to NFAT and Oct family proteins. Furthermore, the Oct family protein Brn-2, which cannot recruit OCA-B, repressed NFAT/Oct

enhancer activity. Hence, the combination of NFAT, AP-1, Oct, NIP45, and OCA-B proteins may provide a general mechanism for activating the T cell-specific expression of a subset of cytokine genes [68].

#### ***1.4.4 MADS-box proteins***

##### ***MEF-2***

Calcineurin signaling has been shown to stimulate the transcriptional activity of preexisting myocyte enhancer binding factor 2 (MEF-2) [69], a transcription factor that, in turn, controls genes essential for muscle differentiation. MEF-2 proteins are encoded by at least four genes, *Mef2A–D* [70]. An adjacent binding site for the MEF-2 transcription factor cooperates with the NFAT site to confer calcineurin sensitivity. Indeed, transgenic mice that harbor a lacZ transgene linked to a multimerized MEF-2 site show slow fiber-specific expression of the transgene, which can be inhibited by CsA or by muscle specific expression of exogenous MCIP1 [71]. The physical interaction between NFAT and MEF-2 proteins provides a mechanism for linking calcineurin signaling to MEF-2 activation [72]. The mechanism of the control of MEF-2 proteins by calcineurin appears to involve the Ca<sup>2+</sup>-dependent dissociation of histone deacetylase 4 (HDAC) [73]. In addition, Ca<sup>2+</sup> activates calmodulin kinase, which in turn phosphorylates and exports HDAC4 from the nucleus. Greenberg and colleagues [74] recently found that Ca<sup>2+</sup> stimuli that protected neurons from cell death activated MEF-2-dependent transcription in a calcineurin-dependent fashion. Presumably, the genes that are activated by MEF-2 in neurons protect them against cell death. In lymphocytes, the Ca<sup>2+</sup>-dependent activation of MEF-2 appears to lead to programmed cell death by activating the transcription factor Nur77 [75].

#### ***1.5 NFAT Target Genes***

NFAT is thought to regulate a large number of target genes expressed by activated immune cells, including the cytokine genes IL-2, IL-3, IL-4, IL-5, IL-8, IL-13, GM-CSF, and IFN $\gamma$ ; the cell receptor ligands CD40L, FasL, and IL-2R $\alpha$  (CD25) and the transcription factor EGR3 in T cells; CD5 and Ig $\kappa$  in B cells; IL-4, IL-5, and TNF $\alpha$  in mast cells; and TNF $\alpha$  and GM-CSF in NK cells (reviewed in [9]). Expression of these genes meets three or more of the following criteria for involvement of NFAT: (i) the genes are induced by signals that include calcium entry; (ii) their expression in activated cells is inhibited by CsA; (iii) their promoter/enhancer regions contain specific binding sites for NFAT; (iv) in transient transfection assays, NFAT

augments reporter activity driven by these promoter/enhancer regions; and (v) when introduced into the reporter plasmid, mutations in the NFAT binding sites of the promoter/enhancer regions abolish (or significantly diminish) reporter activity. The expression of many of these genes (IL-2, IL-3, IL-13, GM-CSF, TNF $\alpha$ , MIP-1 $\alpha$ ) in T cells was inhibited by expression of a selective NFAT inhibitor, i.e. by the high-affinity PxxIT peptide [29]. In contrast, the PxxIT peptide did not affect the induction of other CsA-sensitive genes such as lymphotoxin- $\beta$  or TNF $\beta$ , which do not fit the other criteria for NFAT control.

### ***1.6 Phenotypes of NFAT-deficient Mice***

To elucidate the specific roles of mammalian NFAT protein, mouse strains with inactivated NFAT genes were generated. The phenotypes of mice lacking single NFATc1, NFATc2, NFATc3, NFATc4; double mutants lacking NFATc2/c3, NFATc1/c2, NFATc3/c4 and triple mutant on NFATc2/c3/c4 have been reported.

#### ***NFATc1 deficient mice***

NFATc1-deficient mice die in utero before day 13.5 because of defects in the morphogenesis of cardiac valves and septa. Consistent with the observed developmental deficits, NFATc1 mRNA and protein are present in murine cardiac endothelium throughout the period of cardiac morphogenesis from a simple tube to a four-chambered heart [76, 77]. Peripheral T cells deficient in NFATc1 show variable (2-to 10-fold) impairment of IL-4 production, a reduced synthesis of IL-6 and serum IgE. RAG<sup>-/-</sup> mice containing NFATc1 deficient lymphocytes showed reduced number of thymocytes and display mild defects in activation and proliferation [78, 79].

#### ***NFATc2 deficient mice***

NFATc2<sup>-/-</sup> mice survive to adulthood but suffer from severe immunodeficiencies. Mice older than 3 months spontaneously develop a moderate splenomegaly [80] and alterations in thymus morphology [81]. The experimental findings indicate that NFATc2 deficiency results in a decrease in Th1 responses (i.e., a decrease in IFN- production) and in an increase in Th2 responses (i.e., an considerable increase in IL-4 and IL-5 production) [82]. As a result, NFATc2<sup>-/-</sup> mice display enhanced allergic reactions and increased susceptibility to *Leishmania* infection in vivo [80, 83, 84]. In the peripheral lymphoid system approximately twofold increase in number of T cells was detected. Many of these cells were CD44<sup>high</sup> CD62L<sup>high</sup> CD69<sup>+</sup> [81], indicative of their “pre-activation”. At least part of the hyperproliferative

syndrome is likely to be due to a failure to induce the Fas ligand, leading to the survival of cells that would normally undergo activation-induced death (AICD).

***NFATc3 deficient mice***

Mice with a mutation of the NFATc3 gene show mild defects in thymic development characterized by a partial loss of DP cells by programmed cell death [85]. This is likely related to the failure to induce Bcl-2 during thymic development. No defects in positive selection were noted, and the excessive activation of the Fas ligand in the periphery produced excessive activation-induced cell death. It is also important to note that NFATc3 mutant mice exhibit skeletal muscle hypoplasia that apparently reflects their impaired embryonic muscle development [86].

***NFATc4 deficient mice***

NFATc4 null mice were viable and fertile and showed no major macroscopic or microscopic abnormalities after 36 months of observation. In situ hybridization indicated that NFATc4 expression significantly overlaps with that of NFATc3, which is the closest homolog of *NFATc4*, suggesting that the two genes might have redundant functions [87].

***NFATc1+c2 deficient mice***

Double deficient T cells remained capable of TCR-mediated activation, as demonstrated in proliferation assays, but significantly impaired effector functions, as demonstrated by cytokine production, effector molecule expression, and allogeneic cytotoxicity. NFATc1/c2-deficient T cells were unable to generate significant levels of any cytokine, Th1 nor Th2, suggesting a global deficit in T cell differentiation and T cell effector function in general [88]. In contrast, double deficient B cells displayed signs of hyperactivation and hyperdifferentiation, as evidenced by significantly elevated titers of some serum immunoglobulins and expanded populations of plasma cells. On the other hand, CD69 expression, which is activated by only a stress or Ras/PKC signal and CsA insensitive and calcineurin independent, was induced normally in these double knockout cells, indicating that NFATc1 and NFATc2 are not involved in stress responses but are essential for activation of cytokine genes [88].

***NFATc2+c3 deficient mice***

Double deficient mice for NFATc2+c3 show a spontaneous differentiation towards Th2 cells, the highest levels of IgE yet recorded in mice, as well as severe allergic responses [11]. T cells



from these mice also show spontaneous hyperproliferation and are independent of CD28 stimulation for activation. The paradox of hyperproliferation, enlarged lymphoid tissue and excessive cytokine (IL-4, IL-5, IL-6, IL-10 and GM-CSF) production is likely to be related to defective activation of Fas ligand and hence an inability to undergo activation-induced cell death. In addition, NFATc2+c3 deficient mice developed multiple disease symptoms in several organs, including allergic blepharitis, pneumonitis and lymphadenopathy. Moreover, NFATc2+c3 mice have spontaneous nuclear accumulation of NFATc1, indicating that compensation for the lack of NFATc2 and c3 involves nuclear import of NFATc1 by an as yet unknown mechanism.

### ***NFATc3+c4 deficient mice***

Mice with disruptions of both *NFATc4* and the related *NFATc3* genes die around E11 in utero with general defects in vessel assembly as well as excessive and dissignaling organized growth of vessels into the neural tube and somites. These mutants were smaller, pale, and showed an underdeveloped yolk sac vasculature, and 20% had enlarged pericardial sacs [87]. Additionally, differentiation of E8.5 and E10.5 NFATc3/c4 null hematopoietic precursors into erythroid and myeloid lineages in vitro appeared to be normal. NFATc3/c4 null mice have no defect in the initial ability of endothelial cells to differentiate. But rather these differentiated cells fail to respond to and give signals essential for the assembly of vessels along specific pathways [87].

### ***NFATc2+c3+c4 deficient mice***

The triple-mutant embryos are smaller than stage-matched control littermates, but were at the same stage, and were not developmentally delayed. The smaller size is likely due to the requirement for calcineurin/NFAT signaling in patterning vertebrate vasculature [87]. Profound defects in sensory axon projections were observed in embryos with combined deletions of *NFATc2*, *NFATc3*, and *NFATc4* mutants. At E10.5, most peripheral trigeminal axons observed in the c2/c3/c4 embryos were stunted, but neurite outgrowth appeared to initiate in the correct direction for cranial and dorsal root ganglia [89]. Triple-mutant embryos also displayed profound disturbances in commissural axon growth. Crabtree's research group concluded that embryonic axon outgrowth stimulated by growth factors, such as neurotrophins and netrins, requires these factors not only to stimulate the tips of growth cones, but also to selectively activate a calcineurin/NFAT-dependent transcriptional program controlling the rate of axonal extension [89].

## 2. RESULTS

### 2.1 Induction of NFATc1/ $\alpha$ A in T cells

Activation of human Jurkat T cells (Fig. 2.1) or human and murine primary effector T cells [13, 14] by TPA+ionomycin (T+I), pharmacological agents that activate Protein Kinase-C (PKC) and calcium-dependent pathways to mimic signal through the TCR and co-receptor or by  $\alpha$ CD3+ $\alpha$ CD28 Abs for 4 h or longer led to a strong induction of synthesis of the short NFATc1 isoform  $\alpha$ A while the synthesis of the other NFATc1 isoforms, B and C, and of NFATc2 remained unaffected (Fig. 2.1). The massive induction of NFATc1/ $\alpha$ A at 4 hours was completely suppressed by pharmacological doses of CsA (100 ng/ml) which selectively inhibits Calcineurin, and therefore, NFAT factors suggesting that NFATs autocontrol the inducible transcription of NFATc1/ $\alpha$ A. This prompted us, first, to identify the NFATc1 gene structure, promoter region and analyse its activity, and, second, to study the role that NFATc1/ $\alpha$ A might play in effector T cells where it is strongly induced.

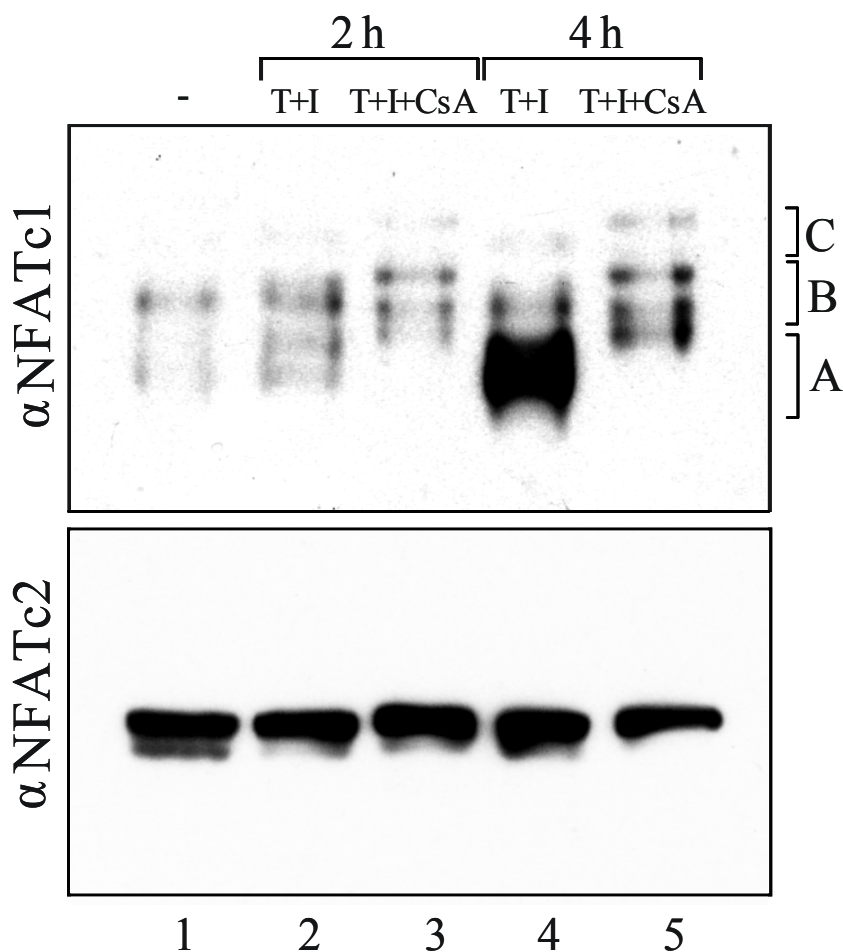


**Figure 2.1 NFATc1/ $\alpha$ A induction in Jurkat T cells.** Western blot with whole cellular proteins from Jurkat cells which were either left untreated (lane 1) or treated with TPA/ionomycin (T/I) in the absence or presence of 100 ng/ml CsA for 2 or 4 hr.  $\alpha$ NFATc1 and  $\alpha$ NFATc2 antibodies were used for IP.

## 2.2 Structure and organization of the chromosomal murine NFATc1 gene

To begin to analyze the regulatory mechanisms controlling transcription in the mNFATc1 gene, genomic DNA fragments containing the gene were cloned and characterized. Eleven independent exons are spread over more than 100 kb DNA (Fig. 2.2 A). The murine gene is expressed in six isoforms which differ both in their N- and C-terminal peptides. The short NFATc1/ $\alpha$ A isoform is predominantly expressed in T effector cells and lacks the B+C-specific C terminal peptide sequences that are encoded in exons 10 and 11 [13]. They share 31% sequence homology with the C terminal peptide of murine NFATc2 [91]. Similar to the generation of human NFATc1 isoforms the synthesis of murine NFATc1 isoforms is controlled by the activity of (at least) two poly A sites which are located downstream of exon 9 (pA1) and exon 11 (pA2), respectively (see Fig. 2.2 A).

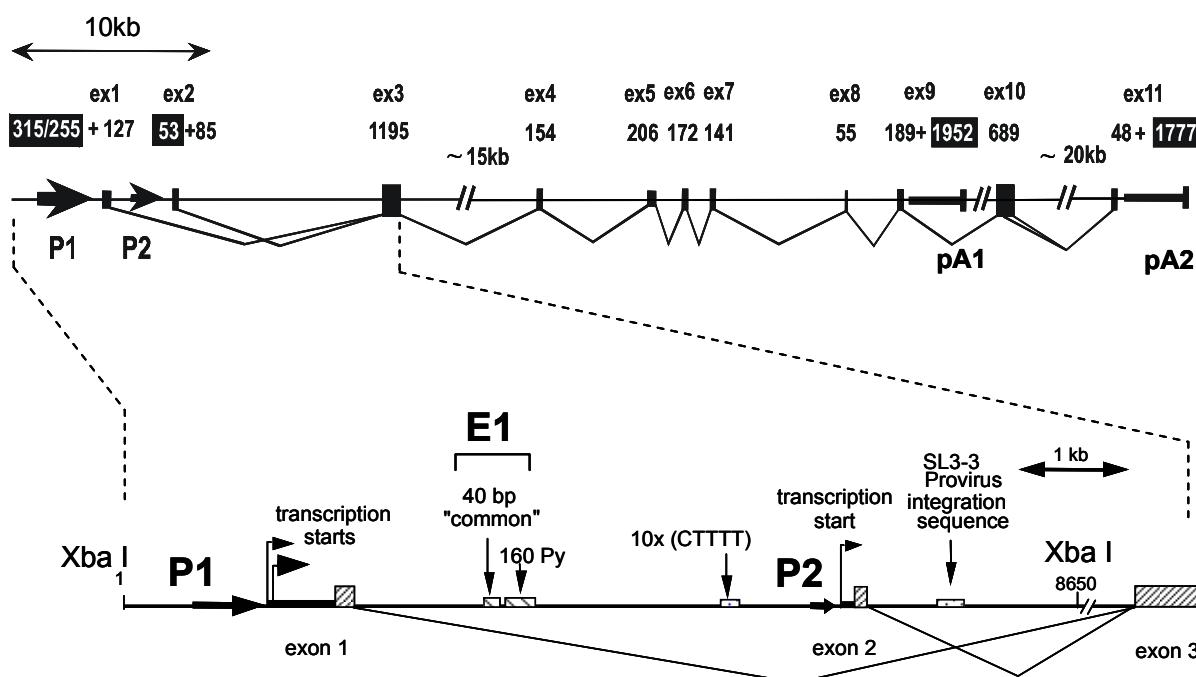


**Figure 2.2 A. Schematic structure of the NFATc1 gene.** The size of 11 exons in bp is indicated above the gene. White numbers in black fields indicate the lengths of 5' and 3' untranslated mRNA regions; black numbers indicate the lengths of protein coding segments. The positions of promoters P1 and P2 and poly A sites pA1 and pA2 are indicated.

**B. Structure of the 8.65 kb XbaI DNA fragment** harboring the two promoters P1 and P2. The protein coding portions of exons 1 and 2 are indicated by dashed boxes, and their 5' untranslated mRNA regions are indicated by thick black bars. Horizontal arrows before both 5' mRNA regions indicate the promoters P1 and P2. Conspicuous sequence motifs are a stretch of 40 bp which is found in several other genes alternatively spliced at their 5' ends [92], a stretch of 160 pyrimidines, ten copies of sequence CTTTT, and an integration site for the retrovirus SL3-3, a potent inducer of T cell lymphomas [93].

Cloning and sequencing of NFATc1 cDNAs from various human and murine hematopoietic cells showed that both P1 and P2 direct the synthesis of three different RNAs. P1 transcripts start at exon 1 and encode NFATc1 proteins bearing the so-called N-terminal  $\alpha$  peptide of 42 amino acids (aa), whereas P2 transcripts start at exon 2, and code for proteins with the N-

terminal  $\beta$  peptide of 29 aa [94], The C termini of these proteins comprise either a short stretch of 19 aa in the A isoform, or longer stretches of 128 aa in the B isoform or 246 aa in the C isoform [14]. The B and C isoforms arise from alternative splicing and poly A addition at the distal site pA2, whereas the short isoform A results from polyadenylation at the proximal poly A site pA1. Together with the inducible activity of the promoter P1, polyadenylation at the proximal poly A site pA1 results in the strong induction of the short isoform NFATc1/ $\alpha$ A [14]. In resting T cells, the NFATc1/ $\beta$  RNAs are the most prominent nfatc1 transcripts and their synthesis is reduced upon T-cell activation [95]. However, following activation in primary effector T cells or in T-cell lines of human or murine origin, a 15–20-fold induction of NFATc1/ $\alpha$ A RNA was detected, whereas only a 2–5-fold increase was observed for the NFATc1/ $\alpha$ B or NFATc1/ $\alpha$ C RNAs [95].

These findings and the structure of NFATc1 5' region suggest that NFATc1 RNAs are

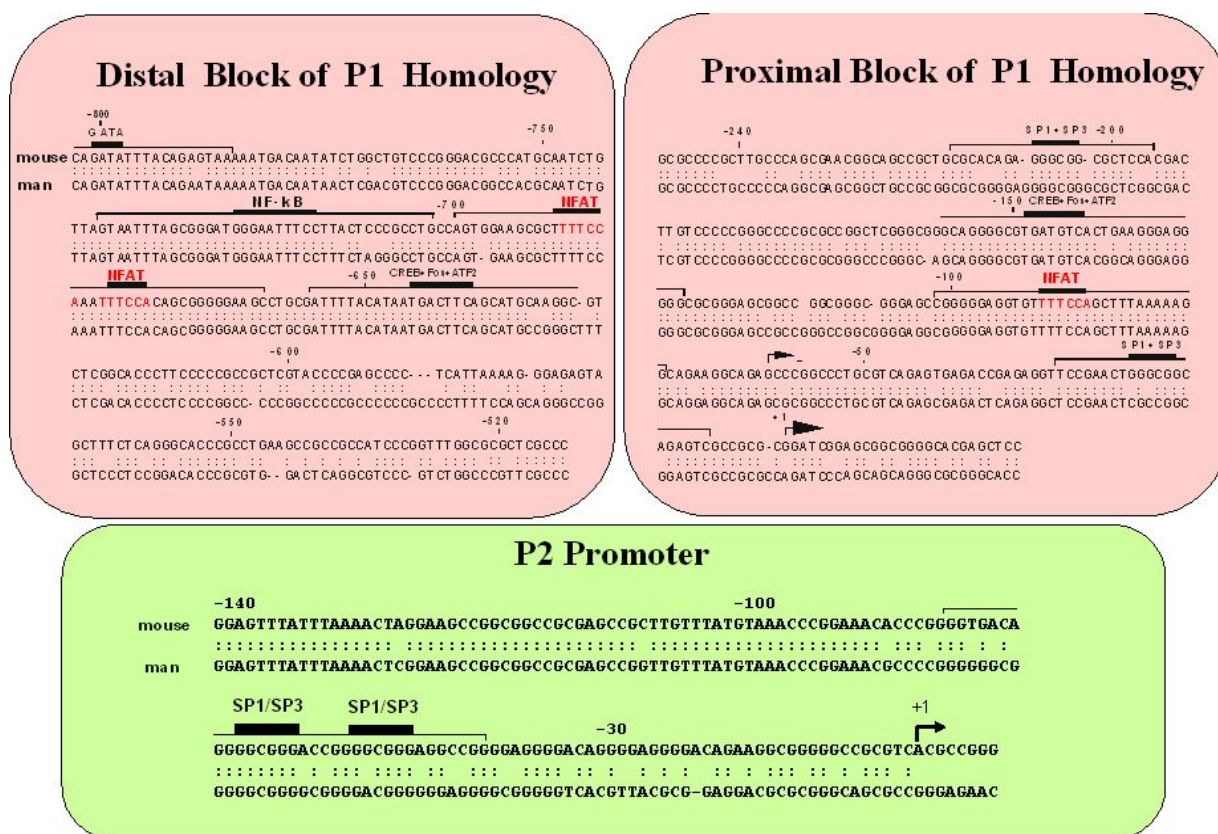


**Figure 2.3** P1 and P2 sequences are highly conserved between the human and murine *NFATc1* genes. Transcriptional start sites are indicated by horizontal arrows; potential binding sites for transcription factors are indicated by black bars above the sequences. Brackets above the sequences indicate the oligonucleotides used in EMSAs for the identification of transcription factors binding.

synthesized from two promoters and by alternative splicing events. The 5' region of murine NFATc1 gene (Fig. 2.2 B) which we cloned as an Xba I fragment of 8650 bp contains the most distal exon 1 encoding the 42 aa of NFATc1 $\alpha$ , and exon 2 encoding the 27 aa in NFATc1 $\beta$ .

Exons 1 and 2 are separated from each other by an intron of approximately 4 kb. Conspicuous sequence characteristics are 375 CpG dinucleotides, i.e. potential targets for DNA methylation, which are clustered around the transcriptional start sites and within the 5' untranslated mRNA regions. Sequence features within intron 1 are a stretch of 160 pyrimidines, 10 copies of the pentanucleotide CTTTT and a sequence of 40 bp that is 87.5 % identical to a sequence within intron 1 of the murine *whn* nude gene that is also controlled by two promoters and alternate splicing events [92]. In addition, approximately 430 bp downstream from exon 2 an integration sequence was detected for the retrovirus SL3-3, a potent inducer of T cell lymphomas in mice [93]. Since it had not been previously reported, we also determined the mouse and human exon/promoter sequences. More detailed look at the nucleotide structure of two main blocks of homology demonstrates an exceptionally high degree of sequence conservation of the more upstream, 5' noncoding exon, between the *NFATc1* genes of the two mammalian species. This is suggestive of an evolutionarily conserved regulatory function for these (transcribed) regions. We analyzed these sequences by TRANSFAC which searches within sequenced fragments *versus* the TFMATRIX transcription factor binding site profile data. We found a number of putative transcription factors binding sites (Fig. 2.3).

### 2.3 Cell-specific utilization of the P1 and P2 promoters

To identify a cell-specific expression pattern, RNase protection assays were performed using RNA samples recovered from various cell types. For mapping of exon 1 transcripts, a 126 bp fragment was used for probe synthesis corresponding to the protein coding region of exon 1.

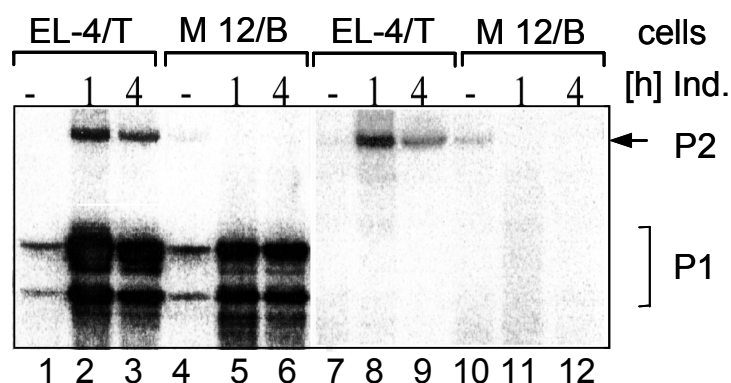


**Figure 2.4 Detection of transcripts directed from the NFATc promoters P1 and P2 in EL-4 T and M12 B cells.** Probes for the detection of exon 1 transcripts (P1) and of transcriptional start site at P2 were hybridized with whole RNA from EL-4 T cells (lanes 1-3) and M12 B cells (lanes 4-6) which were either left uninduced (-) or induced by T+I for 1 or 4 h. In lanes 7-12, the P2 probe was used alone.

First, using RNA from EL-4 T cells and M12 B cells and an exon 1-specific probe, a strong, inducible P1 activity was detected in both cell types. Inducible P2 activity was observed in EL-4 but not M12 cells, where a week induction downregulated P2 activation (Fig. 2.4).

None or at most a very weak P1-directed transcription was observed in all other non-lymphoid cells investigated, such as in embryonic stem (ES) cells, F9 embryonic carcinoma (EC) cells, L cells, 3T3 cells, HL-1 cardiomyocytes and N2A neuronal cells treated with T+I for 1 or 4 h (Fig. 2.5). These results show that NFATc1 P1 promoter is strongly activated in lymphoid T cells. We also examined the expression of P1 and P2 mRNAs by RT-PCR. We used three primers for this purpose; primers 1 and 2 were specific for the sense strand sequence of the first and second exons, respectively, and primer 3 for the antisense strand sequence of the common exon 3. For this analysis we used several B cells lines (such as in 70Z pre B cells, WEHI 231, M12 and A20J B cells) treated with T+I for 4-48 hr and EL-4 cell line treated for 30 min - 16 hr. In all these cells lines low basal level of P2-directed transcripts was present. P1 transcripts were slightly inducible in B cells lines at 4hr of induction comparing to around 10 fold increase of mRNA level at 4hr in EL-4 cells (data not shown).

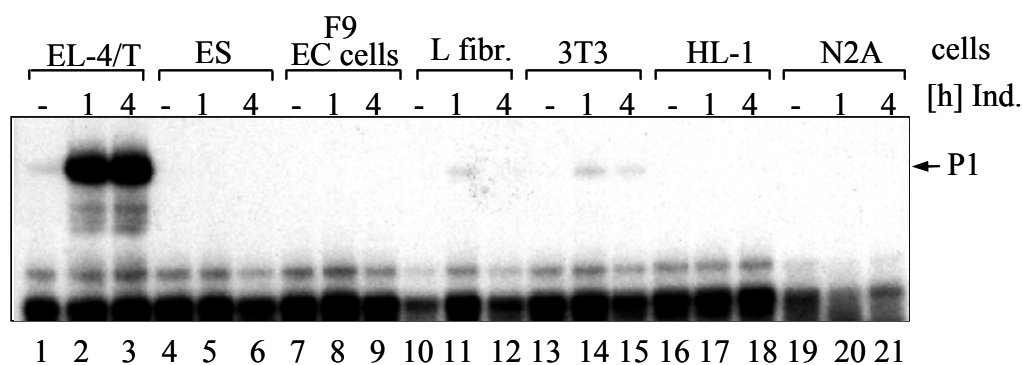


**Figure 2.5 Detection of P1 activity in various murine cells.** An exon 1 probe was hybridized with 10  $\mu$ g RNA from EL-4 T cells, embryonic stem (ES) cells, F9 embryonic carcinoma (EC) cells, L fibroblast, NIH 3T3 cells, HL-1 heart cells, and N2A nerve cells, which were either left uninduced or treated by T+I for 1 or 4 hrs.

#### 2.4 Transcription initiation sites for the alternative mNFATc1 first exons

To identify the transcription initiation sites of the P1 and P2 exons, RNase protection assays were performed using RNA samples recovered from naïve T cells, Th0, Th1 and Th2, or EL-4 cells. We generated antisense RNA probes to determine transcriptional start sites. For the mapping of transcriptional start sites at promoter P1, a 386 bp Kpn I/Sac II fragment of 8.65 kb XbaI fragment (Figure 2.2B) was cloned in PKS plasmid and used for the synthesis of an antisense probe. For mapping of P2 transcripts, a 244 bp NotI/NotI fragment of 8.65 kb XbaI fragment was used. A single start point situated 53 bp in front of the first translational start

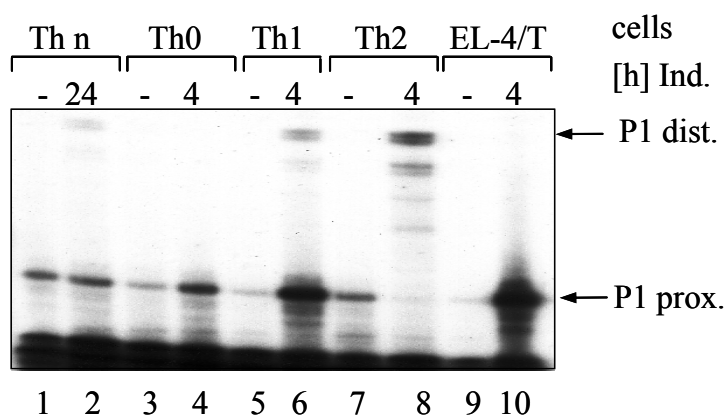


**Figure 2.6 Mapping of the transcriptional start sites at P1.** A probe recognizing upstream start sites of exon 1 transcription was hybridized with 5 $\mu$ g of RNA from naive T cells, Th0, Th1, and Th2 cells, or EL-4 cells. The primary Th cells were induced by  $\alpha$ CD3 and  $\alpha$ CD28 Abs and EL-4 cells by T+I for the times indicated.

codon is used for transcription from P2, while two transcriptional start points are used for transcription directed by P1. These are located 315 and 255 bp upstream of the first ATG and appear to be used alternatively. As shown in Fig. 2.6, the distal site, P1<sub>dist</sub>, is used after induction of naive T cells, Th1 and Th2 cells, whereas the P1<sub>prox</sub> site is predominantly used in naive Th and Th1 but not Th2 cells.

Moreover, P2 activity was found to be markedly weaker, reaching only about 5% of P1 activity. In EL-4 cells, P1 activity was induced by T or I alone, and T+I double treatment enhanced P1 induction, which could be abolished by CsA. Forskolin (F) treatment which

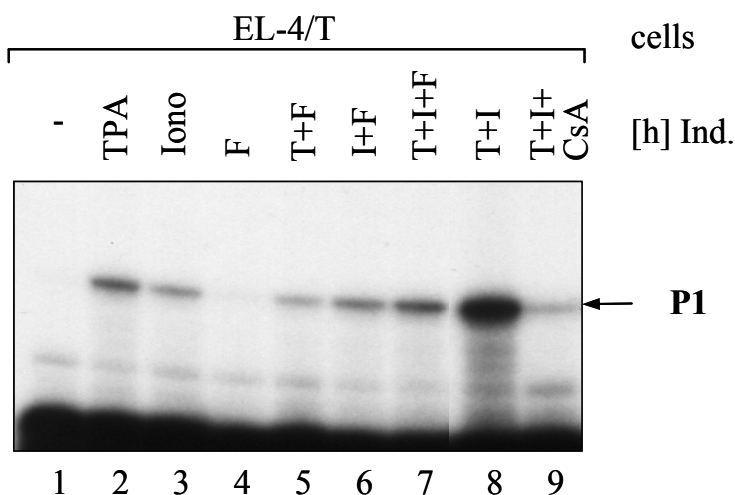


**Figure 2.7 P1 induction.** RNAs from EL-4 cells induced for 1 hr by TPA (T), ionomycin (I), or forskolin (F) alone or in combination were investigated. In lane 9, cells were induced by T+I in the presence of 100 ng/ml cyclosporin A (CsA).

enhances cAMP levels and upregulates the expression of Th2-type NFAT target genes, e.g., *IL-5*, exerted a very weak stimulatory effect on P1, either alone or in combination with ionomycin, and it impaired T+I-mediated P1 induction (Fig. 2.7).

### 2.5 Characterization of the P1 core promoter

We next attempted to localize cis-acting elements involved in the determination of the EL-4 cell-specific expression of the P1 promoter. We first examined four constructs bearing rather large deletions of cosmid 262 sequence containing the P1 promoter of NFATc1 gene. This fragment was digested by *EspI*, *EcoRI* and *Cfr45I* restriction enzymes and using Southern blott method, different 5' size fragments, containing NFATc1 upstream area and P1 promoter with transcriptional start site were isolated and cloned into pGL3 basic vector. The largest construct in this analysis pGL3b-5.5kb, containing 5.5 kbp upstream from the transcription initiation site (*EspI* restriction sites) showed a similar transcriptional activity comparing to shortest construct pGL3b-0.8kb and other constructs. Luciferase (LUC) activity was determined using total cellular extracts and normalized for transfection efficiency. Deletion of the upstream sequence from -5.5 kbp to -0.8 kbp resulted in no significant decrease in promoter activity. This indicates that the proximal segment of 0.8 kb harbors the most important promoter elements and, therefore, was designated as P1 'core' promoter. P1 activity was induced by F but markedly less by T or I alone. A combination of I+F, i.e. by inducers of Ca<sup>2+</sup>-involved signaling cascades or protein kinase A, resulted in a strong synergistic activation of P1 whereas T+I induction was markedly less efficient (Fig. 2.8), contrary to the strong effect on the P1 promoter in its chromo

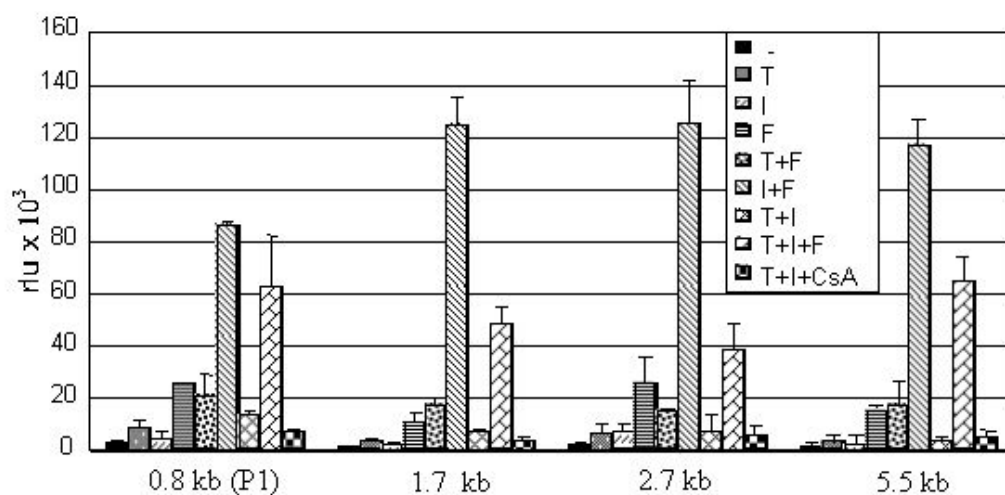


**Figure 2.8 Characterization of the P1 core promoter.** Luciferase gene constructs directed by P1 segments of 0.8, 1.7, 2.7, or 5.5 kb were transfected into EL-4 cells. After 24 hr, the cells were treated with TPA (T), ionomycin (I), or forskolin (F) alone or in combination for an additional 24 hr in the absence or presence of cyclosporin A (CsA).

somal context (Fig. 2.7). This indicates that (i) the chromosomal context and/or (ii) additional transcription factors binding to sequence elements located outside the core promoter region which we have identified contribute to NFATc1 induction in T cells. Sequence alignment of human, mouse and rat chromosomal sequences indicated several regions of strong homology



upstream and downstream from transcriptional start site (Fig. 2.9A). Surprisingly, chromosomal NFATc1 -11.6 kb region of about 500 bp demonstrated 70 % homology between mouse and human and 92% homology between mouse and rat sequences. Moreover, the presence of classical NFAT binding site suggests the presence of the putative regulatory element within this area (Fig. 2.9B). To check the functional activity of this region by transient transfection in EL-4 cells we isolated and cloned 534 bp fragment into pGL3-0.8bp construct upstream of P1 "core" promoter.

**Alignment of human, mouse and rat chromosomal sequences of NFATc1 gene**

A.



B. -11.6kb region

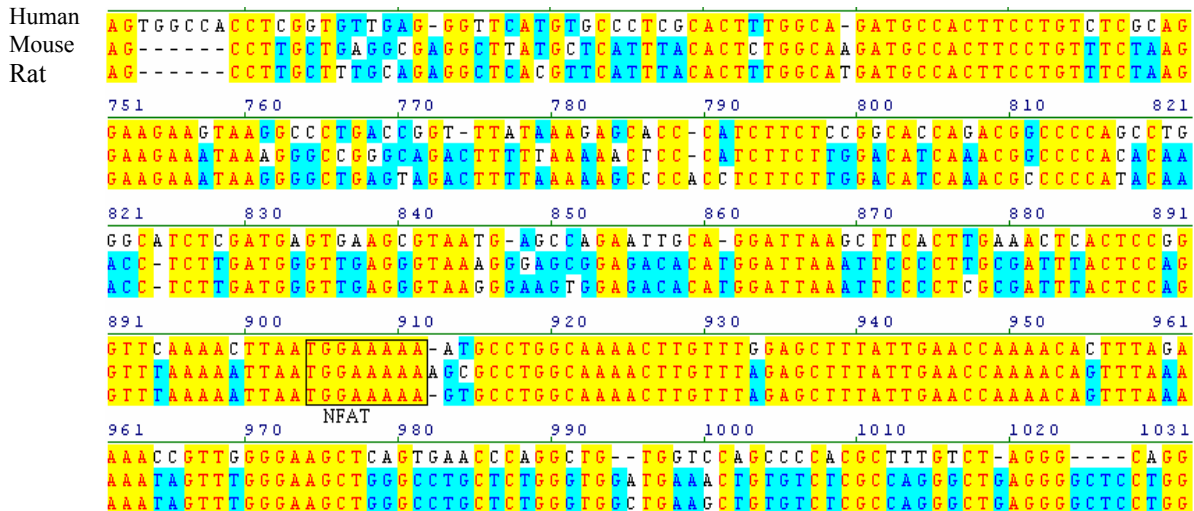
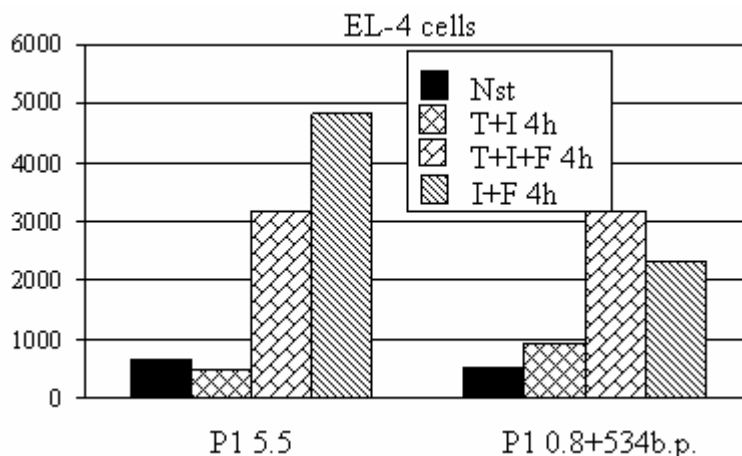


Figure 2.9 A. mNFATc1 gene locus. Homology regions are marked by red points in exons (E) and non-coding sequences (yellow line). Promoters are marked by P1 and P2.

B. Detailed homology map between human, mouse and rat chromosomal sequences in -11.6kb region upstream of transcriptional start site. 534 bp fragment located 11.6 kbp upstream transcriptional start site of P1 promoter contains consensus NFAT site and showed in black box.

Figure 2.10 highlighted the inhibitory effect of 534 bp fragment when cells were treated by I and F agents. P1 promoter activity was twice less compared to largest pGL3b-5.5kb construct. Cells induced by T+I resulted in a slight increase of promoter activity whereas transcriptional level in triple treatment remained the same. This supported our suggestion of the presence of several



**Figure 2.10 Characterization of the P1 core promoter.** Luciferase gene constructs directed by P1 segments of 0.8+534bp or 5.5 kb were transfected into EL-4 cells. After 24 hr, the cells were treated with TPA (T) + ionomycin (I), I + forskolin (F) or in triple combination for an additional 4h.

regulatory elements within gene locus, including promoter core which contribute to NFATc1 complex regulation upon different stimulatory signals.

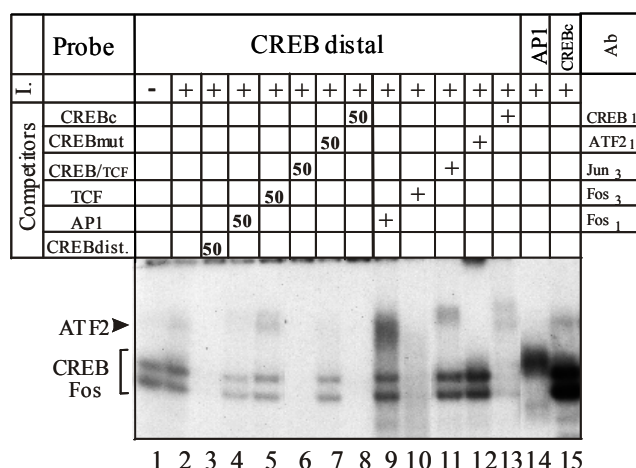
## ***2.6 P1 promoter activation and NFATc1 regulation depends on well organized TF machinery***

### ***2.6.1 CREB contribution to P1 induction***

Two DNA segments of approximately 270 bp from the P1 core promoter spanning the nucleotides from -25 to -250 and from -520 to -800 show more than 80% sequence homology between mouse and human (Fig. 2.3). Two conserved (TATA-like?) boxes are located around 15 and 30 bp in front of the distal transcriptional start site, and, in addition, the motif TGATGTCA. This motif centered around position -145 corresponds to a CREB consensus binding sequence, the cAMP responsive element binding factor. Therefore, using nuclear proteins from EL-4 cells in EMSAs we observed the generation of two prominent DNA/protein complexes which – as shown by competition and supershift EMSAs – consist of CREB and Fos proteins. A third, inducible factor complex contains ATF-2 (Fig. 2.11A).

A similar CREB binding site was detected around position -640 within the distal block of homology and might contribute, along with the proximal site, to the strong effect of elevated cAMP levels on P1 induction. Introduction of mutations into the -145 CREB site impaired P1 induction to approximately 25% of its wild-type level (Fig. 2.11B) indicating that the binding of CREB<sub>distal</sub> and Fos factors to the P1 promoter is important for its activity.

A.



B.

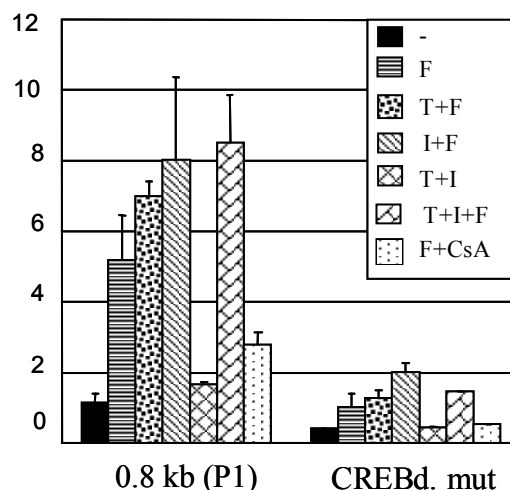


**Figure 2.11 A. CREB-like, ATF-2 and Fos complexes bind to the CREBdist sites of P1.** Nuclear proteins from noninduced EL-4 cells (lanes 1) or cells treated with T+I for 1 hr were incubated with CREBdist, AP1, or CREBc (consensus site) probes (lines 2,14 and 15). For competition, 50 ng of a wild-type CREBc site (lane 8), a mutated CREB site unable to bind CREB (lane 7), a wild-type CREB from TCF site used as a positive control (lane 6), TCF binding site used as a negative control (lane 5), AP1 binding site (line 4) or CREBdistal site (lane 3) were added. Abs raised against CREB, ATF-2, Jun and Fos-3 and 1  $\mu$ l (lanes 13, 12, 11 and 10 or 9) were used in supershift assays.

**B. Introduction of mutations into CREBdist abolishes P1 induction.** Two micrograms DNA of luciferase constructs driven by wild-type (wt) P1 or a P1 fragment mutated in CREBdist sites were transfected into EL-4 cells which were either left untreated (-) or treated different agents.

### 2.6.2 NF- $\kappa$ B binds to P1 promoter

A  $\kappa$ B-like motif centered on position -720 is inducibly bound by the typical p50/p65 NF- $\kappa$ B heterodimers in EMSAs using nuclear proteins from dendritic cells, similar to an NF- $\kappa$ B 'consensus' site (Fig. 2.12). Introduction of mutations abolished any NF- $\kappa$ B binding. p50/p50

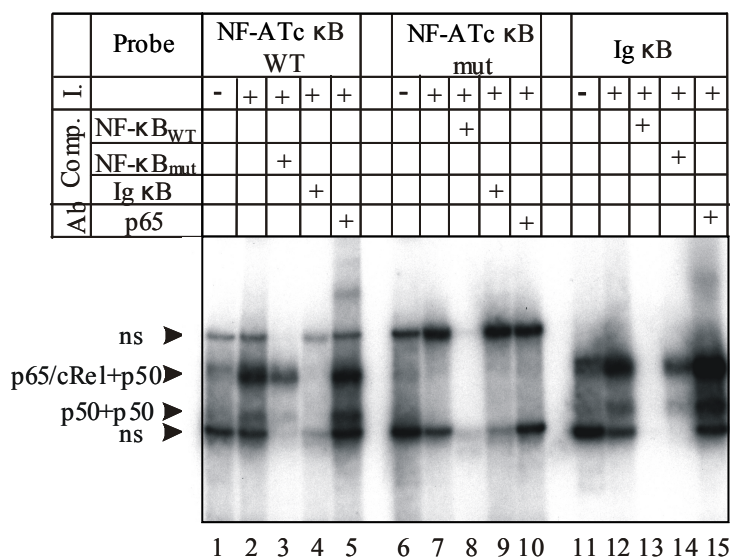


**Figure 2.12 p50/p65 NF- $\kappa$ B heterodimers complexes bind to the NF- $\kappa$ B site of P1.** Nuclear proteins from noninduced dendritic cells (lanes 1,6 and 11) or cells treated with T+I for 1 hr were incubated with NF- $\kappa$ B from P1, NF- $\kappa$ B mutated or Ig  $\kappa$ B probes. For competition, 50 ng of a wild-type NF- $\kappa$ B site (lanes 8 and 13), a mutated NF- $\kappa$ B site unable to bind Ig  $\kappa$ B and NF $\kappa$ B (lanes 14 and 3) were added. Abs raised against Ig  $\kappa$ B (lanes 4 and 9) and p65 (lanes 5, 10 and 15) were used in supershift assays.

complex was detected to be bound to Ig  $\kappa$ B site when cells were induced by T+I for 1h. These data show the capability of NF- $\kappa$ B factor to bind to P1 promoter of NFATc1 gene. It's important to note that dendritic cells don't express NFAT proteins at all.

**2.6.3 NFATs autoregulate P1 induction and enhance NFATc/ $\alpha$ A synthesis**

Within P1 DNA upstream of position -250, there are four additional consensus sequences for the binding of NFAT factors. However, only two of them, which are tandemly arranged around position -675, formed specific NFAT factor complexes when they were incubated with GST-NFATc1-protein in EMSAs (Fig. 2.13). When a probe spanning the tandem sites (NFAT<sub>tand</sub>) was incubated with nuclear proteins from EL-4 cells, several prominent inducible protein complexes were generated which were very similar in mobility to those generated the proto -

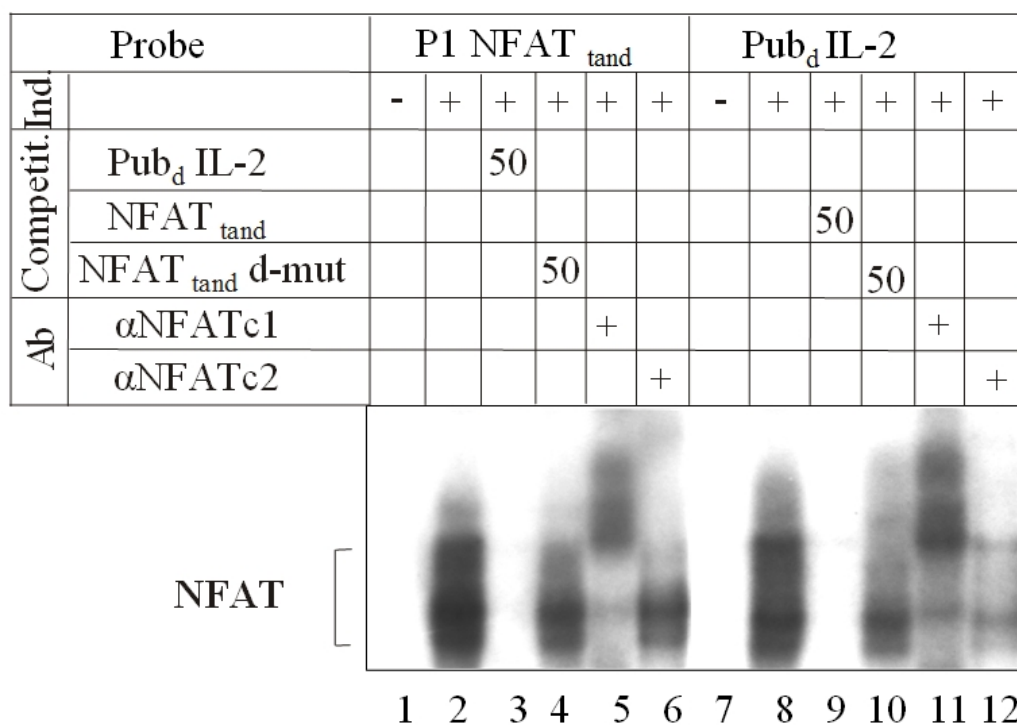


**Figure 2.13 NFAT-like complexes bind to NFAT tand.** Nuclear proteins from noninduced EL-4 cells (lanes 1 and 7) or EL-4 cells treated by T+I for 1 h (lanes 2-6 and 8-12) were incubated with an NFAT tand or IL-2 NFAT (Pu-bd) probe, a typical NFAT site. For competition, 50 ng of Pu-bd (lane 3), NFAT<sub>tand</sub> (lane 9), or mutated NFAT tand d-mut (lanes 4 and 10) oligos were added. Abs raised against NFATc (lanes 5 and 11) or NFATc2 (lanes 6 and 12) were used in supershift assays.

typical NFAT site (compare lanes 2 and 8 in Fig. 2.13). Since an excess of distal IL-2 NFAT site suppressed NFAT binding to NFAT<sub>tand</sub> (see lane 3 in Fig. 2.13), an excess of P1 NFAT<sub>tand</sub> site with intact NFAT motifs but not of a site mutated in both NFAT motifs suppressed factor binding (lanes 9 and 4, 10 in Fig. 2.13), and Abs specific for NFATc1 or

NFATc2 led to supershifts of NFATtand complexes (lanes 5 and 6 or 11 and 12 in Fig. 2.13), NFATtand is a genuine NFAT binding site. Compared to the NFAT -90 site of P1 (see also Zhou et al., 2002) and to Pu-bd of *IL-2* promoter, NFATtand is a stronger NFAT binding site (the EMSA probes used in Fig. 2.13 and 2.14 were of about the same specific radioactivity).

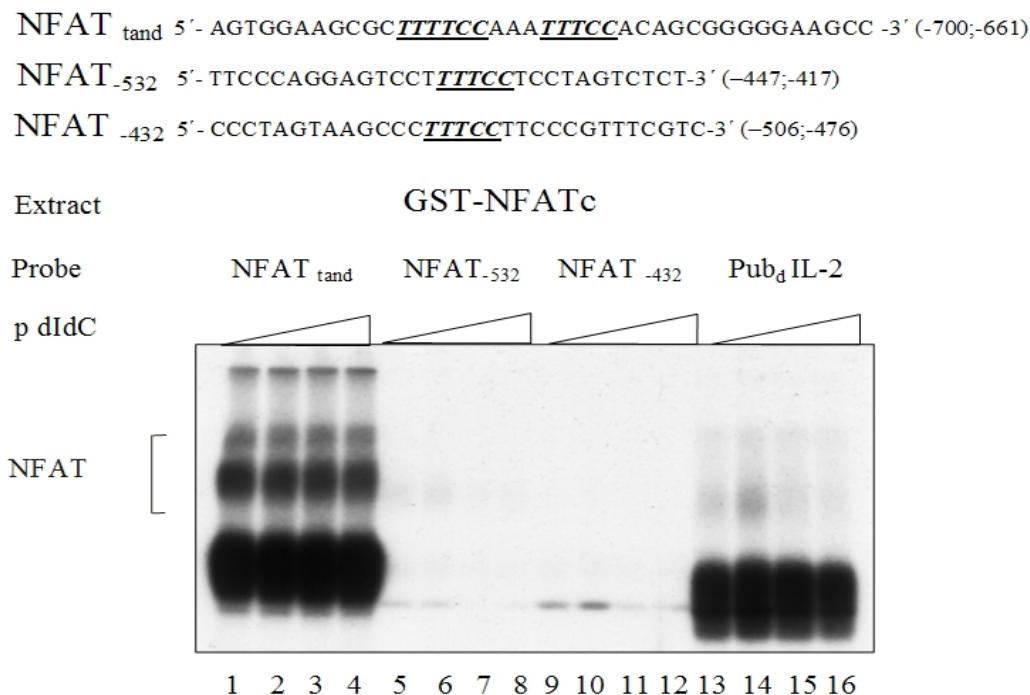


**Figure 2.14 NFATc1 complexes bind to the -675 tandemly arranged NFAT site of P1.** GST-NFATc1-protein was incubated in presence of three NFAT sites and Pubd IL-2 site. NFAT tand demonstrated formation of specific NFAT complexes (lines 1-4, pIdC increasing concentration) comparing to classical Pubd IL-2 NFAT complexes (lanes 14-16). NFAT -532 (lanes 5-8) and NFAT -432 (lanes 9-12) were unable to bind GST-NFATc1.

According to supershift assays, the NFATtand complexes exhibiting the slowest and fastest mobility contain NFATc1 whereas complexes with intermediary mobility contain NFATc2 (lanes 5 and 6 in Fig. 2.14). Both types of complexes are also formed with Pu-bd and the NFAT -90 site. Contrary to P1, the activity of P2 is not regulated by NFAT factors. The inability of P2 oligonucleotides to compete for the generation of NFAT complexes (Fig. 2.18) and missing NFAT binding motifs indicate that NFAT factors do not bind to P2. The configuration of tandemly arranged *TGGAAA* NFAT core sequences at NFATtand led to the question of whether, contrary to a typical NFAT site which is bound by monomeric NFAT and AP-1,

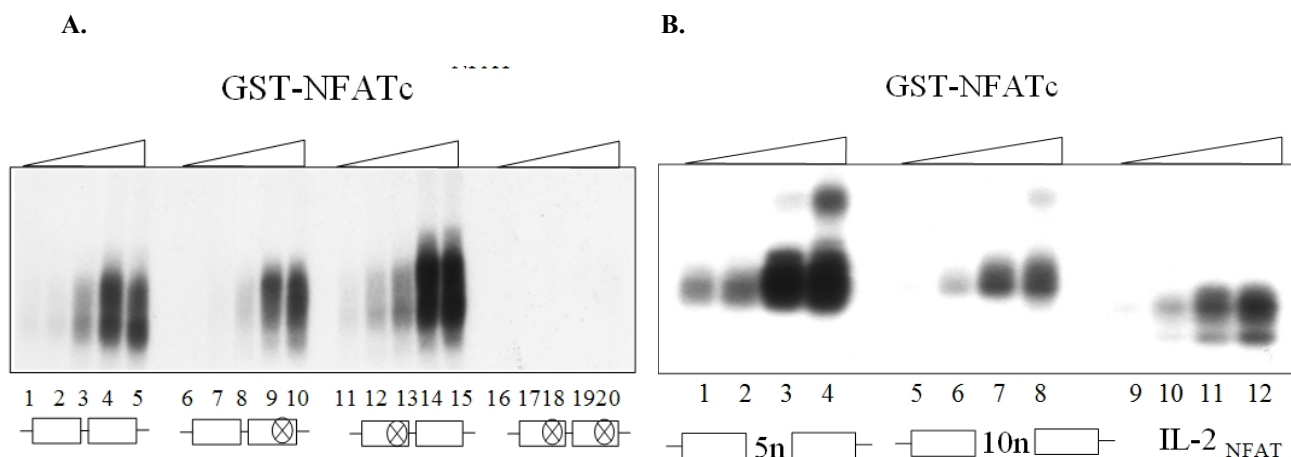


**Figure 2.15 A.** NFATc1 can bind to each of both NFAT core motifs within the NFATtand element. Increasing concentrations of GST-NFATc1-RSD protein were incubated with a wild-type NFATtand probe or probes mutated in one of two or both NFAT motifs.

**B.** Introduction of 5 or 10 spacer bp between the NFAT core motif leads to the generation of NFAT dimers. Increasing concentrations of GST NFATc1-RSD protein were incubated with probes carrying 5 or 10 spacer nucleotides between the two NFAT motifs or an *IL-2* NFAT site probe.

NFAT dimers can bind to NFATtand. When we incubated mutated NFATtand sites which should suppress NFAT binding to one or the other NFAT core motif in EMSA titration experiments with increasing concentrations of bacterially expressed GST-NFATc1-RSD protein, a very similar complex formation was observed with the wild-type or mutated probes. A probe mutated in both motifs did not bind any GST-NFATc1-RSD protein (Fig. 2.15A). However, dimer formation, i.e., the binding of two NFAT proteins to one NFATtand probe, was observed when we introduced 5 or 10 bp between both NFAT motifs. This is shown in

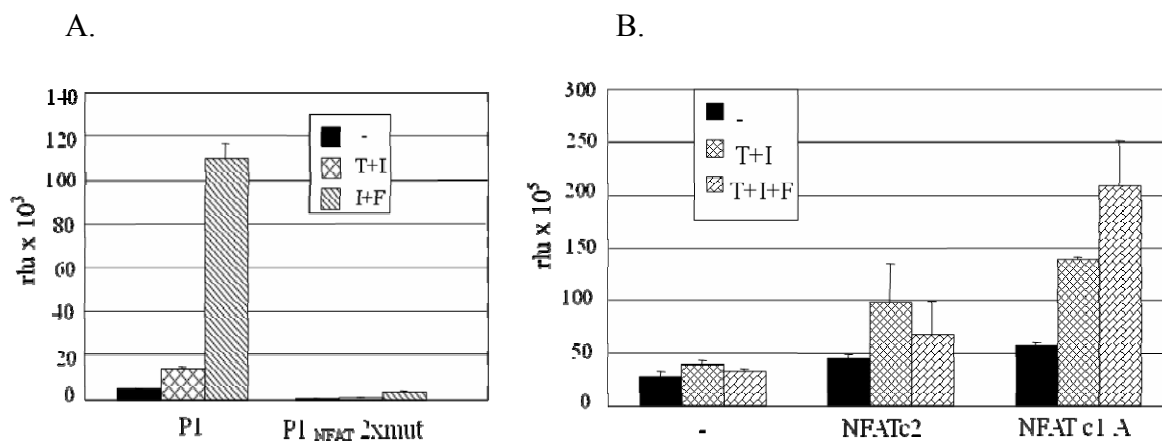


**Figure 2.16 A.** Introduction of NFAT mutations into NFATtand abolishes P1 induction. Two micrograms DNA of luciferase constructs driven by wild-type (wt) P1 or a P1 fragment mutated in both NFAT sites of NFATtand (d-mut) was transfected into EL-4 cells which were either left untreated (-) or treated by T/I or I/F.

**B.** Ectopic expression of NFATc2 or NFATc1/A in EL-4 cells enhances P1 activity. 0.2 micrograms of a P1-directed luciferase construct was transfected into EL-4 cells either with 0.5 g empty vector DNA (-) or vectors expressing NFATc2 or NFATc1/A.

Fig. 2.15B where dimer formation could be observed with a NFATtand\_5n or NFATtand\_10n probe whereas no dimer formation was detected with the distal *IL-2* NFAT site (Fig. 2.15B). The importance of NFAT activity in P1 induction is demonstrated by introducing mutations into P1 at the NFATtand site which suppress NFAT binding and by cotransfections of a P1-directed luciferase reporter gene into EL-4 and 293 cells with vectors expressing NFATc proteins. As shown in Fig. 2.16A, mutation of both NFAT sites abolished any P1 activity. In cotransfections, ectopic NFATc2 expression resulted in a 2- to 3-fold increase and NFATc1/A expression in a 4- to 5-fold increase in inducible P1 activity in EL-4 cells which express relatively high levels of endogenous NFAT (Fig. 2.16B). All these results indicate that NFAT proteins control NFATc1/A expression.

## 2.7 Characterization of the P2 promoter

In contrast to highly inducible P1 promoter, P2 promoter demonstrated basal activity upon different stimulation signals. We cloned into pGL3 basic vector the core P2 promoter of 243 bp with transcriptional start site and two 5' upstream areas of 1.2 kbp and 3.5 kbp. The largest construct in this analysis pGL3b-3.5kb showed a three fold elevated activity compared to enhancer elements in upstream area. Luciferase (LUC) activity was determined using total

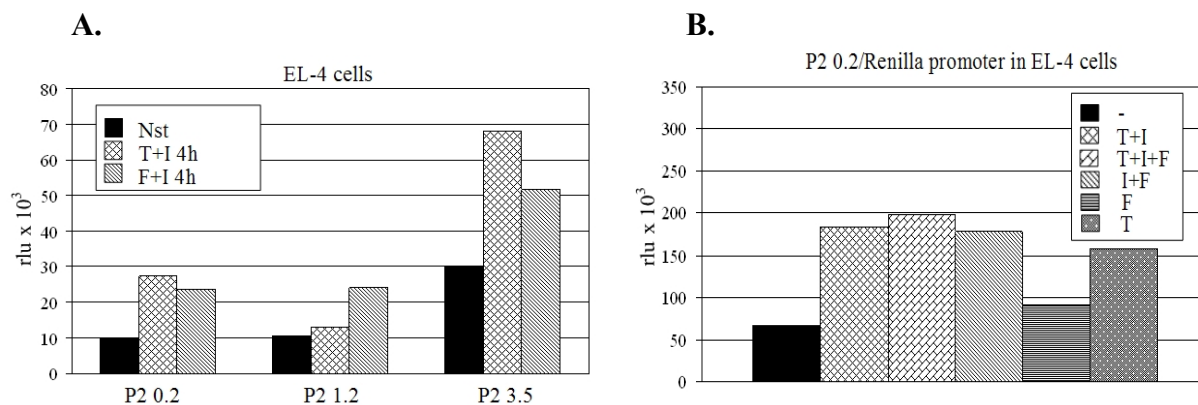


**Figure 2.17 A. Characterization of the P2 core promoter.** Luciferase gene constructs directed by P2 segments of 0.2, 1.2 or 3.5 kbp were transfected into EL-4 cells. After 24 hr, the cells were treated with TPA (T) + ionomycin (I), or forskolin (F) + ionomycin (I).

**B. Renilla gene construct directed by P2 "core"** of 0.2kbp was transfected into EL-4 cells. After 24 hr, the cells were treated with T+I, F+I, triple T+I+F or F and T alone.

cellular extracts pGL3b-0.2kb and pGL3b-1.2kb constructs (Fig. 2.17A). That can be explained by presence of and normalized for transfection efficiency. However, we didn't find any drastical changes in P2promoter behaviour. This indicates that the proximal segment of 0.2 kb harbors the most important promoter elements and, therefore, was designated as P2 'core' promoter. P2 activity was induced by F+I or T+ I agents (Fig. 2.17A). Our suggestion was

confirmed by transfection of pRL-null-0.2kb in EL-4 cells when cells were stimulated by combination of different agents (Fig. 2.17B).

### 2.7.1 NFATs don't bind to P2 promoter

The activity of P2 is not regulated by NFAT factors. The inability of P2 oligonucleotides to compete for the generation of NFAT complexes (Fig. 2.18) and missing NFAT binding motifs indicate that NFAT factors do not bind to P2 directly.

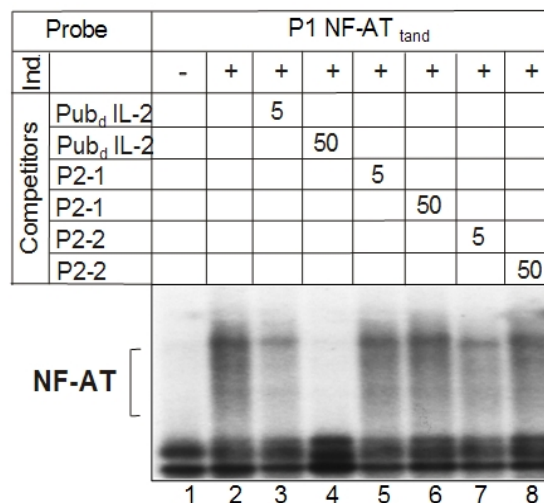


**Figure 2.18 NFATs do not bind to P2.** Nuclear proteins from noninduced EL-4 cells (lane 1) or EL-4 cells treated by T+I for 1 hr (+, lanes 2–8) were incubated with an NFAT<sub>tand</sub> probe and 5 or 50 ng of *IL-2* NFAT site or oligos spanning the nucleotides from position -107 to -142 (P2-1) or -72 to -107 from P2 (P2-2).

## 2.8 Inducible alternative polyadenylation events contribute to the generation of NFATc/ $\alpha$ A

The structure of NFATc cDNAs suggested a contribution of alternative polyadenylation events in the inducible generation of NFATc/ $\alpha$ A. To address this question, we analyzed the 3' half of the NFATc gene. As presented in Fig. 2.2A, the NFATc/B and C specific gene segments are organized in two exons encoding isoform specific peptides and 16 aa in common exon 11. In addition, the exon 11 contains the 3' untranslated mRNA sequences of 1777 bp of NFATc/B and C, respectively. At the splice point, a termination codon is generated such that the following 48 bp become part of the 3' untranslated mRNA tail of 1777 nucleotides. In NFATc/ $\alpha$  $\beta$ A, the last 19 aa (which are absent in NF-ATc/B and C) are encoded by the last exon 9, which also contains 133 bp DNA encoding the foregoing 44 aa and a 3' untranslated mRNA segment of 1952 bp (Fig. 2.3A and 2.3B). This 3' segment harbors the proximal AATAAA poly A addition motif and second, tandemly arranged pA tand. site. In order to demonstrate that the pA1 and pA2 fragments contain functionally active polyadenylation motifs, we introduced



these fragments downstream of the translational stop codon of a luciferase gene in the construct pPKLT55 that was used to characterize the proximal poly A site of the  $\mu$  heavy chain gene

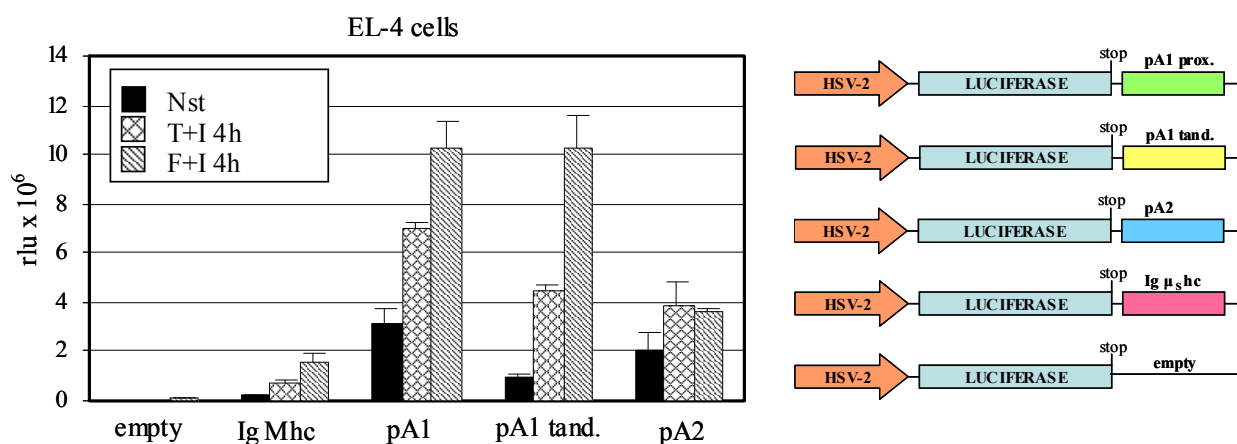


**Figure 2.19** The pA1prox, pA1tand and pA2 sites from NFATc1 can act as poly A addition motifs when cloned behind a luciferase gene. The pA1prox, pA1tand and pA2 fragments (spanning 417, 240 and 325 bp, respectively) were cloned behind the translational stop codon of the luciferase gene by replacing the proximal poly A site of the  $\mu$  heavy chain gene ( $\mu$ s hc) for the generation of secreted IgM in the vector pPKLT55 ( $\mu$ pA2) [90]. These vectors and a vector containing a HSV-2/luciferase gene lacking a poly A site were transfected into EL-4 cells. Untreated cells or cells stimulated by T+I and I+F for 4 hr were harvested for luciferase assays. The data of three independent transfection experiments are shown.

for the synthesis of secreted IgM [24]. Whereas transfection of a pPKLT55 construct lacking a poly A site into EL-4 cells gave rise to a very low luciferase activity, transfections of a pPKLT55 construct containing the proximal  $\mu$ s poly A site resulted in a 10-fold increase of luciferase activity upon F+I treatment. A strong increase of activity was also found when constructs carrying the pA1prox or pA1tand NFATc1 fragments were transfected. In resting cells the strongest activity demonstrated pA1prox site whereas pA1tand and pA2 showed three and two fold reduced activity. Interestingly, in EL-4 cells treated with F+I or T+I for 4 hr, pA2 was approximately 2 fold increased comparing to uninduced cells. That indicates the relative constitutive activity of pA2 site. In contrast, pA1prox and pA1tand demonstrated 3 and 10-fold increased luciferase activity upon F+I treatment (Fig. 2.19). We can conclude that pA1tand site is rather weak in resting cells but highly inducible upon inductive signals. These results indicate the efficient use of pA1 sites for the generation of NFATc1/ $\alpha$ A RNA upon T cell stimulation. Optimal induction conditions lead to the predominant synthesis of NFATc1/ $\alpha$ A by the use of the proximal polyA site pA1.

## 2.9 Quantification of RNA expression level of NFATc1 gene isoforms in Th cells

One step Real-Time PCR was performed for the accurate quantification of RNAs corresponding to NFATc1  $\alpha$ /A, B, C isoforms, directed by P1 promoter; NFATc1  $\beta$ /A, B, C isoforms, directed by P2 promoter and isoforms  $\alpha+\beta$ /A, B, C. RNAs of NFATc1  $\alpha$ /A, B, C were generated by forward primer from exon 1 and sharing sequences of exons 1/3 as a reverse primer. Similarly to P1, RNAs generated by P2 promoter were observed when forward primer sequence was from exon 2 and reverse primer from exons 2/3 gap.  $\alpha+\beta$  isoforms RNA (C terminus) were generated by reverse primers from exon 11 and isoform specific forward primers from exon 10 for long isoforms B and C and exon 9 TYLPAN forward primer and pA1 UTR region for isoforms A (Fig. 2.20).

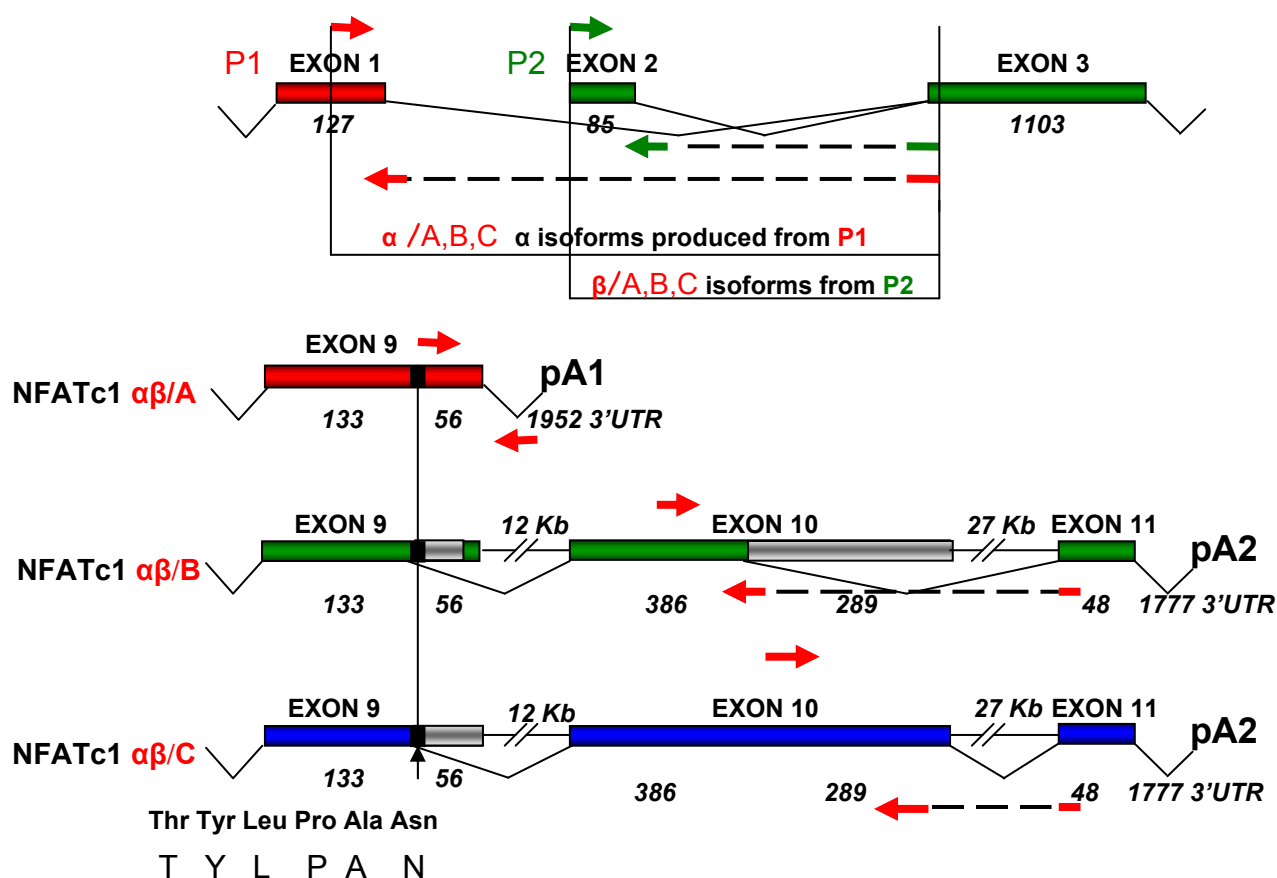


**Figure 2.20 Organization of Murine NFATc1 Isoforms and of the 3' Half of Murine Chromosomal NFATc1 Gene.** The 3' untranslated mRNA segments of 1952 bp (in NFATc1 $\alpha\beta$ /A) and 1777 bp (NFATc1 $\alpha\beta$ /C and  $\alpha\beta$ /B) are indicated. The 5' untranslated mRNA segments are shown as first three exons; promoters indicated by P1 and P2. Arrows indicate primers used in Real Time PCR. The alternative splicing events for the generation of isoforms  $\alpha\beta$ /A, B and C as well as the position of pA1 and pA2 polyadenylation sites are indicated. TYLPAN position marked by vertical black arrow in exon 9. Gray boxes indicate UTR regions in different isoforms during alternate splicing.

To confirm our previous results (transfection assays, RNase protection assays and protein assays) we first analyzed EL-4 cells, induced by various stimuli. This experiment clearly shows that RNAs generated by P2 promoter are weakly expressed at basal level. That fact well fits to

our results on long  $\alpha+\beta/B$  and  $\alpha+\beta/C$  which are constitutive and non-inducible. In contrast to P2 transcripts, exons 1/3 RNAs and short isoform  $\alpha/A$  ( $\alpha+\beta/B$  and  $\alpha+\beta/C$  are non-inducible) are highly inducible in 4 h after TPA + I is added and suppressed by CsA. In non-induced cells all RNA targets are expressed at equal, rather low level predominantly using P2 promoter (Fig. 2.21). These results provoked us to check the RNA expression level in naïve and Th cells to understand the natural situation in cells.

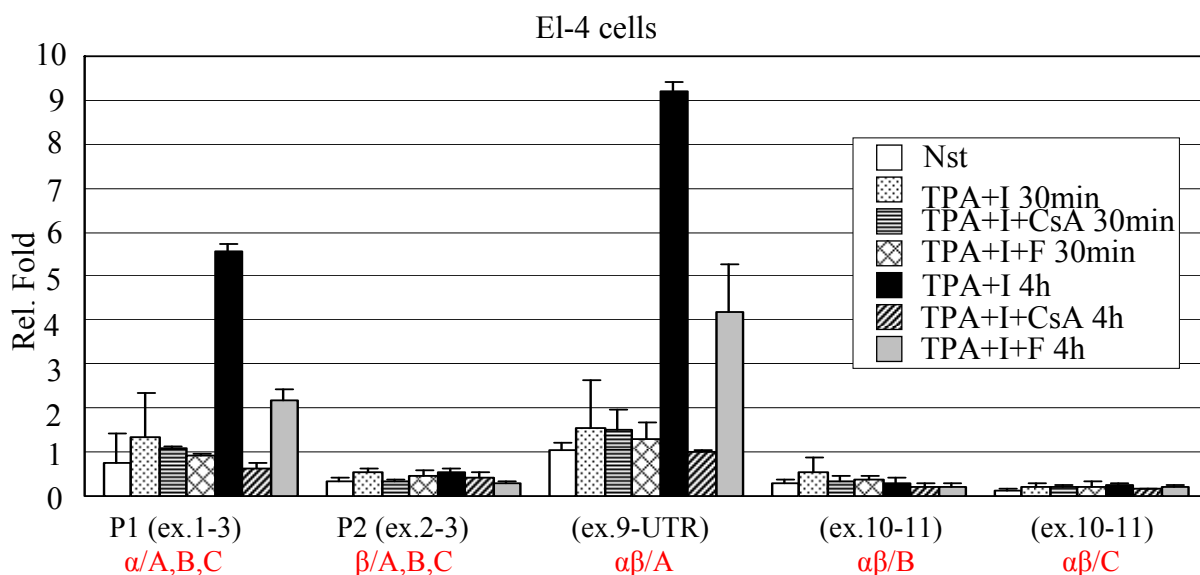


**Figure 2.21 RNA expression level in EL-4 cells.** RNA from EL-4 cells was extracted and used in real-time PCR analysis. Cells were non-induced, TPA+I 30 min and 4h alone or on combination of CsA agent and TPA+I+F 30min or 4h. RNAs directed by different pairs of primers corresponding to  $\alpha/A,B,C$  isoforms (P1),  $\beta/A,B,C$  isoforms (P2) and  $\alpha\beta A/B/C$  isoforms were detected by fluorescent dye SYBR Green I readout using ABI PRISM 7000 Sequence Detection System. Data were analyzed initially using LinRegPCR software. ‘Window-of-linearity’ method, based on calculation of the fluorescence measured per cycle of each sample was used for the relative quantification of mRNA transcripts.

Naïve T helper (Thp) cells exist in peripheral lymphoid organs as immunocompetent precursors which represent a set of relatively recent thymic emigrants that have not yet encountered antigen. When stimulated by receptor engagement in the context of a costimulatory signal, naïve Th cells produce IL-2 but little or no IL-4 or IFN- $\gamma$  [109]. Upon priming, Thp lymphocytes can develop into at least two distinct subsets with different cytokine production profiles and functional capabilities in immune regulation, namely Th1 and Th2 cells. Fig. 2.22 demonstrates the predominant usage of P2 promoter and generation of  $\beta$  long (B and C) isoforms whereas P1 promoter is 3 times weaker than P2. Seems P1 promoter produces  $\beta/A$  constitutive isoform in comparable level to  $\beta/B$  and  $\beta/C$  transcripts. In contrast  $\alpha/A$  is inducible. Generally, Th1 cells produce IFN- $\gamma$  and lymphotoxin, and retain the capacity to produce IL-2, whereas Th2 cells produce IL-4, IL-5, and IL-13 and do not retain the capacity to produce IL-2. Mature T cells secreting both IFN- $\gamma$  and IL-4 are known as Th0 cells.

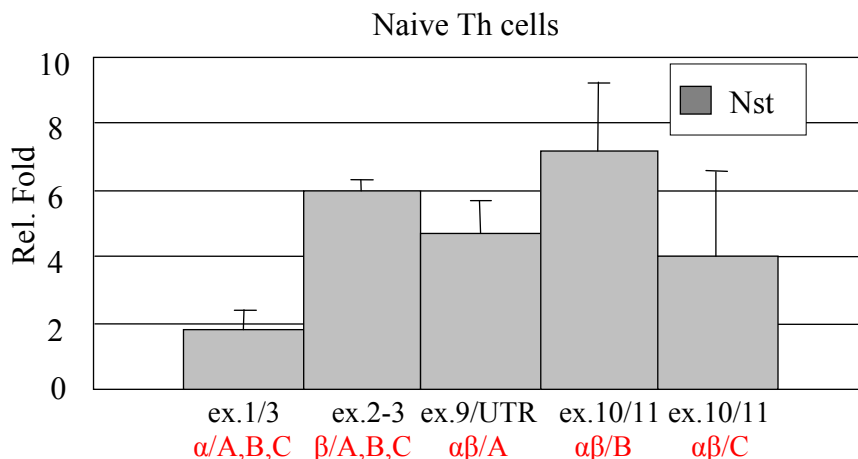


**Figure 2.22 RNA expression level in naïve Th cells.** RNA from naive cells was extracted and used in real-time PCR analysis. Cells were non-induced RNAs directed by different pairs of primers corresponding to  $\alpha/A,B,C$  isoforms (P1),  $\beta/A,B,C$  isoforms (P2) and  $\alpha\beta A/B/C$  isoforms were detected by fluorescent dye SYBR Green I readout using ABI PRISM 7000 Sequence Detection System. Data were analyzed initially using LinRegPCR software. ‘Window-of-linearity’ method, based on calculation of the fluorescence measured per cycle of each sample was used for the relative quantification of mRNA transcripts.

These Th0 cells are lymphocytes that do not polarize during maturation and thus retain the attributes of both Th1 and Th2 cells [110]. Non induced Th0 cells demonstrated 2-fold higher activity of P2 directed  $\beta$ -transcripts and elevated expression of shortest isoform, while C and B isoforms remained at the same low level. Upon activation in 30 min TPA+I we observed approximately 2-fold induction of P1 and P2 directed transcripts and slight elevation in all three isoforms (Fig. 2.23). When cells were incubated during 4 hours TPA+I,  $\alpha$  transcripts demonst-

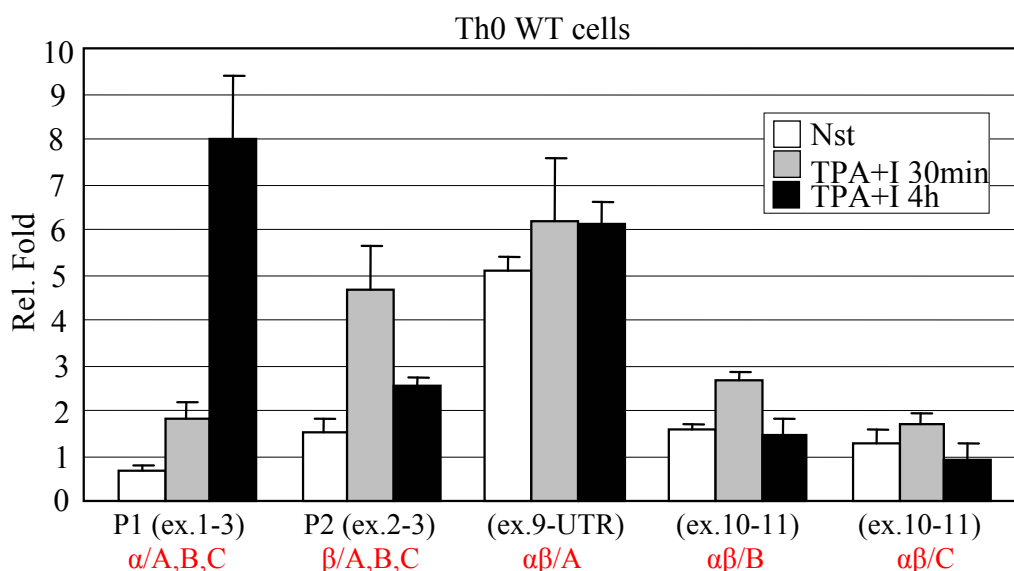
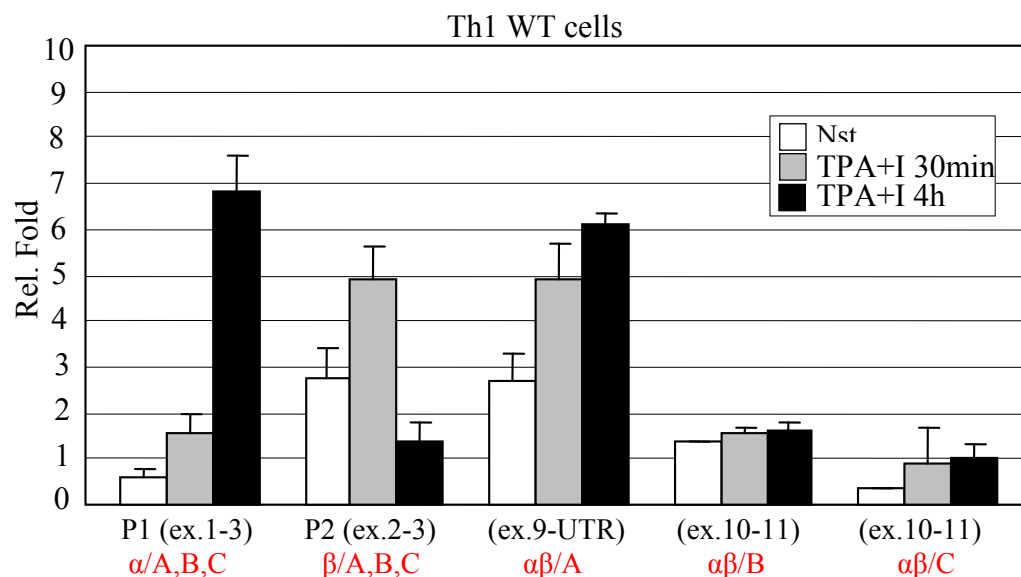


**Figure 2.23 RNA expression level in Th0 cells.** RNA from Th0 cells was extracted and used in real-time PCR analysis. Cells were non-induced (Nst) or treated by TPA+I 30 min or 4h. RNAs directed by different pairs of primers corresponding to  $\alpha/A,B,C$  isoforms (P1),  $\beta/A,B,C$  isoforms (P2) and  $\alpha\beta A/B/C$  isoforms were detected by fluorescent dye SYBR Green I readout using ABI PRISM 7000 Sequence Detection System.

-rated 13-fold induction with simultaneous 2-fold suppression of  $\beta$  isoforms. Isoform transcripts were expressed on the same level. The most probable explanation is that N terminus of NCATc1/ABC is different for  $\alpha$  and  $\beta$  versions, so exon 1/3 pair primers include all  $\alpha$  isoforms (A,B and C) and exon 2/3 pair primers result in  $\beta$ , while RNA C terminus is the same

A.



B.

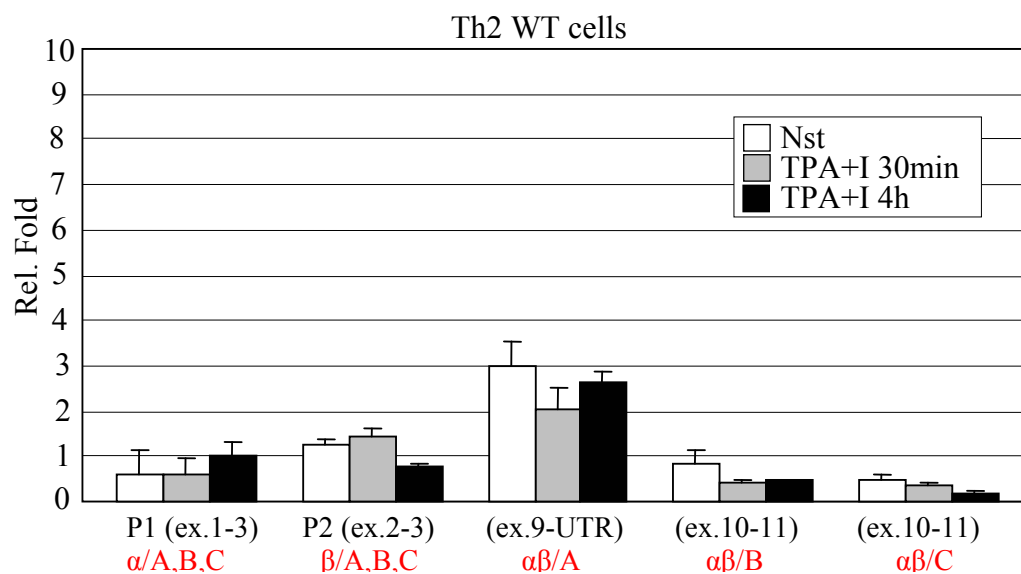


**Figure 2.24 RNA expression level in (A.) Th1 and (B.) Th2 cells.** RNA from the cells was extracted and used in real-time PCR analysis. Cells were non-induced (Nst) or treated by TPA+I 30 min or 4h. RNAs directed by different pairs of primers corresponding to  $\alpha/A,B,C$  isoforms (P1),  $\beta/A,B,C$  isoforms (P2) and  $\alpha\beta A/B/C$  isoforms were detected by fluorescent dye SYBR Green I readout using ABI PRISM 7000 Sequence Detection System.

for all isoforms, i.e  $\alpha+\beta$ . Probably is not correct to compare results between RNA expression level of all three A,B,C  $\alpha$  types and single A isoform both  $\alpha$  and  $\beta$  types. More accurate interpretation would be analysis of  $\alpha/A, B, C$  and  $\beta/A, B, C$  from the one hand and  $\alpha\beta/A, \alpha\beta/B, \alpha\beta/C$  from the other. The same expression pattern was observed in Th1 cells (Fig. 2.24A).

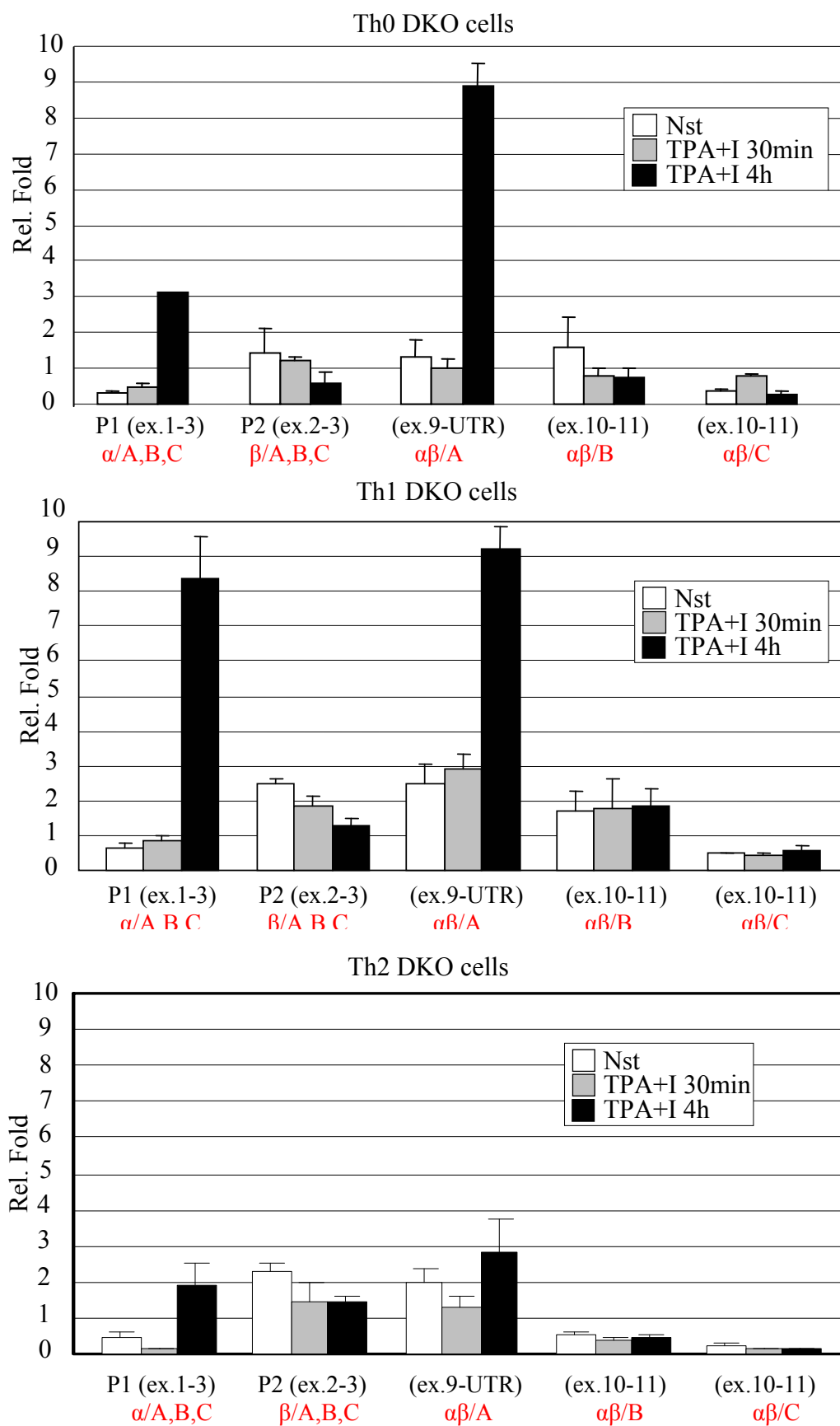


**Figure 2.25 RNA expression level in NFATc2+c3 deficient Th0, Th1 and Th2 cells.** RNA from DKO cells was extracted and used in real-time PCR analysis. Cells were non-induced (Nst) or treated by TPA+I 30 min or 4h. RNAs directed by different pairs of primers corresponding to  $\alpha/A,B,C$  isoforms (P1),  $\beta/A,B,C$  isoforms (P2) and  $\alpha\beta A/B/C$  isoforms were detected by fluorescent dye SYBR Green I readout using ABI PRISM 7000 Sequence Detection System.

Interestingly, when Th2 cells were tested in similar experiment we found completely different situation. All transcripts demonstrated non-inducible expression level similar to naïve cells where P2 promoter usage was predominant and no positive auto regulation loop was observed. However, the expression level of A isoform was 3,5 fold elevated in non-induced nor activated cells. Obviously, the major part of A isoform is a  $\beta$  type directed by P2 promoter, while P1 promoter is rather weak (Fig. 2.24B).

To ensure that NFATc1  $\alpha/A$  is autoregulated without the impact of NFATc2 or NFATc3 we have performed a similar set of experiments using primary Th cells from NFATc2+c3 deficient mice. The experiment reflected on Fig. 2.25 doesn't bring any solid support to the idea that other NFATs are potential players in autoregulation of shortest NFATc1  $\alpha/A$  isoform.

### 3. DISCUSSION

NFAT (nuclear factor of activated T cells) transcription factors were originally described as nuclear proteins that bind to and control the activity of the interleukin 2 (IL-2) promoter and further lymphokine promoters/enhancers in T lymphocytes. However, NFAT factors are also expressed in other cell types and regulate the activity of numerous genes that control the generation of cardiac septa and valves in embryonic heart, the formation of blood vessels, the outgrowth of neuronal axons and the differentiation of osteoclasts during bone formation [10, 24]. Among the five members of the NFAT factor family, the activity of four NFATc proteins (NFATc1, c2, c3 and c4) is controlled by the  $\text{Ca}^{2+}$ /calmodulin-dependent phosphatase calcineurin (CN) that, by dephosphorylating numerous sites within the regulatory region of NFAT, stimulates cytosolic/nuclear translocation and subsequent DNA binding of NFAT factors [10, 24]. CN is a direct target of two immunosuppressants, cyclosporin A (CsA) and FK506, which, when complexed with immunophilins, can bind to CN and inhibit its enzymatic activity. Without active CN, the activity of NFAT factors is suppressed, T cell activation is blocked and rejection of transplanted organs can be prevented [10, 24]. In activated T cells, in which NFATc1 and c2 are predominantly expressed, the AP-1 proteins Fos and Jun are the most common partners of these NFATc proteins [96]. Within lymphokine promoters and other promoters activated upon T cell stimulation, multiple composite sites of the consensus structure 5'-GGAAAaxxxxTGAXTCA-3' have been identified [97], to which NFAT and AP-1 proteins bind as heteromeric complexes with high affinity. Other bZIP factors that have been described to cooperate with NFAT factors through composite NFAT sites are c-Maf, ICER and p21SNFT. In my work I focus on NFATc1 gene regulation during Th cells differentiation. We have identified mechanism of autoregulation of NFATc1 $\alpha$ /A isoform in Th1 cells (Fig. 3.1) and propose a new model of NFATc1 gene regulation in lymphoid cells (Fig. 3.2). Positive autoregulation has been described for several transcription factors, such as for Myo-D, Pit-1 and GATA-1 in the commitment of non-lymphoid cells and for GATA-3 in the commitment of naive  $\text{CD4}^+$  T cells to Th2 effector cells [98-101]. Recently, a positive autoregulatory loop has also been postulated for NFATc4 in non-lymphoid cells in Down's syndrome [102], further illustrating how important medical consequences might arise from subtle changes in autoregulatory networks. The inducible synthesis of NFATc1/ $\alpha$ A was shown to be essential for the generation of osteoclasts. The receptor activator of nuclear factor kB ligand (RANKL) has been identified as an inducer of the synthesis of NFATc1/ $\alpha$ A but not of NFATc2 or of any other NFATc1 protein, illustrating the NFAT-mediated autoregulation of NFATc1/ $\alpha$ A induction in osteoclasts [113]. Positive autoregulation ensures the formation and maintenance of high concentrations of important



‘master regulators’ of cell differentiation for maintaining a committed differentiation state. Although the conditions for the induction of NFATc1/ $\alpha$ A and other commitment factors differ in detail, their common strategy to enhance the factor levels by autoregulation suggests that NFATc1/ $\alpha$ A determines the fate of peripheral CD4<sup>+</sup> T-cell subsets in a similar decisive way.

### 3.1 The *nfatc1* gene: control by two promoters, alternative splicing and two poly A sites

The human and murine *nfatc1* genes span ~150 kb of chromosomal DNA (Fig. 2.2). The immediate upstream sequences of *nfatc1* exons 1 and 2 are highly conserved between human and mouse and they contain numerous transcription-factor-binding sites (Fig. 2.3). In addition, transfection assays have shown that both upstream regions confer transcriptional activity when cloned in front of a reporter gene (Fig. 2.8 and 2.17). We have therefore designated these regions as the *nfatc1* P1 and P2 promoters. Both P1 and P2 direct the synthesis of three different RNAs. P1 transcripts start at exon 1 and encode NFATc1 proteins bearing the so-called N-terminal a peptide of 42 amino acids (aa), whereas P2 transcripts start at exon 2, and code for proteins with

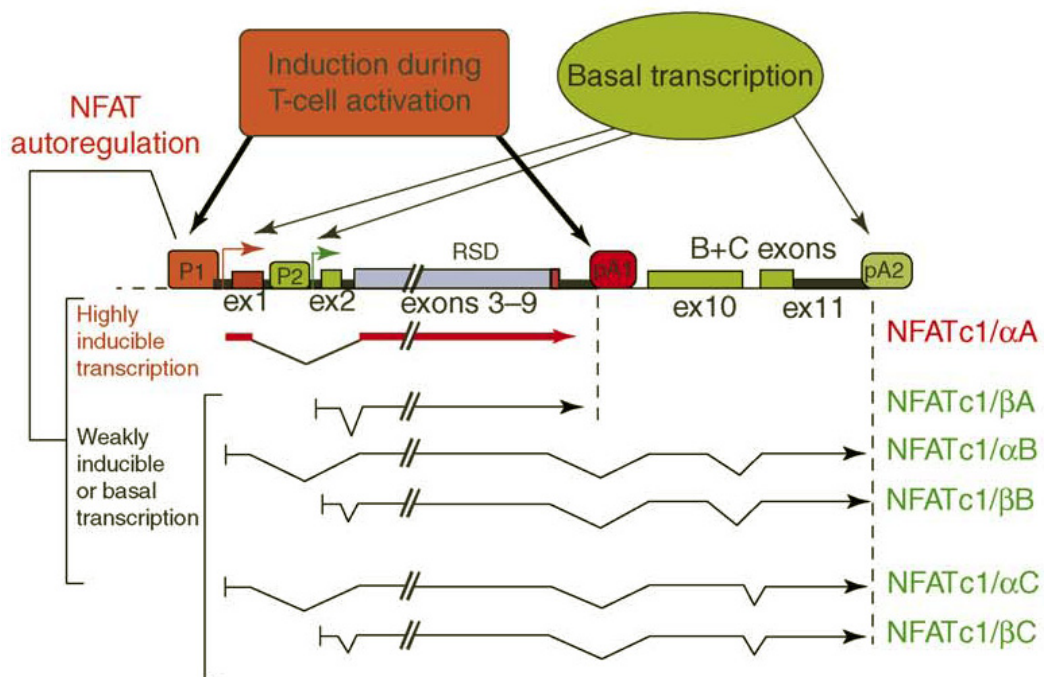


**Figure 3.1. The expression of the murine *nfatc1* gene as six individual NFATc1 RNAs.** A model of *nfatc1* gene expression. In resting (or naive) T cells, the activity of the promoter P2 results in the transcription of exon 2, splicing to exon 3 and in the generation of three  $\beta$  isoforms. T-cell activation leads to a promoter switch, from P2 to P1, and the transcription of exon 1, splicing to exon 3 and the generation of a isoforms. Optimal induction conditions lead to the predominant synthesis of NFATc1/ $\alpha$ A (red) by the use of the proximal polyA site pA1. Unlike the two promoters, this site is not conserved between mouse and human. Although in both species NFATc1 proteins of about the same sizes are synthesized, the human NFATc1/A RNA spans ~3 kb [13], whereas the murine RNA spans 4.5 kb. Moreover, the relatively strong pA1 site in mouse seems to generate more NFATc1/A transcripts in resting T cells than the relatively weak human pA1 site [13]. NFATc1/ $\alpha$ A lacks the C-terminal transactivation domain TAD-B.

the N-terminal b peptide of 29 aa [95]. The C termini of these proteins comprise either a short stretch of 19 aa in the A isoform, or longer stretches of 128 aa in the B isoform or 246 aa in the C isoform [95]. The B and C isoforms arise from alternative splicing and poly A addition at the distal site pA2, whereas the short isoform A results from polyadenylation at the proximal poly A site pA1 (Fig. 2.19 and 2.20). Together with the inducible activity of the promoter P1, polyadenylation at the proximal poly A site pA1 results in the strong induction of the short isoform NFATc1/ $\alpha$ A [14]. In resting T cells, the NFATc1/ $\beta$  RNAs are the most prominent nfatc1 transcripts and their synthesis is reduced upon T-cell activation (Fig. 2.21, 2.22). However, following activation in primary effector T cells or in T-cell lines of human or murine origin, a 15–20-fold induction of NFATc1/ $\alpha$ A RNA was detected, whereas only a 2–5-fold increase was observed for the NFATc1/ $\alpha$ B or NFATc1/ $\alpha$ C RNAs (Fig. 2.21). The inducible P1 promoter needs more than one signal for its optimal induction. One signal is provided by a persistent increase in free cytosolic  $Ca^{2+}$  induced by ionomycin, which stimulates the nuclear translocation and transcriptional activation of all NFATc factors [10]; another signal is provided by phorbol esters, which activate protein kinase C and other protein kinase pathways in T cells. This suggests that both TCR and co-receptor signals contribute to give full P1 nfatc1 induction (Fig. 2.7). However, in transient transfection assays using EL-4 T cells, the induction of the P1 promoter differed markedly from that of the endogenous P1 promoter, suggesting that additional remote regulatory sequence elements contribute to nfatc1 transcription. Instead of ionomycin- and phorbol-ester-mediated signals (mimicking TCR and co-receptor signals), P1 requires ionomycin and cyclic AMP (cAMP) signals for its maximal induction in the transfection model (Fig. 2.8). We also identified two CRE sites (Fig. 2.3) within P1 to which CREB, Fos and ATF-2 factors were detected to bind in Electrophoretic mobility shift assays (EMSAs) (Fig. 2.11A). ATF-2 is a known target of p38 protein kinase, which was shown to support nfatc1 induction in T cells [103]. Other transcription-factor binding sites include those for Sp1, NF- $\kappa$ B, GATA and NFATs (Fig. 2.3). There are two NFAT-binding sites within P1. The distal site around position -675 to which NFATs bind with high affinity is composed of two repeats of the NFAT core binding motif TGGAAA. However, it does not constitute any TPA-responsive (TRE)-like motif of palindromic structure, TGAC/GTCA, for the binding of AP1 factors. Mutations that abolished NFAT binding to the repeat motifs resulted in a strong decrease in P1 induction (Fig. 2.16A). However, a strong P1 induction was detected in effector Th0 and Th1 cells from NFATc2+c3 double-deficient mice, indicating that these NFATs are of minor importance for P1 induction in these cells (Fig. 2.25). Despite the strong NFAT binding to the P1 NFAT repeat, no NFAT dimer formation could be detected using this site as a probe in EMSAs (Fig. 2.15). It is conceivable that, supported by the closely linked NF- $\kappa$ B-like site, NFATs could form larger complexes at P1.

The formation of NFAT dimers has been described for the composite NF- $\kappa$ B/NFAT sites of HIV long terminal repeats (LTRs) [104] and for a pseudo-palindromic NF- $\kappa$ B-like site from the human IL-8 promoter.

### ***3.2 NFATc1: Autoregulation results in the predominant synthesis of NFATc1/ $\alpha$ A***

The regulatory region of NFATc1 overlaps with the strong N-terminal transactivation domain, TAD-A. Most of the transactivation potential was detected within a peptide spanning residues 113 to 205 and additional activity was detected within the N-terminal peptide of residues 1–108. A second transactivation domain, TAD-B, was mapped within the unique 240 aa C terminus of NFATc1/C [105]. Although TAD-B seemed to be markedly weaker in transactivation assays, its activity could be induced several fold by phorbol esters and (other) stress signals, similar to TAD-A. Remarkably, neither stimulation of calcineurin activity by ionomycin nor inhibition by CsA affected induction of TAD-A or TAD-B [105, 13]. A transactivation domain was also mapped within the C-terminal peptide of NFATc2 [25] that shares ~30% homology with that of NFATc1/C. In addition, the TAD-B domains in NFATc1/C and NFATc2 contain two potential  $\Psi$ KxE sumoylation motifs (where  $\Psi$  corresponds to a hydrophobic aa, mainly isoleucine or valine) within highly conserved aa stretches around aa positions 684 and 897 (in NFATc2). For NFATc2, it has been shown that both motifs are sumoylated *in vivo*, and mutating the proximal 684 site to a non-sumoylated motif resulted in a strong decrease in NFATc2 activity and localization in nuclear (SUMO-1/PML?) bodies [106]. Following ectopic expression, NFATc2 and NFATc1/ $\alpha$ C facilitated activation induced cell death (AICD) of primary murine T cells following anti-CD3 antibody stimulation, whereas NFATc1/ $\alpha$ A had no effect. This supports the view that AICD of T cells is controlled by mechanisms involving the C-terminal TAD-B of NFATc proteins [12]. Contrary to NFATc1/ $\beta$ B and NFATc1/ $\beta$ C, the inducible short NFATc1/ $\alpha$ A isoform does not harbor either the conserved hydrophobic decapeptide or sumoylation sites and, therefore, its activity is not controlled by sumoylation. Instead of containing the acidic N-terminal b-peptide of 29 aa, it bears the N-terminal a-peptide of 42 aa that harbors seven Ser/Thr residues for potential protein modifications.

### ***3.3 T lymphocytes: NFATc1 autoregulation is a property of effector T helper cells***

In murine T-cell development, NFATc1 expression can be observed as early as in double-negative DN1 thymocytes (A. Patra et al. unpublished), that is, before the expression of pre-TCR at the late DN3 stage [107]. This shows that (pre-) TCR signals do not control the ‘opening’ of the *nfatc1* locus in early thymocytes (Figure 21). However, TCR (and co-receptor) signals induce

the transcription from the seemingly ‘repressed’ *nfatc1* locus in naive CD4<sup>+</sup> T cells, and persistent Ca<sup>2+</sup> signals are necessary for maintaining full NFATc1 transcription. The initial phase of *nfatc1* transcription in naive CD4<sup>+</sup> T cells is controlled by the promoter P2 which is constitutively active in resting T cells. The activation of resting T cells results in a decrease of P2

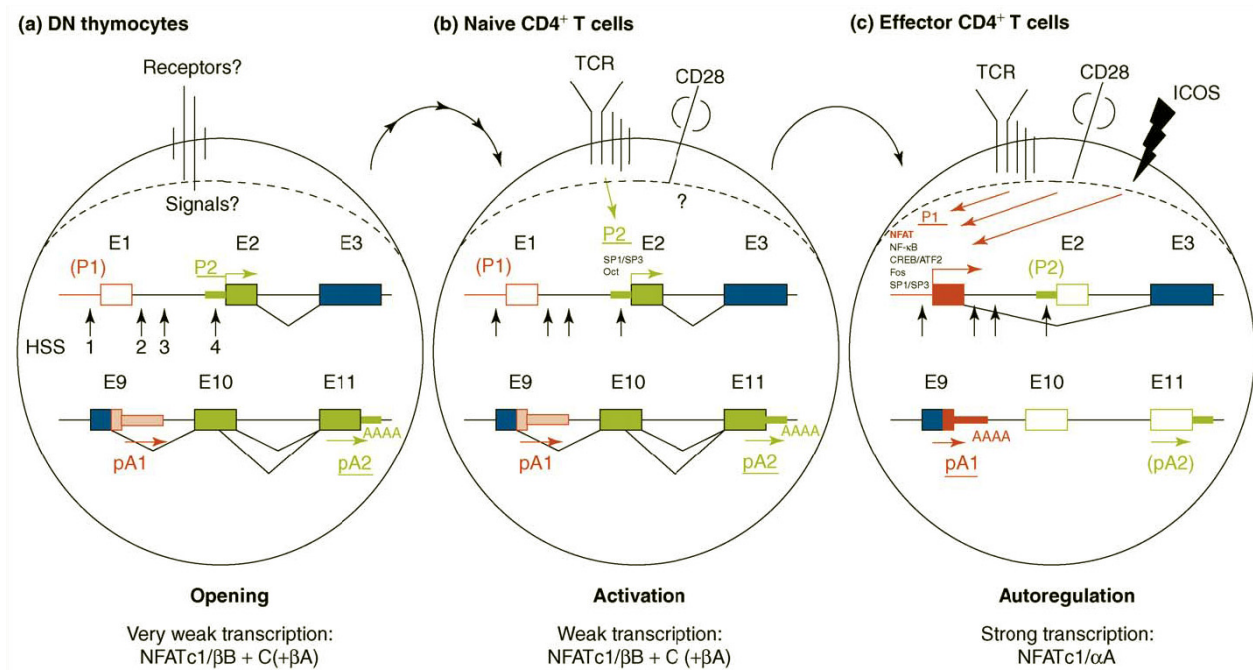


**Figure 3.2 A model of activation of the *nfatc1* gene locus during T-cell development [95].** Portions of the *nfatc1* promoter and polyA site regions are shown. (a) Opening of the locus. NFATc1 expression can be detected in early DN thymocytes, before the expression of pre-TCR in late DN3 thymocytes. We assume that (lymphokine?) signals will lead to the generation of DNase I hypersensitive sites, DNA hypomethylation and histone acetylation at the *nfatc1* promoter region, resulting in the activation of the P2 promoter. This will lead to the generation of NFATc1/β transcripts. It is currently unknown whether at any stage in thymocyte development NFATc1 expression is controlled by positive autoregulation. (b) The activation of the locus in naive CD4<sup>+</sup> T cells. TCR (and co-receptor?) signals stimulate transcription from P2 into NFATc1/β transcripts. This is supported by Sp1/Sp3, Octamer (Oct) and other transcription factors that bind to P2 (and, probably, other regulatory DNA elements) and trigger the synthesis of low NFATc1/β RNA levels. The pA2 site is predominantly used. (c) Transcription of the locus in effector T cells by positive NFATc1 autoregulation. At high concentrations of NFATs and other transcription factors, splicing and polyA addition factors, upon TCR and co-receptor stimulation, transcription initiation switches from the use of promoter P2 to P1, and polyadenylation from the distal pA2 site to the proximal pA1 site. Prominent transcription factors binding to P1 include NFATs (NFATc2, NFATc1), NF-κB, CREB, ATF2 and Fos members. This results in the predominant synthesis of high levels of NFATc1/αA, the short NFATc1 isoform containing an N-terminal peptide (encoded in exon 1) and lacking the C-terminal TAD-B (encoded in exons 10 and 11). Thus, for optimal NFATc1/αA (auto-) induction, the coordinated activities of Ca<sup>2+</sup>/calcineurin, NF-κB- and MAP/p38-kinase signaling pathways are necessary to induce P1 activity, transcription and polyadenylation at pA1. Due to NFATc1/αA induction is unaffected in NFATc2+c3 double-deficient T cells, NFATc1 autoregulates its own synthesis by controlling P1 activity and NFATc1/αA induction.

and the induction of P1 activity (Fig. 3.2) and, under optimal conditions, in the predominant synthesis of NFATc1/αA in effector T cells (Figure 2.21). In addition to the high concentrations of poly A factors required for optimal pA1 function [14], the levels of transcription factors, in particular NFATs, must also increase for P1 induction. Using single-cell assays, it was shown, by the Herzenberg laboratory more than 15 years ago [108], that NFATs must exceed certain

threshold levels for transcriptional activation. Although the inactivation of one NFAT factor, either NFATc1 or NFATc2, in mice didn't affect IL-2 production [83, 80, 11, 79], the inactivation of both factors completely abolished IL-2 production [88]. This illustrates that a threshold level provided by one or both NFAT factors was sufficient for IL-2 promoter/enhancer induction, whereas below a certain threshold (provided by NFATc3, which is expressed at low levels in peripheral T cells) the IL-2 promoter/enhancer remained inactive. The P1 promoter might also be controlled by this binary ('all or nothing') mode of induction. In addition to TCR signals leading to NFAT activation, CD28 (and further co-receptor) mediated signals exert a (co-)stimulatory effect on P1 induction, in particular in Th1 cells. In Foxp3-expressing murine CD4<sup>+</sup>CD25<sup>+</sup> T regulatory cells (Tregs), the NFATc1 RNA levels were decreased ~20-fold compared with levels in conventional CD4<sup>+</sup> T cells [111], which might be owing to a low P1 activity in these ('semi-nergic') cells.

### **3.4 Conclusion**

The induction of CD4<sup>+</sup> effector T cells by TCR and co-receptor signals leads to the synthesis of NFATc1/ $\alpha$ A, a short NFATc1 isoform. In T cells, NFATc1/ $\alpha$ A is the only NFAT protein for which synthesis is controlled by positive autoregulation, resulting in high NFATc1 threshold levels. For the generation of osteoclasts it has been demonstrated that these high NFATc1 levels generated by autoregulation are necessary for cell lineage commitment, and it is likely that NFATc1/ $\alpha$ A autoregulation has a similar crucial role in the differentiation of naive T cells to the various T effector cell populations. In addition, the altered transactivation potential of NFATc1/ $\alpha$ A suggests a specific role for this NFATc1 protein in gene control, such as in Th1 effector cells where NFATc1/ $\alpha$ A is synthesized at high concentrations. The theoretical analysis demonstrates that NFATc1/ $\alpha$ A expression has a switch-like dependence on calcineurin activity because of autoactivation feedback loop [99]. By contrast, the feedforward activators NF- $\kappa$ B, CREB, ATF-2 and Fos exert a graded effect on NFATc1/ $\alpha$  levels. Provided that the calcineurin activity has exceeded a threshold value, these activators will determine the actual level of NFATc1/ $\alpha$  expression. Thus, the expression of the inducible NFATc1/ $\alpha$ A isoform can be regulated both in a switch-like and in a gradual manner by different stimuli.

## 4. SUMMARY

NFAT transcription factors play critical roles in gene transcription during immune responses. Besides regulation of lymphokine promoters in T lymphocytes, NFAT factors are also expressed in other cell types and regulate the activity of numerous genes that control the generation of cardiac septa and valves in embryonic heart, the formation of blood vessels, the outgrowth of neuronal axons and the differentiation of osteoclasts during bone formation [10, 24].

Here we show that the induction of NFATc/ $\alpha$ A in effector T cells is controlled by a strong inducible promoter, P1. It results in splicing of exon 1 to exon 3 transcripts and, in concert with the activity of a poly A site downstream of exon 9, leads to the massive synthesis of NFATc/ $\alpha$ A in effector Th1 cells. A second, weak promoter, P2, lies in front of exon 2 and directs the synthesis of longer NFAT  $\beta$  isoforms. Both P1 and P2 direct the synthesis of three different RNAs:  $\alpha$ A,  $\alpha$ B,  $\alpha$ C and  $\beta$ A,  $\beta$ B,  $\beta$ C correspondingly. The B and C isoforms arise from alternative splicing and poly A addition at the distal site pA2.

P1 but not P2 activity is autoregulated by NFAT factors which bind to two tandemly arranged NFAT sites within P1 and enhance its induction. In resting T cells, the NFATc1/ $\beta$  RNAs are the most prominent nfatc1 transcripts and their synthesis is reduced upon T-cell activation. However, following activation in primary effector T cells or in T-cell lines of human or murine origin, a 15–20-fold induction of NFATc1/ $\alpha$ A RNA was detected, whereas only a 2–5-fold increase was observed for the NFATc1/ $\alpha$ B or NFATc1/ $\alpha$ C RNAs. Optimal induction of P1 promoter require involving of a persistent increase in free cytosolic Ca<sup>2+</sup> induced by ionomycin, which stimulates the nuclear translocation and transcriptional activation of all NFATc factors and phorbol esters, which activate protein kinase C and other protein kinase pathways in T cells. This suggests that both TCR and co-receptor signals contribute to give full P1 nfatc1 induction. Because NFATc1/ $\alpha$ A induction is unaffected in NFATc2+c3 double-deficient T cells, NFATc1 autoregulates its own synthesis by controlling P1 activity and NFATc1/ $\alpha$ A induction.

P1 promoter contains tandemly arranged NFAT core binding motif TGGAAA to which bind monomeric NFATc1 proteins and numerous conservative binding sites of other transcriptional factors like CREB, Fos, ATF-2, Sp1, NF- $\kappa$ B and GATA suggesting complex multi-factor regulation of NFATc1 gene.

We also highlight that initial phase of nfatc1 transcription in naive CD4<sup>+</sup> T cells is controlled by the promoter P2 which is constitutively active in resting T cells. The activation of resting T cells results in a decrease of P2 and the induction of P1 activity and, under optimal conditions, in the predominant synthesis of NFATc1/ $\alpha$ A in effector T cells. In addition to the high concentrations of poly A factors required for optimal pA1 function, the levels of transcription factors, in particular NFATs, must also increase for P1 induction. That could be explained by achievement of certain threshold levels for transcriptional activation.

Finally, the altered transactivation potential of NFATc1/ $\alpha$ A suggests a specific role for this NFATc1 protein in gene control, such as in Th1 effector cells where NFATc1/ $\alpha$ A is synthesized at high concentrations.

## Zusammenfassung

Die Familie der NFAT-Transkriptionsfaktoren (NFATc1-c4) ist im Zuge einer Immunreaktion entscheidend an der transkriptionellen Regulation der Genexpression beteiligt. Wurden NFAT-Faktoren zunächst als T-zell-spezifische Aktivatoren von Zytokinpromotoren beschrieben, so hat sich inzwischen gezeigt, dass sie in einer Vielzahl von Geweben eine wichtige Rolle spielen. Als Beispiele seien die Herzklappenentwicklung, die Bildung von Blutgefäßen, die Ausbildung neuronaler Axone oder die Osteoklastendifferenzierung genannt [10, 24].

In der hier vorliegenden Arbeit zeigen wir, dass die starke Expression der kurzen Isoform NFATc1/ $\alpha$ A in Effektor-T-Lymphozyten durch die induzierbare Aktivität des Promoters P1 kontrolliert wird. Die P1 Aktivierung führt zum Splicing des Exon 1 zu 3 ( $\alpha$ -Isoformen) und endet meist durch Benutzung der Polyadenylierungsstelle pA1 hinter Exon 9 (A-Isoformen). Der zweite, schwächerer Promoter P2 befindet sich vor dem zweiten Exon und ist für die konstitutive Synthese der  $\beta$ -Isoformen verantwortlich. Der Transkriptionstart am zweiten Exon geht meist mit der Benutzung einer zweiten, hinter dem 11. Exon gelegenen Polyadenylierungsstelle pA2 einher, die durch alternatives Splicing zur Synthese der Isoformen B und C führt. Insgesamt können so vom *nfatc1*-Lokus sechs verschiedene Isoformen ( $\alpha$ A,  $\alpha$ B,  $\alpha$ C,  $\beta$ A,  $\beta$ B und  $\beta$ C) generiert werden.

Die induzierbare Aktivität des P1-Promoters ist, im Gegensatz zum eher konstitutiv aktiven P2-Promoter, NFAT-abhängig und somit eine Form der Autoregulation. In ruhenden T-Lymphozyten sind einzig die Transkripte der NFATc1/ $\beta$ -Isoformen nachweisbar. Nach einer T-Zell-Aktivierung nimmt ihre Häufigkeit dann ab, während nun die  $\alpha$ -Isoformen dominant werden. In dieser Arbeit wird gezeigt, dass es nach Induktion primärer Effektor-T-Helfer-Zellen oder in T-Zell-Linien zu einer 15-20-fachen Akkumulation der NFATc1/ $\alpha$ A mRNA bzw. einer 2-5-fachen Zunahme der NFATc1/ $\alpha$ B und C mRNAs kommt. Zur maximalen Induktion des P1-Promoters bedarf es zum einen eines anhaltenden Anstiegs der intrazellulären Kalziumkonzentration, die zur Aktivierung der Phosphatase Calcineurin und damit zur Kernlokalisierung der NFAT-Faktoren führt. Zum anderen ist die Aktivierung der Proteinkinase C-Enzyme und der MAP-Kinasen notwendig, wie sie durch Phorbolster in der Zelle vermittelt wird. Dies lässt darauf schließen, dass für eine optimale Aktivierung des P1-Promoters sowohl Signale des T-Zell-Rezeptors als auch Signale von Korezeptoren - wie von CD28 - notwendig sind. Da die Induktion von NFATc1/ $\alpha$ A in NFATc2/NFATc3 doppeldefizienten Mäusen normal erfolgt, kann man schlussfolgern, dass NFATc1 in Form einer Autoregulation die Aktivität des P1-Promoters und damit die Synthese der  $\alpha$ -Isoformen kontrolliert.

Die NFAT-vermittelte Aktivierung des P1-Promoters erfolgt über zwei tandemartig angeordnete NFAT-Bindungsstellen der Nukleotidsequenz TGGAAA, an die jeweils ein NFAT-Protein binden kann. Daneben enthält der Promoter konservierte Bindemotive für CREB-, AP-1, Sp-, NF- $\kappa$ B- und GATA-Faktoren, die wahrscheinlich an der komplexen Kontrolle dieses induzierbaren NFATc1-Promoters beteiligt sind.

Zusammengefasst ergibt sich aus diesen Daten das folgende Modell. Die Transkription im *nfatc1*-Genlokus erfolgt in naiven und in ruhenden Effektor-T-Zellen konstitutiv und gesteuert durch den P2-Promotor. In Folge einer Aktivierung der Zelle verringert sich die Aktivität des P2-Promoters, während gleichzeitig der P1-Promotor induziert wird, der zusammen mit einer verstärkten Nutzung der pA1-Polyadenylierungssequenz für die massive Zunahme der NFATc1/ $\alpha$ A-Isoform verantwortlich ist. Dies deutet auf eine besondere Bedeutung dieser kurzen Isoform in der Effektorphase der T-Zell-Aktivierung hin, insbesondere in Th1-Zellen, die NFATc1/ $\alpha$ A in hohen Konzentrationen produzieren.

## **5. MATERIALS AND METHODS**

The methods described in this section are all based upon today's standard molecular and cellular biology techniques.

### **5.1. Materials**

#### **5.1.1. Instruments**

##### **Hardware**

Autoclave  
Bacterial shaker  
Balance machine  
Cold centrifuge  
DNA sequencer 373A  
Gel documentation system  
Gel camera  
Gel dryer  
Heating blocks  
Hybridization Oven  
Ice machines  
Intensifying screen  
Laminar hoods  
Light microscope  
Liquid nitrogen tank  
Luminometer  
Microliter pipettes  
Microcentrifuge  
Multichannel pipette  
Multi dispenser pipette  
PCR machine  
pH meter  
Phosphoimager  
Quartz cuvettes  
Refrigerators (-20°C; -70°C)  
Rotors (JA-10, JA-14)  
Scintillation counter

##### **Manufacturer**

Stiefenhofer  
New Brunswick Scientific  
Sartorius  
Heraeus  
Applied Biosystems  
Herolab  
Stratagene, Hoefer  
H.Hölzel  
Eppendorf  
Bachofer  
Genheimer  
DuPont  
Heraeus, Gelaire  
Olympus, Leica  
Tec-lab  
Berthold  
Eppendorf, Brand  
Eppendorf  
Eppendorf  
Eppendorf  
Perkin Elmer, MWG  
Ingold  
Fujix BAS-2000 III, Fuji  
Hellma  
Privileg, Bosch, Heraeus  
Beckman  
Canberra Packard



Shaking incubator	Eppendorf
Power supplier	Amersham Pharmacia
SDS-PAGE apparatus	BioRad
Spectrophotometer	Amersham Pharmacia
Ultracentrifuge	Beckman
UV lamp (UVT-20M)	Herolab
Vortexer	Eppendorf
Waterbath	Eppendorf
Water filtration unit (MilliQ Plus)	Millipore
Western blot apparatus	Hofer
Real-Time RCR machine	ABI Prism 7000

### ***5.1.2. Chemical reagents and general materials***

<b>Reagent</b>	<b>Purchased from</b>
Cell strainer (70 $\mu$ M)	Falcon
2 ml cryotubes	Greiner bio-one
Disposable needles, Cuvettes & Syringes	Greiner bio-one
Glasswares	Schott
Nitrocellulose Membrane	Schleicher & Schuell
Polypropylene tubes	Greiner bio-one, Nunc
Parafilm	Greiner bio-one
Pipette tips	Eppendorf
Pipettes	Sarstedt
Röntgen film (13x18 cm, BioMax)	Kodak
Sterile filters (0.2 $\mu$ M/ 0.45 $\mu$ M)	Schleicher & Schuell
Tissue culture plates	Greiner bio-one, Falcon
Tissue culture flask (50, 250, 500 ml))	Greiner bio-one
Tissue culture dish (60 mm, 90 mm)	Falcon, Greiner bio-one
Tubes (1.5 & 2 ml)	Sarstedt, Eppendorf
Whatmann paper	Schleicher & Schuell

**5.1.3. Chemical reagents**

Acrylamid solution	Carl Roth
Agar-Agar	Carl Roth
Agarose	Sigma-Aldrich
Ampicillin	Hoechst
APS	Merck Eurolab
β-mercaptoethanol	Carl Roth
BioRad protein assay (5x Bradford reagent)	BioRad
Bromophenol blue	Merck Eurolab
Calcium chloride [CaCl <sub>2</sub> ]	Carl Roth
CD62L MACS beads	Miltenyl Biotech
Chloroform [CHCl <sub>3</sub> ]	Carl Roth
Citric acid [C <sub>6</sub> H <sub>8</sub> O <sub>7</sub> ·H <sub>2</sub> O]	Carl Roth
Column for murine CD4 <sup>+</sup> cell	CEDARLANE <sup>®</sup>
Coomassie brilliant blue R-250	Roche Applied Science
Cyclosporin A [CsA]	Novartis Pharma
DEPC	Carl Roth
Disodiumhydrogenphosphate [Na <sub>2</sub> HPO <sub>4</sub> ·7H <sub>2</sub> O]	Merck Eurolab
D-Luciferin [C <sub>11</sub> H <sub>8</sub> N <sub>2</sub> O <sub>3</sub> S <sub>2</sub> ]	AppliChem
DMSO	Carl Roth
dNTPs	MBI-Fermentas
DTT	Carl Roth
ECL Chemiluminescence Kit	Amersham, Roche
EDTA [Na <sub>2</sub> EDTA·2H <sub>2</sub> O]	Carl Roth
EGTA	Sigma-Aldrich
Ethanol [C <sub>2</sub> H <sub>5</sub> OH]	Carl Roth
Ethidium Bromide [EtBr]	Sigma-Aldrich
Formaldehyde [CH <sub>2</sub> O]	Carl Roth
Forskolin	Calbiochem,
Gel extraction kit (Jetsorb)	Genomed
Glutathione sepharose	Sigma-Aldrich
Glycerin (87%)	Carl Roth
Hepes	Carl Roth, Gibco BRL
Hydrochloric Acid [HCl]	Merck Eurolab
Ionomycin	Sigma-Aldrich
Isoamylalcohol	Carl Roth
Isopropanol [2-Propanol, C <sub>3</sub> H <sub>8</sub> O]	Carl Roth
Leupeptin hydrochloride	Roche Applied Science
Lithium chloride [LiCl]	Sigma-Aldrich
Milk powder	Saliter
Magnesium acetate [Mg(C <sub>2</sub> H <sub>3</sub> O <sub>2</sub> ) <sub>2</sub> ·4H <sub>2</sub> O]	Sigma-Aldrich
Magnesium chloride [MgCl <sub>2</sub> ]	Carl Roth
Magnesium sulfate [MgSO <sub>4</sub> ·7H <sub>2</sub> O]	Carl Roth
Manganese chloride [MnCl <sub>2</sub> ]	Fluka
Methanol [CH <sub>4</sub> O]	Carl Roth
MOPS	Carl Roth
PCR purification kit	Qiagen
PEG 4000	NEB
Phenol [C <sub>6</sub> H <sub>6</sub> O, TE equilibrated]	Carl Roth

PIPES	Serva
Plasmid-DNA Isolation kit (Maxi)	Macherey-Nagel, Qiagen
Plasmid DNA Isolation kit (Mini)	Genomed
PMSF	Serva
Poly dI/dC	Boehringer Ingelheim
Ponceau Red	Sigma Aldrich
Potassium acetate [C <sub>2</sub> H <sub>3</sub> KO <sub>2</sub> ]	Carl Roth
Potassium chloride [KCl]	Sigma-Aldrich
Potassium dihydrogen phosphate [KH <sub>2</sub> PO <sub>4</sub> ]	Sigma-Aldrich
Potassium hydrogen phosphate [KHPO <sub>4</sub> ]	Sigma-Aldrich
Potassium hydroxide [KOH]	Carl Roth
Propidiumiodide (PI 1 mg/ ml ddH <sub>2</sub> O)	Sigma Aldrich
Protease inhibitor tablet (complete mini)	Roche Applied Science
Protein-A/G sepharose	Santa Cruz
Radioactive nucleotides	
[ $\gamma$ <sup>32</sup> P-ATP, $\alpha$ <sup>32</sup> P-dCTP, $\alpha$ <sup>32</sup> P-UTP]	Amersham Pharmacia
RNase Protection Assay Kit (RiboQuant)	BD Pharmingen
RPMI 1640	Gibco BRL
Rubidium chloride [RbCl]	Carl Roth
Sodium acetate [CH <sub>3</sub> COONa·3H <sub>2</sub> O]	Merck Eurolab
Sodium carbonate [Na <sub>2</sub> CO <sub>3</sub> ]	Carl Roth
Sodium chloride [NaCl]	Carl Roth
Sodium fluoride [NaF]	Sigma-Aldrich
Sodium hydrogen phosphate [NaH <sub>2</sub> PO <sub>4</sub> ·H <sub>2</sub> O]	Merck Eurolab
Sodium hydroxide [NaOH]	Carl Roth
Sodium orthovanadate [Na <sub>3</sub> VO <sub>4</sub> ]	Fluka
Sodium pyruvate [C <sub>3</sub> O <sub>3</sub> H <sub>3</sub> Na]	Gibco BRL (100 mM)
Sodium citrate [C <sub>6</sub> H <sub>5</sub> Na <sub>3</sub> O <sub>7</sub> ·2H <sub>2</sub> O]	Carl Roth
SDS	Carl Roth
Sephadex G50	Amersham Pharmacia
Tamoxifan	Sigma
TEMED	Carl Roth
TPA	Sigma Aldrich
Transfection reagents (SuperFect™, PolyFect™)	Qiagen
Trichloroacetic acid [C <sub>2</sub> HCl <sub>3</sub> O <sub>2</sub> ]	Sigma Aldrich
Tris	Carl Roth
Triton X-100	Aldrich
Trizol reagent	Gibco BRL
Trypan blue 0.1%	Gibco BRL
Tween 20	Carl Roth
Western blotting substrate (Lumi light)	Roche
X-VIVO 15	BioWhittaker
Xylene cyanol FF	Serva
2-YT Broth	GibcoBRL

#### **5.1.4. DNA size markers**

The GeneRuler 100 bp and 1 kb DNA size markers were procured from MBI-Fermentas. The size of fragments in markers was as following:

100 bp Marker            1,031 / 900 / 800 / 700 / 600 / 500 / 400 / 300 / 200 / 100 / 80

1 kb Marker 10,000 / 8,000 / 6,000 / 5,000 / 4,000 / 3,500 / 3,000 / 2,500 / 2,000 /  
1,500 / 1,000 / 750 / 500 / 250

**5.1.4.1. Protein standards**

The protein size marker BENCHMARK™ was procured from Gibco BRL.

**5.1.5. Enzymes**

All restriction endonucleases and modifying enzymes MBI-Fermentas  
Proteinase K and RNase [Ribonuclease] Type I-A Sigma-Aldrich

**5.1.6. Antibodies**

<b>Antibodies</b>	<b>Provided by</b>
α-Oct 1	T. Wirth
α-Oct 2	T. Wirth
α-NFATc1 N-term	ImmunoGlobe
α-NFATc1 C-term	ImmunoGlobe
α-NFATc1 PAN	ImmunoGlobe
α-NFATc2	Anjana Rao
α-EGR-1	Santa Cruz
α-Sp1	Santa Cruz
α-CREB	Santa Cruz
α-ATF-2	Santa Cruz
α-Jun	Santa Cruz
α-p65	Santa Cruz
α-Fos	Santa Cruz

**5.1.7. Oligonucleotides and primers**

All oligonucleotides and primers were procured from MWG Biotech. The lyophilized oligos were dissolved in 10 mM Tris, pH 7.5 to a final concentration of 100 pmol/μl. For the sequencing reaction, lyophilized oligos were dissolved in 10 mM Tris, pH 7.5 to a final concentration of 10 pmol/μl. Primers were stored in -20°C.

**Sequencing primers**

T3 promoter 5'-ATTAACCCTCACTAAAGGGA-3'  
T7 promoter 5'-AAGGCTAGAGTACTTAATACGA-3'

**Generation of mouse 534 bp -11 kb RE element**

Dir 5'-CACACGCATTCACACACAAA-3'

Rev 5'-GCGAGACACAGTTTCATCCA-3'

**ChIP**

Human IL3 enhancer

Dir 5'-TGGCAAGACGGCAAGAACCC -3'

Rev 5'-CAGGGGTTGGAGCACATACT -3'

Human NFATc1 P1 promoter distal (-950 bp tandem NFAT site)

Dir 5'-GAGACGTGAGAGAGGAAAGTG -3'

Rev 5'-CGGCATGCTGAAGTCATTATG -3'

Human FasL promoter

Dir 5'-GGGAGCAGTTCACACTAACAGG -3'

Rev 5'-GCTGGATCTCTCTTATAGAGTTTC -3'

Human  $\beta$ -Actin

Dir 5'-GAGCAAGAGAGGCATCCT -3'

Rev 5'-CAGTGGTACGGCCAGAGG -3'

Human NFATc1 P2 promoter

Dir 5'-CAGGGCACAAGAGGCCGGGGGAC -3'

Rev 5'-GTCGCGGCCGCCAGGGGTTC -3'

**EMSA**

Mouse P1 NFAT tand (-700;-661)

5'- AGTGGAAGCGCTTTTCCAAATTTCCACAGCGGGGGAAGCC -3'

Mouse P1 NFAT tand 3' mutation (-700;-661)

5'- AGTGGAAGCGCTTTTCCAAATTTA~~AA~~ACAGCGGGGGAAGCC -3'

Mouse P1 NFAT tand 5' mutation (-700;-661)

5'- AGTGGAAGCGCTTTT~~G~~CAAATTTCCACAGCGGGGGAAGCC -3'

Mouse P1 NFAT tand-mut (-700;-661)

5'- AGTGGAAGCGCTTTT~~G~~CAAATTTA~~AA~~ACAGCGGGGGAAGCC -3'

Mouse P1 NFAT -90 (-102;-74)

5'- CGGGGGAGGTGTTTTCCAGCTTTAAAAAGG -3'

Mouse P1 NFAT -90-mut (-102;-74)

5'- CGGGGGAGGTGTTTT~~GG~~AGCTTTAAAAAGG -3'

Mouse P1 NFAT (-447;-417)

5'- TTCCCAGGAGTCCTTTTCCTCCTAGTCTCT-3'

Mouse P1 NFAT (-506;-476)

5'- CCCTAGTAAGCCCTTTCCTTCCCGTTTCGTC-3'

Mouse P2-1 Oct (-107;-142)

5'- GGAGTTTATTTACTAGGAAGCCGGCGGCCGCG -3'

Mouse P2-2 Oct (-72;-107)

5'- AGCCGCTTGTTTATGTAAACCCGGAACACCCGGG -3'

Mouse CREB -660

5'- ATTTTACATAATGACTTCAGCATGCAAGGC -3'

Mouse CREB -660-mut

5'- ATTTTACATAAT~~CC~~CTTCAGCATGCAAGGC -3'

Mouse Pu-b<sub>d</sub> IL-2

5'- CCAAAGAGGAAAATTTGTTTCATACAGAAGG-3'

Mouse NFATc  $\kappa$ B 5'- GTAATTTAGCGGGATGGGAATTTTCCTTACTCCCGCCTG-3'

Mouse NFATc  $\kappa$ B mut 5'- GTAATTTAGCGGGAT TTGAATTTTCCTTACTCCCGCCTG-3'

Mouse Ig  $\kappa$ B

5'-TGCACAGAGGGGACTTTCC GAGAGGC-3' Mouse NFAT<sup>tand+5</sup>  
5'-AGTGGAAAGCGCTTTTCCAATGTACATTTCCACAGCGGGGGAAGCC-3'  
Mouse NFAT<sup>tand+10</sup>  
5'-AGTGGAAAGCGCTTTTCCAATGTACAGTCAATTTCCACAGCGGGGGAAGCC-3'

pA1<sub>prox</sub>  
dir- 5' AGA AAG GTG TGT TCC CAG GCG 3'  
rev- 5' CTA GGG GTT TCC TGA TAA GAC 3'  
pA1<sub>tand</sub>  
dir- 5' GCC ACA GTT AGG GTT GAA TG 3'  
rev- 5' AAT CTG AGA CCA GGG GAG C 3'  
pA2  
dir- 5' GCT GGC GCG AAC TGC CTT GTA C 3'  
rev- 5' GAG CCA TGT TGC AAA GCA CTT G 3'

### **Real-time PCR SYBR**

P1 promoter (ex.1/3-ex.3)  
Dir 5' - GGGAGCGGAGAACTTTGC-3'  
Rev 5' - CAGGGTCGAGGTGACACTAGG -3'  
P2 promoter (ex.2/3-ex3)  
Dir 5' - AGGACCCGGAGTTCGACTTC -3'  
Rev 5' - GCAGGGTCGAGGTGACACTAG -3'  
Isoform c1/A (ex.8/9-UTR area)  
Dir 5' - ACCTGTGCAAGCCAAATTCC -3'  
Rev 5' - AGAGTTACCATTTGGCAGGAAG-3'  
Isoform c1/B (ex.10 (c1/B specific region)-ex.11/10)  
Dir 5' - ACTTCAGCCACCCGCTTC -3'  
Rev 5' - GATCTCATTTACTGCGGCTG -3'  
Isoform c1/C (ex.10 (c1/C specific region)-ex.11/10)  
Dir 5' - GCAAGAGCCTGAGGAATTGG -3'  
Rev 5' - CAGCTCCGATGTGCTGAATTAG -3'

### **Cloning of mouse P2 promoter (224 b.p.)**

Dir 5' - CGAGTGGAGCTTGGGCTACG -3'  
Rev 5' - GGTCGCGCGGCACTGGTG-3'

#### **5.1.8. Antibiotics**

Ampicillin (100 mg/ ml); final Conc. 100 µg/ ml

#### **5.1.9. Solutions and Buffers**

All chemicals of molecular biology research grade were procured from respective manufacturers and all solutions were prepared using pure distilled (Milli-Q grade) autoclaved water. Wherever necessary, solutions were sterile filtered or autoclaved.

*APS stock solution (10 %, 10 ml)*

APS 1 g

*Blocking buffer for Western blot:*

Milk powder 5 g

Dissolved in 100 ml of 1x TBS-T.

*Calcium chloride stock solution (1 M, 1000 ml)*

CaCl<sub>2</sub> 110.98 g

*ChiP assay*

**SONIFICATION buffer**

Hepes pH 7.9 50mM

NaCl 140mM

EDTA 1mM

Triton X-100 1%

Na-deoxycholat 0,1%

SDS 0,1%

Water

**HIGH SALT buffer**

NaCl 500mM

Water

**LiCl buffer**

Tris pH 8.0 20mM

EDTA 1mM

LiCl 250mM

NP-40 0,5%

Na-deoxycholat 0,5%

Water

**TE buffer**

Tris Ph 8.0 20mM

EDTA 1mM

Water

**SWELLING buffer**

Hepes pH 7.8 25mM

MgCl<sub>2</sub> 1,5mM

KCl 10mM

NP-40 0,1%

Water

**ELUTION buffer**

Tris pH 8.0 50mM

EDTA 1mM

SDS 1%

Water

*Colony hybridization solutions*

CH solution I (always prepared fresh)

NaOH 0.5 N

CH solution II

Tris- HCl (pH 7.5) 0.2 M

NaCl 1.0 M

CH solution III

SDS 1%

EDTA 1 mM

Na<sub>2</sub>HPO<sub>4</sub> (pH 6.8) 40 mM

CH pre-hybridization solution

SSC 5x

SDS	0.2%
Denhardt solution	2x
Salmon sperm DNA	100 µg/ml
CH stop buffer	
Loading dye	6x
SDS	0.5%
EDTA	50 mM
CH washing buffer	
SSC	2x
SDS	0.2%

*Coomassie blue solution (1000 ml)*

Coomassie Brilliant Blue R-250	2.5 g
Methanol	100 ml
Acetic Acid	100 ml
H <sub>2</sub> O	800 ml

*DEPC-treated ddH<sub>2</sub>O (RNase-free, 1000 ml)*

DEPC 1 ml  
 DEPC was mixed thoroughly, incubated overnight (~ 16 h) under hood at RT, autoclaved and stored at RT; all solutions and buffers for RNA work were prepared in DEPC-treated ddH<sub>2</sub>O.

*Denaturing PAA-Gel for RNase Protection Assay (1000 ml; 6% gel solution)*

Urea	280.0 g (8M)
30% Acryl-Bisacrylamide solution	240 ml
10x TBE buffer	100 ml
Composition of one gel (Polymerization takes approx. 1 -2 hours at RT)	
6% gel solution	30 ml
10% APS	300 µl
TEMED	60 µl

*DNA Electrophoresis Buffer (1000 ml)*

TAE (50x) 20 ml  
 The solution was supplemented with 0.25 ml EtBr stock solution per liter of TAE and boiled for dissolving the agarose.

*DNA gel composition*

	0.7%	1.0 %	2.0 %
Agarose	1.05 g	1.5 g	3.0 g
20x TAE	7.5 ml	7.5 ml	7.5 ml
ddH <sub>2</sub> O	142.5 ml	142.5 ml	142.5 ml
EtBr (5mg/ml)	25 µl	25 µl	25 µl

*DTT stock solution (1 M, 20 ml)*

DTT 3.09 g  
 DTT powder was dissolved in 10 mM sodium acetate (pH 5.2), aliquoted and frozen in -20°C.

*EDTA stock solution (0.5 M, 1000 ml)*



## Materials and Methods

Na<sub>2</sub> EDTA·2H<sub>2</sub>O 186.1 g  
pH of the solution was adjusted to 8.0 with 10 M NaOH (~ 50 ml); EDTA gets dissolved only in correct pH.

### *EGTA stock solution (0.25 M, 1000 ml)*

EGTA 95 g  
pH of the solution was adjusted to 8.0 with KOH; EGTA gets dissolved only in correct pH.

### *EMSA Solutions*

PAA gel for the preparation of radioactive DNA probes (50 ml, 12%)

ddH<sub>2</sub>O 30 ml  
30% acryl-bisacrylamide solution 15 ml  
10x TBE buffer 5 ml  
10% APS 300 µl  
TEMED 60 µl

Gel polymerization takes approx. 1 hour.

### *EMSA gel (6%, 100 ml)*

dd H<sub>2</sub>O 70 ml  
30% acryl-bisacrylamide solution 20 ml  
10x TBE buffer 10 ml  
10% APS 500 µl  
TEMED 50 µl

### *EMSA binding buffer (3x, 50 ml)*

1M HEPES/KOH (pH 7.9) 3 ml  
1 M KCl 7.5 ml  
0.5 M Na<sub>2</sub>EDTA·2H<sub>2</sub>O (pH 8.0) 300 µl  
1 M DTT 150 µl

### *EMSA running buffer (1x, 1000 ml)*

TBE (10x) 25 ml  
EMSA stop buffer  
SDS 0.5 %  
EDTA 20 mM  
Bromophenol blue

### *Ethidium bromide stock solution (100 ml)*

EtBr 1 g

The solution was stored at 4°C in a dark bottle.

### *Gel loading sample buffer, 6x (MBI Fermentas)*

Glycerine 60%  
EDTA 60 mM

Bromophenol blue 0.09%  
Xylene Cyanol FF 0.09%

### *HEPES/ KOH stock solution (1 M, 1000 ml)*

HEPES 238.33 g

pH of the solution was adjusted to 7.2/ 7.4/ 7.9 with KOH.

*Luciferase harvesting buffer (50 ml)*

1.5 M Tris/HCl (pH 7.8)	1.7 ml
1 M MES	2.5 ml
Triton X-100	50 $\mu$ l

The solution was freshly prepared and 50  $\mu$ l DTT stock solution (1M) was added just before use.

*Luciferase assay buffer (50 ml)*

1.5 M Tris/HCl (pH 7.8)	4.17 ml
1 M MES	6.25 ml
1 M Mg(C <sub>2</sub> H <sub>3</sub> O <sub>2</sub> ) <sub>2</sub> ·4H <sub>2</sub> O	1.25 ml

The solution was freshly prepared and supplemented with very little ATP just before use.

*Luciferin solution for luciferase assay (100 ml)*

Luciferin	28 mg
1 M KHPO <sub>4</sub> (pH 7.8)	0.5 ml

The solution was aliquoted and stored at -20°C.

*Extraction buffer A (Hypotonic, 1000 ml)*

1 M Hepes/KOH (pH 7.9)	10 ml
1 M KCl	10 ml
0.5 M Na <sub>2</sub> EDTA·2H <sub>2</sub> O (pH 8.0)	200 $\mu$ l
0.25 M EGTA (pH 8.0)	400 $\mu$ l

Solution was stored at 4°C. For 10 ml Buffer A, following inhibitors were added before experiment: 10  $\mu$ l DTT stock solution (1M) and 50  $\mu$ l AEBSF (0.2 M).

*Extraction buffer C (High salt, 1000 ml)*

1 M Hepes/KOH (pH 7.9)	20 ml
1 M KCl	400 ml
0.5 M Na <sub>2</sub> EDTA·2H <sub>2</sub> O (pH 8.0)	2 ml
0.25 M EGTA (pH 8.0)	4 ml

Solution was stored at 4°C. For 10 ml Buffer C, following inhibitors were added before experiment: 10  $\mu$ l DTT-stock solution (1M), protease inhibitors [100  $\mu$ l AEBSF (0.2 M), 10  $\mu$ l leupeptin (2 mM) and 10  $\mu$ l aprotinin (0.3 M)].

*PBS (10x, 1000 ml)*

NaCl	80 g
KCl	2 g
CaCl <sub>2</sub>	1 g
MgCl <sub>2</sub>	1 g
Na <sub>2</sub> HPO <sub>4</sub> ·7H <sub>2</sub> O	26.8 g
KH <sub>2</sub> PO <sub>4</sub>	2.4 g

pH of the solution was adjusted to 7.4 with 1 N HCl.

*Ponceau red solution (100 ml)*

Ponceau red	2.0 g
Chloracetic acid (2%)	2.0 g

*Potassium chloride stock solution (1 M, 1000 ml)*

KCl	74.6 g
-----	--------

*Potassium hydrogen phosphate stock solution (1 M, 1000 ml)*

*Potassium phosphate buffer (0.2 M, 1000 ml)*  
 KH<sub>2</sub>PO<sub>4</sub> 27.2 g  
 pH was adjusted to 7.0 with 1 M KOH.

*Protease inhibitors (final working concentration is indicated)*  
 Aprotinin [Stock solution (0.3 M): 2 mg/ml H<sub>2</sub>O] 0.3 μM  
 Leupeptin [Stock solution (2 mM): 1 mg/ml H<sub>2</sub>O] 2 μM  
 AEBSF [Stock solution (0.2 M): 50 mg/ml H<sub>2</sub>O] 1 mM

*RNA loading buffer (5x, 10 ml, stored at 4°C)*  
 Saturated bromophenol blue solution 16 μl  
 500 mM EDTA, pH 8.0 80 μl  
 37% (12.3 M) formaldehyde 720 μl  
 100% glycerol 2 ml  
 Formamide 3.084 ml  
 10x RNA gel buffer 4 ml  
*RNA gel buffer (10X, Stored in dark bottle at RT, 1000 ml)*  
 MOPS (0.2M) 41.85 g  
 NaOAc (0.051M) 6.8 g  
 EDTA (0.01M) 2.92 g  
 Adjust pH to 7.0 with NaOH (~15 ml)

*RNA gel running buffer (1x, 1000 ml in DEPC - treated H<sub>2</sub>O)*  
 10x RNA gel buffer 100 ml  
 37% (12.3 M) formaldehyde 20 ml

*SDS stock solution (10%, 1000 ml)*  
 SDS 100 g  
 The solution was warmed to 70°C to dissolve and pH was set to 7.2 with 1 N HCl.

*SDS-PAGE sample buffer (4 x, 100 ml)*  
 1.5 M Tris/HCl (pH 6.8) 20 ml  
 SDS 2.4 g  
 Glycerine (87 %) 50 ml  
 β-mercaptoethanol 25 ml  
 Bromphenol blue 0.04%  
 The solution was warmed to 70°C and stored at -20°C.

*SDS-PAGE running buffer (10x, 1000 ml)*  
 Tris 30.3 g  
 Glycin 144.1 g  
 10% SDS 100 ml  
 pH of the solution was adjusted to 8.5 with 1 N HCl.

*Sodium acetate stock solution (3 M, 1000 ml)*  
 CH<sub>3</sub>COONa·3H<sub>2</sub>O 408.24 g  
 pH of the solution was adjusted to 5.2 with concentrated acetic acid.

*Sodium chloride stock solution (5 M, 1000 ml)*  
 NaCl 292.22 g  
 The solution was dissolved by heating to 60°C.

*Sodium hydroxide stock solution (10 M, 1000 ml)*

NaOH 400 g

*Sodium phosphate buffer (0.2 M, 1000 ml)*

NaH<sub>2</sub>PO<sub>4</sub>·H<sub>2</sub>O 27.6 g

*Stripping buffer for nitrocellulose membrane (1000 ml)*

1.5 M Tris/HCl (pH 6.8) 41.7 ml

10% SDS 200 ml

Before use, 100 ml buffer was supplemented with 700 µl β-mercaptoethanol.

*TAE buffer (Tris/Acetate/EDTA, 50x, 1000 ml)*

Tris 242 g

0.5 M Na<sub>2</sub>EDTA·2H<sub>2</sub>O (pH 8.0) 100 ml

Concentrated acetic acid 57.1 ml

*TBE buffer (Tris/Borate/EDTA, 10x, 1000 ml)*

Tris 108 g

Boric Acid 55 g

0.5 M Na<sub>2</sub>EDTA·2H<sub>2</sub>O (pH 8.0) 40 ml

*TBS (20x, 1000 ml)*

Tris 121.0 g

NaCl 175.2 g

KCl 7.5 g

pH of the solution was adjusted to 7.6 with 1M HCl (~ 10.2 ml)

*TBS/Tween (TBS-T, 1x, 1000 ml)*

TBS (20x) 50 ml

Tween 20 1 ml

*TE buffer (Tris/EDTA, pH 8.0, 1000 ml)*

1.5 M Tris/HCl (pH 8.0) 6.7 ml

0.5 M EDTA (pH 8.0) 0.2 ml

*Transfer buffer for Western blot (1000 ml)*

Glycine 2.9 g

Tris 5.8 g

10% SDS 3.7 ml

Methanol 200 ml

*Tris/ HCl stock solution (1.5 M, 1000 ml)*

Tris 181.7 g

pH of the solution was adjusted to 6.8/ 7.5/ 7.8/ 8.0/ 8.8 with 1 N HCl.

*Whole cell extract preparation buffer (Kyriakis Lysis Buffer Modified, 1000 ml)*

1 M HEPES/KOH (pH 7.4) 20 ml

0.25 M EGTA (pH 8.0) 8 ml

NaF 2.1 g

β-Glycerophosphate 10.8 g

Glycerine (87%) 115 ml

Triton X-100 10 ml  
NaN<sub>3</sub>-solution (10%) 4 ml

The solution was stored at 4°C. For 10 ml KLBM<sup>+</sup> buffer, following inhibitors were added before experiment: 10 µl DTT-stock solution (1M), protease inhibitors [50 µl AEBSF (0.2 M), 10 µl leupeptin (2 mM) and 10 µl aprotinin (0.3 M)] and phosphatase inhibitor [50 µl Sodium orthovanadate (0.2 M)].

### **5.1.10. DNA Vectors**

P1 (NF-ATc1) probe preparation - pKS vector + P1/386 b.p.

P2 (NF-ATc1) probe preparation - pKS vector + P2/244 b.p.

pGL3b-0.8kb – P1 core promoter

pGL3b-1.7kb - P1 core promoter and 1.1kb upstream area

pGL3b-2.7kb - P1 core promoter and 2.1kb upstream area

pGL3b-5.5kb - P1 core promoter and 4.7kb upstream area

pGL3b-0.8kb +534b.p. - P1 core promoter and 534b.p. from -11,6kbp upstream area

pGL3b-0.8kb\_CREBdistal mut - P1 core promoter with mutated CREB

pGL3b-0.8kb\_2xNFATmut - P1 core promoter with 2xmutated NFAT sites

pGL3b-0.2kb - P2 core promoter

pGL3b-2.2kb - P2 core promoter and 1kb upstream area

pGL3b-3.5kb - P2 core promoter and 3.3kb upstream area

pRL-null+P2 - P2 core promoter, renilla reporter gene

pPKLT55\_pA1- polyA motif introduced downstream of the stop codon of a luciferase gene

pPKLT55\_pA1tandem - polyA motif introduced downstream of the stop codon

pPKLT55\_pA2 - polyA motif introduced downstream of the stop codon

### **5.1.11. Growth Medium**

#### **5.1.11.1. Liquid medium and agar plates for bacterial culture.**

##### *2xYT Medium*

2-YT Broth 31 g

Powder was dissolved in 1000 ml ddH<sub>2</sub>O and autoclaved at 121°C, 15 psi for 30 minutes. After autoclaving, the medium was cooled down to 60°C and then respective antibiotic (ampicillin, final conc. 100 µg/ml) was added.

##### *2xYT Agar Plate*

2YT Broth 31 g

Agar-Agar 12 g

## *Materials and Methods*

These were dissolved in 1000 ml ddH<sub>2</sub>O and autoclaved at 121°C, 15 psi for 20 minutes. After autoclaving, the medium was cooled down to 60°C to add respective antibiotic (ampicillin, final conc. 100 µg/ml), immediately distributed in bacterial dishes under the laminar hood and allowed to solidify at RT overnight. The plates were stored at 4°C.

### *LB Medium*

Bacto tryptan	10 g
Yeast extract	5 g
NaCl	10 g

The pH of the medium was adjusted to 7.0 with 10N NaOH (~ 200 µl), the total volume was adjusted to 1000 ml with ddH<sub>2</sub>O and autoclaved at 121°C, 15 psi for 20 minutes. The medium was stored at 4°C. Before use, respective antibiotic was added to the medium.

### *LB Agar plate*

Bacto tryptan	10 g
Yeast extract	5 g
NaCl	10 g
Agar-Agar	12 g
ddH <sub>2</sub> O	800 ml

The pH of the medium was adjusted to 7.0 with 10 N NaOH, the total volume was adjusted to 1000 ml with ddH<sub>2</sub>O and autoclaved at 121°C, 15 psi for 20 minutes. After autoclaving, the medium was cooled down to 60°C to add antibiotic, immediately distributed in bacterial dishes under the laminar hood and allowed to solidify at RT overnight. The plates were stored at 4°C.

### **5.1.11.2. Mammalian cell culture media**

#### *Suspension Cell line (Jurkat, EL-4, WEHI-231, and other lymphoid cells)*

RPMI 1640	1000 ml
FCS (Jurkat, EL-4)	5 %

#### *Primary murine CD4<sup>+</sup> T lymphocytes*

X-VIVO 15	1000 ml
FCS	10%
L-Glutamin (200 mM)	10 ml
Penicillin (10.000 IU/ ml), Streptomycinsulphate (10 mg/ ml)	6 ml

$\beta$ -mercaptoethanol (50 mM)	1 ml
Sodium pyruvate (100 mM)	10 ml
Hepes (1 M)	10 ml
MEM (Non-essential amino acids, 100x)	10 ml

## **5.2. Methods**

### **5.2.1. Bacterial manipulation**

Plasmid transformed bacteria are selected on LB plates with the appropriate antibiotic for 24 hr. For overnight mini cultures, single colonies are picked and inoculated into LB medium with antibiotic and shaken overnight at 37°C. This pre-culture is then used for preparing frozen glycerol cultures, plasmid DNA or protein purification. For storage of bacteria, a glycerol stock culture is prepared by growing bacteria to an OD of 0.8 at a wavelength of 600nm in culture medium. 500 $\mu$ l bacterial culture is taken and added to 500  $\mu$ l 80% glycerol and then mixed thoroughly in a small 1.5ml tube. This stock solution is subsequently frozen at -80°C. To inoculate an overnight culture again, bacteria were taken and held at room temperature (RT) until surface is thawed. Pick a small amount of cells and mix into 2-5 ml culture medium and leave to grow for 12-16 hours at 37°C in a bacterial culture shaker. The frozen stock is immediately returned to the -80°C.

#### **5.2.1.1. Preparation of competent cells (CaCl<sub>2</sub> method)**

Inoculate an overnight pre-culture from a single colony on a prestreaked plate (from glycerol stock) in 2ml LB or 2x TY media by incubation at 37°C and shaking to aerate. The second day, inoculate 1 ml of the pre-culture in 100ml fresh media and grow the culture at 37°C until OD at wavelength 600nm of the culture reaches 0.5. Cool down the culture on ice for at least 15 min. (The following procedures should be carried out at 4°C in pre-cooled sterile tubes). Harvest the cells in a centrifuge at 5000 g for 5 min, and discard the supernatant. Resuspend the bacterial pellets thoroughly in a small volume of ice-cold 100mM CaCl<sub>2</sub>. Dilute the suspension with the CaCl<sub>2</sub> solution to a final volume of 30-40 ml, and leave on ice for 25 min with occasional shaking. Spin down the cells as before, discard the supernatant carefully and resuspend the pellet in 5 ml glycerol/CaCl<sub>2</sub>. The suspension can be aliquoted in 100 to 400  $\mu$ l and stored at -70°C. The transformation efficiency of the bacteria prepared by this method should reach at least 5x10<sup>6</sup>cfu/mkg of plasmid DNA.

### ***5.2.1.2 Transformation of competent bacteria***

Thaw the competent bacteria from a desired origin on ice. Add ligated DNA or purified plasmid-DNA to 100 µl competent cells in a cold 1.5 ml microfuge tube. Mix carefully and keep on ice for 30 min. Heat-shock the bacteria then at 42°C for 90 sec, chill on ice for 2 min and add 1 ml antibiotic-free LB medium, and shake at 37°C for 1h. Selection of transformed bacteria is done by plating aliquots of the bacterial suspension on antibiotic containing agar plates. A single colony can then be expanded in LB medium and used for DNA preparation.

### ***5.2.1.3 Screening of transformants by colony hybridization***

Bacterial colonies growing on agar plates were covered by nitrocellulose filter. The spatial arrangement of colonies on the plates was preserved on the filters. After transfer, the filters were processed for hybridization to an appropriate radiolabeled probe while the original (master) plate is incubated for a few hours to allow the bacterial colonies to re-grow in their original positions. The success of colony hybridization depends on high specificity of synthetic oligonucleotide probe used. The transformed *E. coli* culture was plated onto 90-mm LB agar plates, at dilutions roughly to generate up to 2500 transformed colonies. A nitrocellulose filter (disc, 0.45 micron) was placed, numbered side down, on the surface of the LB agar plate, in contact with the bacterial colonies, until it was completely wet. Once the filter was in place, the filter was marked to the underlying agar medium by stabbing in three or more asymmetric locations through the filter with a 23G needle. The edge of the filter was gripped with blunt-ended forceps and, in a single smooth movement, the filter was peeled from the surface of the agar plate and placed on the Whatmann filter paper presoaked with fresh CH solution I, with colonies on the membrane facing up, and left for 10 minutes to let bacterial colonies lyse. After this treatment, membrane was placed on Whatmann filter paper pre-soaked with CH solution II and left for 10 minutes. This step was repeated once. Now disc was air dried on Whatmann filter paper and further incubated for 10 minutes with shaking in CH solution III was performed. Again the membrane was dried on Whatmann paper and baked at 80°C for 30 min. Now membrane was ready for hybridization process. The CH prehybridization solution was pre-warmed at 42°C and membrane was prehybridized for 30 minutes to 1 hour at 42°C in this solution. Radiolabeled probe was prepared by labeling of oligonucleotide by Polynucleotide kinase (PNK). Synthetic oligonucleotides lacking phosphate groups at their 5' termini can be radiolabeled by transfer of the <sup>-32</sup>P from [<sup>-32</sup>P]ATP in a reaction catalyzed by bacteriophage T4 polynucleotide kinase as



following:

Oligonucleotide	100-500 ng
10x PNK buffer	2.0 $\mu$ l
32P- $\gamma$ ATP	3.0 $\mu$ l
H <sub>2</sub> O	12.0 $\mu$ l
PNK	1.0 $\mu$ l

The reaction mixture was incubated at 37°C for 30 minutes and reaction was stopped by adding 5  $\mu$ l of CH stop buffer. The probe was not purified and directly used for hybridization by mixing in CH prehybridization solution. The hybridization was performed at 60°C for 90 minutes in this solution. To remove unbound probe, membrane was washed 4-5 times at 55°C with CH washing solution. Radioactivity on disc was monitored after each washing to avoid excessive washing.

The membrane was air dried, exposed overnight with intensifying screen at -70°C and autoradiogram was developed to detect positive clones.

## **5.2.2 DNA methods**

### ***5.2.2.1. Electrophoresis of DNA on agarose gel***

Double stranded DNA fragments with size between 0.5 kb and 10 kb can be separated according to their lengths on agarose gels. Agarose is added to 1x TAE to obtain a final concentration between 0.7-2%. Boil the suspension in the microwave until the agarose is completely melted. Allow the agarose to cool down to around 50°C before adding ethidium bromide up to 0.5  $\mu$ g/ml and pour into the gel apparatus. Add DNA gel loading buffer to the DNA sample and apply on the gel. Electrophorese in 1x TAE buffer at 100 volts. The DNA can be visualised under UV-light.

### ***5.2.2.2. Isolation of plasmid DNA from agarose (QIAEX II agarose gel extraction protocol)***

This protocol is designed for the extraction of 40-bp to 50-kbp DNA fragments from 0.8-2% standard agarose gels in TAE or TBE buffer. DNA molecules are adsorbed to QIAEX II silica particles in the presence of high salt. All non-nucleic acid impurities such as agarose, proteins, salts, and ethidium bromide are removed during washing steps. Excise the desired DNA band from the agarose gel under the UV light. Weigh the gel slice and add 3 volumes of Buffer QG to 1 volume of gel for DNA fragments 100-bp-4 kbp; for DNA fragments more than 4 kbp, add 2 volume of QG plus 2 volumes of H<sub>2</sub>O. Resuspend QIAEA II by vortexing for 30 sec; add 10  $\mu$ l

(or 30 µl) of QIAEX II to the sample containing not more than 10 µg of DNA (between 2-10 µg). Incubate at 50°C for 10 min to solubilise the agarose and bind the DNA. Mix by vortexing every 2 min to keep QIAEX II in suspension. Centrifuge the sample for 30 sec and carefully remove supernatant with a pipette. Wash the pellet with 500 µl of Buffer QG and then twice with Buffer PE. Air-dry the pellet and elute the DNA in 10 mM Tris-HCL or H<sub>2</sub>O and resuspend the pellet by vortexing. Incubate at RT for 5 min (or at 50°C for 5 min) for DNA fragments not more than 4 kbp (for DNA fragments between 4-10 kbp). Centrifuge for 30 sec and carefully pipette supernatant into a clean tube.

#### ***5.2.2.3. Purification of plasmid DNA (QIAquick PCR purification kit)***

This protocol is designed to purify single- or double-stranded PCR products or DNA plasmids ranging from 100 bp to 10 kbp. DNA adsorbs to the silica-membrane in the presence of high salt while contaminants pass through the column. The impurities are washed away and pure DNA is eluted with Tris buffer or H<sub>2</sub>O. Add 5 volume of buffer PB to 1 volume of the contaminants and mix. Place a QIAquick spin column in a 2 ml collection tube. Apply the mixed sample to the QIAquick column and centrifuge 30-60 sec. Discard flow-through and place QIAquick column back into the same collection tube. Add 0.75 ml Washing Buffer PE to column and centrifuge 30-60 sec. Discard flow-through and place QIAquick column back into the same collection tube. Centrifuge column for an additional 1 min at maximum speed. Place QIAquick column in a clean 1.5 ml microfuge tube. Add 50 µl Elution Buffer EB or H<sub>2</sub>O to the centre of the QIAquick column and centrifuge for 1 min. Store the purified DNA at - 20°C.

#### ***5.2.2.4. Ligation of DNA fragments***

##### ***Calf-intestinal-phosphatase (CIP) reaction (5' dephosphorylation)***

Alkaline phosphatase catalyses the removal of 5' phosphate groups from DNA, RNA and ribo- and deoxyribonucleoside triphosphates. For blunt end ligation, the 5' phosphate group of the vector must be removed by CIP reaction. This reaction is also used to prevent the re-ligation of the vectors. 2.5 µg of DNA fragments is phosphorylated at 37°C for 30 min in 100 µl of reaction volumes consisting of 1x CIP buffer and 1 µl of phosphatase. 5 mM EDTA is then added to the reaction and incubated with the reaction at 65°C for 15 min to inactivate the enzyme. The DNA fragments are purified by phenol extraction and ethanol precipitation before ligation reaction.

##### ***5.2.2.5. Cohesive-end ligation***

Prepare the plasmid DNA or DNA fragment by cutting it with suitable restriction enzymes, which is followed by purification. 1:3 molar ratio of vector: insert DNA fragments together with

1 µl of T4 ligase are incubated in 1x Ligation Buffer in a total volume of 20 µl for 4 hr at RT or overnight at 16°C. Heat the mixture at 65°C for 10 min to inactivate the enzyme.

#### ***5.2.2.6. Mini-preparation of plasmid DNA***

Grow 3 ml overnight culture in LB, 2x TY, or GC media with 100 µg/ml ampicillin at 37°C overnight. Pellet the cells at 14,000 rpm for 1 min. Remove the supernatant and resuspend the pellets in 100 µl Buffer. Add 200 µl Buffer P2 (Lysis Buffer) and incubate at RT for 5 min. Add 150 µl ice-cold 3 M acidic KOAc (Neutralisation Buffer), mix by inverting the tubes for 6-7 times and incubate on ice for 5 min. Centrifuge at 15,000 rpm for 3 min. Transfer the supernatant to a fresh Eppendorf tube and add 900 µl of pre-cooled 100% ethanol, precipitate at -70°C for 10 min. Centrifuge the pellet at 15,000 rpm for 10 min. Wash the pellet with 200 µl 70% ethanol. Air-dry the pellet and resuspend it in 30-50µl 10 mM Tris-HCl, pH 7.8.

#### ***5.2.2.7. Maxi-preparation of plasmid DNA***

Grow culture in 150 ml LB media containing plasmids or recombinant plasmids overnight in a 37°C incubator with shaking at 220 rpm. Collect the bacteria and isolate DNA plasmids by using a Quiagen Plasmid Maxi Kit. This extraction method is based on Birnboim's alkali lysis principle. Resuspend the bacterial pellet in 10 ml of Buffer P1. Add 10 ml of Buffer P2, mix gently, and incubate at RT for 5 min. Add 10 ml of chilled Buffer P3, mix immediately, and incubate on ice for 20 min. Centrifuge at 4,000 rpm for 30 min at 4°C. Filter the supernatant over a prewetted, folded filter. Apply the supernatant to a equilibrated QIAGEN-tip 500 and allow it to enter the resin by gravity flow. Wash the QIAGEN-tip twice with Buffer QC. Elute DNA with 15 ml Buffer QF. These processes result in the isolation of a DNA-salt pellet, which is precipitated by 0.7 volumes (10.5 ml) of isopropanol and centrifuged further at 4000 rpm for 30 min. Washed the resulting pellet twice with 70% ethanol and air-dry at RT. The pellet is then carefully resuspended in TE buffer and used for transfection of cultured mammalian cells.

#### ***5.2.2.8. Measurement of DNA concentration***

The DNA concentration is determined by using an UV spectrophotometer at wavelength of 260 nm. The absorption of 1 at 260 nm corresponds to a concentration of 50 µg/ml double stranded DNA. Identity, integrity and possible purity of the DNA can be subsequently analysed on an agarose gel.

#### ***5.2.2.9. DNA Sequencing (Sanger Dideoxy Method)***

DNA sequencing was done using automatic sequencer based on a method which is a variant of

dideoxynucleotide method. Sequencing of DNA was achieved by generating fragments through the controlled interruption of enzymatic replication (Sanger et al., 1977). DNA polymerase I is used to copy a particular sequence of a single-stranded DNA. The synthesis is primed by complementary fragment, which may be obtained from a restriction enzyme digest or synthesized chemically. In addition to the four deoxyribonucleoside triphosphates (ddNTP), the incubation mixture contained a 2', 3'- dideoxy analogue of one of them. The incorporation of this analogue blocked further growth of the new chain because it lacked the 3'-hydroxyl terminus needed to form the next phosphodiester bond. A fluorescent tag was attached to the oligonucleotide primer, a differently colored one in each of the four chain-terminating reaction mixtures. The reaction mixtures were combined and electrophoresed together. The separated bands of DNA were then detected by their fluorescence as they pass out the bottom of the tube, and the sequence of their colors directly yielded the base sequence. A high sensitivity fluorescent detector measures the amount of each fluorophore as a function of time and hence sequence is determined from the order of peaks of four different dyes.

***PCR for sequencing:***

In sterile PCR microfuge sequencing reaction was set up as following:

Reaction mix: 5 µl plasmid DNA (from miniprep, approx. 1-2 µg),

2 µl primer (20 pM), 7 µl sequencing mix\*.

PCR program: 25 cycle: 96°C/15 s; 52°C (or 55°C)/15 s; 60°C/4 min \*A-dye: Terminator labeled with dichloro[R6G]; C-dye: Terminator labeled with dichloro[TAMRA]; G-Dye: Terminator labeled with dichloro[R110]; T-Dye: Terminator labeled with dichloro[ROX].

***Purification of sequencing products:*** 200 µl of Sephadex G-50 was packed in PCR filter tips and mounted onto microfuge tube with the help of an adapter. About one-tenth (1.4 µl) volume of sequencing reaction mix (14 µl), 3 M sodium acetate, pH 5.2, was added to fresh microfuge tube mounted with G-50 column. Sequencing mixture was loaded onto the G-50 column and centrifuged at 3000 rpm for 5 minutes. To each tube, 70 µl of 96% ethanol was added, followed by centrifugation at 15,000 rpm, for 10 minutes at RT. The supernatant was aspirated completely taking care of DNA pellet. Another quick spin was given to collect and aspirate traces of ethanol, if any, and the pellet of DNA was air dried at 37°C for 5 minutes and submitted for automated sequencing.

DNA sequencing was done by Dr. S. Chuvpilo (Ist. of Pathology, Würzburg).

### **5.2.2.10. DNA amplification by Polymerase Chain Reaction (PCR)**

PCR is an enzymatic method for the *in vitro* synthesis of multiple copies of specific sequences of DNA. The cocktail for PCR contained the following components:

DNA-template (plasmid ~ 9 Kb)	100-250 ng
Forward primer (100 pmol/μl)	0.7 μl
Reverse primer (100 pmol/μl)	0.7 μl
MgSO <sub>4</sub> (25 mM),	6-7 μl (end conc. 3 - 3.5 mM)
10 x buffer without MgSO <sub>4</sub>	5 μl
dNTP-mix (10 mM)	4.5 μl
PWO-polymerase (1 U/μl)	4 μl
ddH <sub>2</sub> O	up to 50 μl

The PCR cocktail was immediately incubated in PCR machine for amplification using the cycling programs.

### **5.2.2.11. Southern blot**

Digest genomic DNA by specific restriction enzymes, separate the fragments on 0.7-1% TAE agarose gel with ethidium bromide at 3V/cm, ON. Photograph the gel, and then capillary transfer DNA onto Hybond-N membrane in 20x SSC Buffer according to manufacturer instruction (Hybond-N, Amersham). Cross-link DNA to membrane using UV-light, 120 mJ/cm<sup>2</sup>. Radioactively label and hybridise a probe. The membrane was first incubated with prehybridising solution for 1 hr at 65°C. The solution was then changed and replaced with hybridisation solution containing the radiolabelled probe and incubated overnight at 65°C. The probe may be frozen, denatured and re-used for up to one week later. Following hybridisation, the membrane is then subjected to washing at 65°C. The membrane is washed once with washing buffer 1, followed by three times with washing buffer 2, each for 15 min. The membrane is then rinsed to remove excess SDS and exposed ON with X-Ray film.

## **5.2.3 RNA Methods**

### **5.2.3.1. Isolation of RNA from mammalian cells**

RNA is extremely sensitive to degradation by RNases, and should therefore be handled with RNase-free materials. Cells can be directly lysed in TRIzol LS reagent, 5x10<sup>6</sup> cells/1ml. Add 0.2 ml Chloroform. Mix on a Vortex for 25 sec then place on ice for 15 min. Transfer to an

Eppendorf tube and centrifuge at 10,000 rpm for 15 min. Transfer the upper aqueous phase to the new tube, add 0.5 ml Isopropanol, incubate 30 min at RT and centrifuge at 10,000 rpm for 15 min. Wash pellet with 75% Ethanol, air dry and resuspend in 100-150µl DEPC-H<sub>2</sub>O. Measure concentration, and store at -20°C under 2.5 volumes ethanol.

### ***5.2.3.2. Running RNA samples on denaturing gels***

Electrophoresis tank was cleaned with detergent solution (0.5% SDS), thoroughly rinsed with RNase-free water followed by ethanol and allowed to dry. The edges of the gel-tray were sealed with tape and appropriate comb cleaned with 70% ethanol was placed. For RNA gel preparation, 1.2 – 1.5 g agarose was dissolved in 70 ml of DEPC – treated water by heating in a micro oven and cooled to approx. 60°C. RNA gel was prepared, poured in the gel tray and allowed to polymerize at RT. In the meanwhile, one volume of 5x RNA loading buffer was mixed with 4 volumes of RNA sample, briefly spun down, incubated for 3-5 minutes at 65°C and chilled on ice. Samples were loaded into the wells of the polymerized agarose gel and electrophoresed at 5-7 V/cm in 1x RNA gel running buffer.

### ***5.2.3.3. Ribonuclease protection assay***

The method can be used to quantitate RNAs, to map the positions of introns, and to identify the locations of 5' and 3' ends of mRNAs on cloned DNA templates. Preparations of RNA containing an mRNA of interest were hybridized to a radiolabeled single-stranded RNA probe. At the end of the reaction, a mixture of RNase A and RNase T1 was used to degrade unhybridized regions of the probe, and the surviving molecules are then separated by denaturing gel electrophoresis and visualized by autoradiography.

***Probe synthesis:*** Before the start of probe synthesis, the heating block was set at 37°C and following reagents were brought to room temp:  $\alpha$ -<sup>32</sup>P-UTP, GACU nucleotide pool, DTT, 5X transcription buffer and RPA template set. For each probe synthesis, following reagents from the kit were added (in order) to a 1.5 ml eppendorf tube, mixed by gentle pipetting or flicking, quickly spun in a microfuge and incubated at 37°C for 1 hour:

1 µl RNasin<sup>®</sup>

1 µl GACU pool

2 µl DTT

4 µl 5X transcription buffer

1 µl RPA Template Set

5  $\mu$ l [ $\alpha$ -<sup>32</sup>P]UTP

1  $\mu$ l T7 RNA polymerase

The reaction was terminated by adding 2  $\mu$ l of DNase, mixed by gentle flicking, quickly spun in a microfuge and incubated at 37°C for 30 minutes. For separation of probes, reaction of each sample mixed with the loading dye was directly loaded on the 6% polyacrylamide gel which was run at 40 mA until the first marker line reaches a marked line, usually 12 cm from the wells. The glass plates were removed carefully and the gel was covered with plastic foil contained fluorescent markers and exposed for 1-2 min to X-ray film at RT. An autoradiogram band, corresponding to specific probe band then was combined with the gel and cut out with a sterile needle. The gel slice was transferred to a new 1.5 ml eppendorf tube and homogenized with a paster pipette. 300  $\mu$ l of 1M ammonium acetate was added and incubated for 1 hour at 60°C then spun in a microfuge for 2 minutes at RT and transferred the upper aqueous phase to a new 1.5 ml tube To precipitate RNA, 900  $\mu$ l ice cold 100% ethanol and 10  $\mu$ g of yeast tRNA were added, mixed by inverting the tube(s), incubated for 2-3 minutes on dry ice (or 30 minutes at -70°C) and centrifuged for 20 minutes at RT (or 15 minutes at 4°C). The supernatant was removed carefully and pellet was dried for 5 to 10 minutes at RT. The RNA pellet was solubilized in 50-100  $\mu$ l of hybridization buffer and 1  $\mu$ l was taken for quantification in the scintillation counter. Usually maximum yield was expected in the range of 1-3 x 10<sup>6</sup> Cherenkov counts/ $\mu$ l (measurement of cpm/ $\mu$ l without the presence of scintillation fluid) with an acceptable lower limit of 3 x 10<sup>5</sup> Cherenkov counts/ $\mu$ l. After quantification, this 1  $\mu$ l probe was used as undigested probe upon dilution to 1:50 in the blue buffer. The probe was stored at -20°C no longer than 2-3 days.

**RNA hybridization:** Following things were arranged before the start of hybridization: heating block at 90°C, precipitated RNA of desired amount and hybridization oven at 56°C. For hybridization, 5  $\mu$ g of target RNA was mixed with 10  $\mu$ l of diluted probe in a 1.5 ml tube. The RNA was solubilized by gentle vortexing for 3-4 minutes followed by quick spin in the microfuge. Samples were placed in a heating block pre-warmed to 90°C for 5-10 minutes (up to 30 minutes). The tubes were transferred to hybridization oven set at 56°C and incubated for 12-16 hours.

**RNase treatment:** The heating block was turned to 30°C for 15 minutes prior to the RNase treatment. For 20 samples, RNase cocktail was prepared by mixing 2.5 ml RNase buffer and 6  $\mu$ l of RNase A + T1 mix. Overnight samples were mixed with 100  $\mu$ l of RNase cocktail, briefly centrifuged, and incubated for at least 45 minutes at 30°C.

**Proteinase K treatment:** The heating block was turned to 37°C. For 20 samples, proteinase K cocktail was prepared by mixing 390  $\mu$ l of proteinase K buffer, 30  $\mu$ l of proteinase K and 30  $\mu$ l

of yeast tRNA. After RNase treatment, 18 µl of proteinase K cocktail was added, mixed and incubated for 30 minutes at 37°C.

**Precipitation and electrophoresis of RNA:** For the precipitation of dsRNA, 100 µl of ammonium acetate and 600 µl of isopropanol were mixed to each sample, incubated for 15 minutes at -20°C and centrifuged at RT for 15-30 minutes. The supernatant was removed and the pellet was dried at 95°C for 2-3 minutes. The pellet was dissolved in 4 µl loading buffer, denatured at 90°C for 3 minutes and transferred on ice. In the meanwhile, gel solution was prepared (for composition see 5.1.5). The polymerized gel was pre-run at 30W for 1 hour in 1x TBE. Samples were loaded on the gel along with undigested probe. After the blue dye reached 2/3<sup>rd</sup> of the length of gel, electrophoresis was stopped, gel was dried in vacuum for 1 hour at 95°C and autoradiogram was established by exposing the gel for 24-48 hours to X-ray film with an intensifying screen at -70°C.

#### **5.2.3.4. One step Real-Time PCR (QIAGEN QuantiTect SYBR Green RT-PCR Kit)**

This method provides accurate real-time quantification of RNA targets. The fluorescent dye SYBR Green I in the master mix enables rapid analysis of many different targets without having to synthesize target-specific labeled probes. The cocktail for the Real-time PCR contained the following components:

<b>Component</b>	<b>Volume/reaction</b>	<b>Final concentration</b>
2x QuantiTect SYBR Green	12,5 µl	1x
QuantiTect RT Mix	0,25 µl	0.25 µl/reaction
Primer A (100p/µl)	0,15 µl	
Primer B (100p/µl)	0,15 µl	
Template RNA	5 µl	100ng/reaction
RNase-free water	7 µl	
Total volume	25 µl	

Primers were designed using “primer3” web based free software and tested to ensure amplification of single discrete bands with no primer-dimers. All primers were synthesised by MWG. Real-time PCR was conducted using an ABI PRISM 7000 Sequence Detection System. Each reaction was run in quartet in a final reaction volume of 25 ml. Cycling parameters were 50°C for 30 min for the reverse transcription reaction, 95°C for 15 min to activate DNA polymerase, then 40 cycles of 95°C for 15 s, 53°C for 30s and 72°C for 30 s. Melting curves were performed using Dissociation Curves software (Applied Biosystems) to ensure only a single product was amplified.



Data were analysed initially using LinRegPCR software. ‘Window-of-linearity’ method, based on calculation of the fluorescence measured per cycle of each sample was used for the relative quantification of mRNA transcripts. This alternative approach is based on linearization of the basic formula for exponential PCR amplification by taking the logarithm on both sides of the equation resulting in  $\text{Log}(NC) = \text{Log}(N0) + \text{Log}(\text{Eff}) \times C$ . The NC and C are measured fluorescence data and cycle number, respectively. The log-linear part of the PCR data can be determined for each sample by selecting a lower and an upper limit of a ‘window-of-linearity’. Linear regression analysis is then used to calculate the intercept and the slope,  $\text{Log}(N0)$  and  $\text{Log}(\text{Eff})$ , respectively, from the straight line that fits best to the included data points. The starting concentration follows directly from the intercept of this linear regression line, and is expressed in terms of SYBR Green I fluorescence.

## **5.2.4 Protein Methods**

### ***5.2.4.1. Preparation of protein extracts***

#### ***Preparation of whole protein extract from mammalian cells:***

Cells were centrifuged (1200 rpm, 5 minutes, 4°C), washed with cold PBS (Without  $\text{Ca}^{++}$  and  $\text{Mg}^{++}$ ), resuspended in 1 ml of PBS (without Ca/Mg), transferred to 1.5 ml tubes and again pelleted down (2000 rpm, 2 minutes, RT). The cell pellet was resuspended in cold whole cell extract preparation buffer supplemented with protease and phosphatase inhibitors (KLB $\text{M}^+$ ) (100  $\mu\text{l}$  per  $1 \times 10^7$  cells). Cells were disrupted by two times freezing and thawing on dry ice or passing the cell suspension through 26G needle 10 times and incubated for further 10 minutes. The cell suspension was centrifuged for 30 minutes at 14,000 rpm, 4°C and supernatant was saved as whole cell extract, which was stored for future use at -70°C. The protein concentration of the supernatant was determined by Bio-Rad protein assay.

#### ***Preparation of nuclear and cytoplasmic protein extracts from mammalian cells:***

Cells were centrifuged at 1200 rpm for 5 min at RT and the cell pellet was resuspended in 1 ml cold PBS buffer (without  $\text{Ca}^{++}$  and  $\text{Mg}^{++}$ ), transferred to a 1.5 ml tube and again centrifuged at 2000 rpm for 2 min at RT to remove the supernatant. The pellet was resuspended in 200  $\mu\text{l}$  to 1 ml of extraction buffer A $^+$  (100  $\mu\text{l}$  per  $1 \times 10^7$  cells) and incubated for 20-30 min at 4°C. Extraction buffer A $^+$  is a low salt buffer ( $^+$  indicates that DTT and PMSF were added to buffer A), which allowed the cells to swell. To destroy the swollen cells, the solution was passed 10 times through 1 ml syringe with 26G needle and centrifuged at 7,000 rpm for 2 minutes in the cold room. The supernatant contained cytosolic fraction and the pellet, which appeared

transparent, contained nuclear fraction. The supernatant was transferred to a fresh tube and kept on ice. The pellet was washed with 800 µl extraction buffer A<sup>+</sup>, centrifuged at 7,000 rpm for 2 minutes in the cold room and the pellet was resuspended in extraction buffer C<sup>+</sup> (leupeptin was added in addition to DTT and PMSF) by pipetting and vigorously mixing with brutal force, followed by vortexing the nuclear extract vigorously for 30 minutes in the cold room. Now the suspension was centrifuged at 14,000 rpm for 30 minutes in the cold room and supernatant containing nuclear proteins was frozen in -70°C. The protein concentration of the supernatant was determined by Bio-Rad protein assay.

**5.2.4.2. Measurement of Protein concentration (Bio-Rad protein assay)**

The Bio-Rad Protein Assay is based on the observation that when Coomassie Brilliant Blue G-250 binds to the protein, the absorbency maximum shifts from 450 nm to 595 nm. Equal volumes of cell lysate containing 1-20 µg of protein is added to diluted Dye Reagent and mixed well (1:5 dilution of Dye Reagent Concentrate in ddH<sub>2</sub>O). After a period of 5-10 min, the absorption at wavelength 595 is measured versus reagent blank (which contains only the lysis buffer).

**5.2.4.3. Immunodetection**

**SDS-polyacrylamide gel preparation and electrophoresis:** SDS-polyacrylamide gels were prepared in 8 cm x 10 cm x 1.5 mm mini gel format according to the standard Laemmli method [91]. Separating or lower gel mix was prepared according to the volume required, poured in the gel apparatus, overlaid gently with 0.1 % SDS and allowed to polymerize at room temperature. After the separating gel was polymerized, the overlay was decanted, thoroughly and gently washed with distilled water. The stacking gel was poured, the comb was inserted and allowed to polymerize at RT. Requisite concentration of protein samples were mixed with 4x Laemmli buffer and denatured by heating at 95°C for 5 min, loaded in the wells of polymerized gel and electrophoresed at constant current, 25-30 mA per gel, in 1x SDS-PAGE running buffer.

	Stacking gel, pH 6.8	Separating gel, pH 8.8			
Percentage of the gel	4%	8%	10%	12%	15%
Distilled water	6.8	5.8	5.0	4.1	2.85
1.5 M Tris-HCl, pH 8.8	-	3.125	3.125	3.125	3.125
1.5 M Tris-HCl, pH 6.8	1.25	-	-	-	-
Acryl-/ Bisacrylamide (29% / 1% w/v)	1.7	3.35	4.15	5.0	6.25
10% (w/v) SDS	0.1	0.125	0.125	0.125	0.125

10% APS	0.1	0.125	0.125	0.125	0.125
TEMED	0.01	0.01	0.005	0.005	0.005
Total Volume	10.0	12.5	12.5	12.5	12.5

Table 5.2: Composition of protein gels (all numerical figures are in ml)

*Western blotting and hybridization:* SDS-PAGE gel was electrotransferred onto nitrocellulose membrane at 40 mA overnight at 4°C. The air dried membrane was incubated in a blocking solution (5% fat free milk in 1X TBS-T) for 30 minutes to 1 hour at RT. Membrane was directly incubated in primary antibody solution (1:2000 in blocking solution) for 2 to 3 hours at RT. After incubation, membrane was washed in 1X TBS-T for 1 x 20 minutes and 3 x 5 minutes each. Now membrane was incubated in secondary antibody conjugate solution (1:2000 in blocking solution) for 1 to 2 hours at room temperature and washed in 1X TBS-T for 1 x 20 minutes and 3 x 5 minutes each. Colour was developed with ECL developing solution according to the instructions of the manufacturer (Amersham).

*Stripping of nitrocellulose membrane:* Nitrocellulose membrane was stripped of the first antibody to detect the level of another protein by hybridization with another antibody. This was done by incubating the membrane in stripping buffer (pre-warmed to 60°C) and placing in a water bath set at 60°C for 30 min with shaking. Now the membrane was washed one time with ddH<sub>2</sub>O and three times with TBS/Tween for 5 min each. The membrane was ready for staining with another primary antibody.

#### **5.2.4.4. DNA/Protein Interaction Assay**

The Electrophoretic Mobility Shift Assay (EMSA) provides a simple and rapid method for detecting DNA-binding proteins in vitro. This method has been used widely in the study of sequence-specific DNA-binding proteins such as transcription factors. The assay is based on the observation that complexes of protein and DNA migrate through a non-denaturing polyacrylamide gel more slowly than free DNA fragments or double-stranded oligonucleotides. The gel shift assay is performed by incubating a purified protein, or a complex mixture of proteins (such as nuclear or cell protein extract preparations), with a <sup>32</sup>P end-labeled DNA fragment containing the putative protein binding site. The reaction products are then analyzed on a non-denaturing polyacrylamide gel. The specificity of the DNA-binding protein for the putative binding site is established by competition experiments using unlabeled DNA fragments

or oligonucleotides containing a binding site for the protein of interest or other unrelated DNA sequences.

Chromatin is comprised of nucleosome subunits, each of which consists of DNA wound around several histone proteins. Recent findings have revealed that large multiprotein complexes are often involved in regulatory processes taking place in the nucleus. The regulation of transcription in eukaryotic cells is critically dependent on the dynamic state of chromatin. Transcriptional activation and inactivation is intimately associated with either the relaxed or taut conformation of chromatin structure. To unravel the structure and dynamics of these nuclear protein complexes and determine their interactions with the DNA template, many scientists use an assay known as the chromatin immunoprecipitation (ChIP) assay. The ChIP assay combines two straightforward steps — first, *in vivo* formaldehyde cross-linking of whole cells that freezes protein-protein and protein-DNA interactions, followed by immunoprecipitation of protein-DNA complexes with specific antibodies from sonicated extracts and PCR.

#### ***5.2.4.5. Radioactive labeling and purification of DNA probe***

Oligonucleotides were dissolved in ddH<sub>2</sub>O to a final concentration, 100 pmol/μl. For each probe, 20 μl of sense and antisense oligonucleotides were mixed, vortexed, spun down briefly, and incubated in a thermoblock at 65°C until they reached this temperature. Now DNA was taken out from 65°C and let it cool down to RT for hybridization. Now the final volume obtained was 40 μl of 100 pmol/μl double stranded DNA. This was diluted to 20 ng/μl (for dsDNA of 25 nucleotides in length, 1pmol corresponds to 9ng, so 100 pmol/μl = 900 ng/μl and therefore dilution factor was 45x). All reactions were setup in tightly fitting screw cap tubes as following:

dd H <sub>2</sub> O	5.0 μl
10x PNK buffer	1.0 μl
ds-Oligo	1.0 μl (40 ng)
<sup>32</sup> P-γATP	2.0 μl (40 mCi)
PNK	1.0 μl

The reaction mix was vortexed, spun down and tubes were placed behind a radioactive shield for incubation at 37°C for 30 min (The incubation time of 30 minutes was strictly followed since the PNK enzyme has the property of removing phosphate group upon longer incubation). In the meanwhile, 12 % acrylamide gel was prepared for purification of labeled probe. After incubation, 5 μl of EMSA stop buffer was added to stop the reaction. Now the samples were loaded on the polymerized gel, run in 1x TBE at 20mA for 2 hours and the desired band was cut after exposing the gel to a film. The gel slice was mixed with 150 μl of 10 mM KCl and kept on

rotation for O/N at 4°C. The radioactivity was measured in 2 µl aliquot and the probe was diluted to 20,000 cpm / µl. If not used immediately, the radioactive probe was stored at -20°C for maximum of 3 weeks.

#### **5.2.4.6. Electrophoretic Mobility Shift Assay (EMSA)**

A 6 % polyacrylamide gel was poured and allowed to polymerize for 1 hour at RT. The polymerized gel was pre-run in 0.4x TBE at 20A (constant 200 V) till the power dropped down to 10A (usually for 2 hours) to let the salt run out off the gel. For EMSA, nuclear proteins were used. The master mix for each sample was prepared as following:

3x binding buffer	3.3 µl
poly dI/dC (1 µg/µl)	0.7 µl
dd H <sub>2</sub> O minus nuclear extract and probe	up to 10.0 µl

The master mix for all similar samples (i.e. same probe) was mixed with radioactive probe (~20,000 cpm for each sample), aliquoted into different tubes for different nuclear extracts, mixed with respective nuclear extracts (2.0 µg) and incubated for 20-30 min on ice. For adjusting the different concentrations of nuclear extracts to the final volume of 10 µl, the buffer C was used. For “Supershift assays”, 1 µl (1 µg/µl) of antibody solution against the transcription factor to be studied was added. A 100-fold excess of cold oligos were added for competition assays. For separation of complexes, 8 µl of each sample was directly loaded on the 6% polyacrylamide gel which was run at 220 V until the marker reaches a marked line, usually 13 cm from the wells. The glass plates were removed carefully and the gel was immersed in 10% acetic acid for 20 min to fix small fragments. A Whatman paper was placed on the gel and carefully separated from the glass plate. The gel was covered with plastic foil and dried for 60-120 min in a vacuum dryer. An autoradiogram was established by exposing the gel for 24 - 48 hours to X-ray film at -70°C with an intensifying screen.

#### **5.2.4.7 Chromatin Immunoprecipitation (ChIP)**

The cells ( $2 \times 10^5$ /ml, 200ml) were grown at RPMI media and induced. Crosslinking was performed by adding 37% formaldehyd to the final concentration of 1% directly into the media and rocked for 10 min at room temperature. The cells were washed with ice-cold PBS/BSA and resuspended on ice for 30 min in 10ml of SWELLING buffer, containing protease inhibitors, 1µg/ml leupeptin and 1mM PMSF. Following dounce homogenization, the nuclei were collected by 7x passing cells through needle on ice and pelleted by centrifugation (2500 rpm for 5 min at

4°C, no brake). The nuclei were resuspended in 2ml of SONIFICATION buffer, containing protease inhibitors as above and incubated on ice for 10 min. Three times freezing/thawing step on dry ice we did as an additional purification point. The chromatin was sonicated to an average length of about 600 bp. Sonication conditions were: 0,5 sec/pulse max power, in 30 sec bursts followed by 1 min cooling on ice for a total sonication time of 2-2.5 min per sample. Debris was cleared by centrifugation at max speed for 10 min at 4°C. The supernatant was transferred to the new tube. To reduce nonspecific background, the sample was pre-cleared with 40-50 µl of a salmon sperm DNA/protein A agarose slurry and 20 µl Rabbit antiserum for 2 hours at 4°C with rotation. The supernatant was divided into two fractions: one for a no antibody control and the second was immunoprecipitated with 3 µl antibodies overnight at 4°C. 30 A260 units of the pre-cleared chromatin we used for one immunoprecipitation. Immune complexes were collected with 50 µl of salmon sperm DNA/protein A agarose slurry for 1 hr 4°C with rotation. Then, beads were washed twice consecutively with 400 µl of each solution: SONIFICATION/ HIGH SALT/ LiCl/ TE. Separate tips for each sample were used to avoid a contamination. The immunocomplexes were eluted with 250 µl of ELUTION buffer for 15 min at 65°C with rotation. Beads were pelleted at max speed for 3 min and supernatant was transferred to clean tubes. Elution step was repeated and both elutions were combined in the same tube.

Formaldehyde crosslinks were reversed by adding of 5M NaCl to a final concentration of 0,3M to the eluates and incubated 4-6 hours at 65°C with rotation. After successive treatment with 1 of 20 µg/ml Proteinase K for one hour at 45°C, the samples were extracted with phenol-chloroform and precipitated with 1/10 V of AcONa pH 5.2 and 3V of 100% ethanol at -20°C for 1 hour. Next, samples were centrifugated 60 min at max speed and pellets were resuspended in 25-30 µl of TRIS or water. 1 µl of the immunoprecipitated DNA and input DNA were analyzed by radioactive PCR using promoter specific primers. Amplifications were performed in the presence of  $\alpha$ -<sup>32</sup>P dCTP and products were analyzed in 5% polyacrylamide gel. To ensure that amounts of PCR products accurately reflected the amounts of template DNA, control PCR reactions (26,27,28,29,30,31 and 32 cycles) were performed.

## **5.2.5 Reporter Gene Analysis**

### ***5.2.5.1. Transfection of EL-4 cells***

DEAE-Dextran method was used for transient transfection of EL-4 cells. One day before transfection, EL4 cells were inoculated at a density of  $50 \times 10^5$  cells/50 ml. Before transfection,

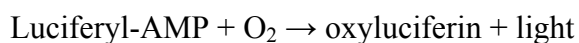
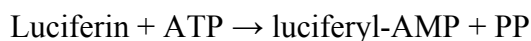
transfection cocktail per sample was made in a cryotube as following, vortexed, spun down and left at RT:

Reporter construct	1 µg
Vector DNA	6 µg
1x TBS	up to 540 µl
DEAE	180 µl

50 ml of overnight cultured cells were centrifuged at 1200 rpm for 3-5 minutes, pooled in TBS (e.g. for 27 dishes, all cells were pooled in 27 ml TBS), aliquoted equally in the different tubes, and again centrifuged at 1200 rpm for 3 minutes to pellet down cells. The transfection cocktail was mixed with the cell pellet and incubated on ice for 20 minutes with shaking. In the meanwhile, 100 mm plate with 19 ml complete RPMI medium was incubated at 37°C. Cells were shocked by adding 400 µl of 25% DMSO (in 1x TBS) for 90 seconds, then 4.0 ml of 1x TBS was added and centrifuged at 1200 rpm for 3 minutes. The cell pellets were resuspended in RPMI medium and pooled all cells transfected with same reporter. Again pooled cells were centrifuged, resuspended in 1 ml / dish of complete RPMI medium and dropped on each plate containing 19 ml complete RPMI medium and incubated in 37°C. Transfected cells were stimulated overnight according to the protocol.

#### **5.2.5.2. Luciferase Reporter Gene Assay**

Bioluminescence is characterized by light emission catalyzed by an enzyme. Firefly (*Photinus pyralis*) luciferase catalyzes the release of light upon addition of luciferin and ATP. The luciferase activity was assayed and quantified by measurement of light production. The photon production by catalytic oxidation of luciferin occurs from an enzyme intermediate, luciferyl-AMP. Luciferin was first activated by the addition of ATP and the activated luciferin, in turn, reacted with oxygen to form dioxetane. Dioxetane decomposes and excites the molecule, which transfers to its ground state by emission of fluorescence light.



Cells were collected in 50 ml tube, centrifuged at 1200 rpm for 3 minutes, resuspended in 1 ml of PBS, and transferred to 1.5 ml tube. Cells were again centrifuged at 6,000 rpm for 2 minutes, added 100 µl of harvesting buffer to the pellet, mixed thoroughly by vortexing and centrifuged at 14,000 rpm for 4 minutes. Now 50 µl of this supernatant was mixed with 50 µl of assay buffer in the luciferase plate, which was placed in a luminometer, injected with 100 µl of luciferin solution and luciferase activity was measured. Results are presented as luciferase units

normalised to protein concentration. Each experiment is performed in duplicates or triplicates. The mean and standard deviations of two independent experiments are shown in the figures.

## **5.2.6 Cell culture techniques**

### ***5.2.6.1. Cell maintenance***

All cell lines were handled in highly sterile condition under laminar hood and cultivated in appropriate media supplemented with antibiotics. Cells were incubated at 37°C, 5 % CO<sub>2</sub> in humidified incubator. EL-4 is a murine thymoma cell line established from 9,10-dimethyl-1, 2-benzanthrazen - induced T cell lymphoma. These cells express constitutively active calcineurin, a phosphatase, which activates NFAT by dephosphorylation. Upon phorbol ester (plus ionomycin) stimulation, this cell line secretes several cytokines like IL-2, IFN- $\gamma$ , IL-10 and GM-CSF (ATCC Nr. TIB-39). Primary murine CD4<sup>+</sup> T lymphocytes were isolated from lymph nodes of DO11.10 TCR transgenic (tg) Balb/c mouse. Suspension cell lines like EL-4 and Jurkat T cells were split every 3-4 days just by refreshing with complete RPMI medium to a small aliquot of cell suspension.

### ***5.2.6.2. Induction of cells***

T lymphocytes were induced by pharmacological agents TPA and ionomycin that activate Ras/Protein Kinase and calcium-dependent pathways, respectively, to mimic signal through the TCR.

TPA :20 ng/ml for stimulation of stable cell line, 10 ng/ml for primary cells and EL-4 cells

Ionomycin :1  $\mu$ M for stimulation of stable cell line, 0.5  $\mu$ M for primary cells and EL-4 cells

### ***5.2.6.3. Preparation and activation of naïve CD4<sup>+</sup> T lymphocytes***

***Isolation of peripheral CD4<sup>+</sup> T lymphocytes from lymphnodes (LNs):*** CD4<sup>+</sup> T lymphocytes were isolated from LNs of 5-6 weeks old healthy mice which were sacrificed by cervical dislocation. Before dissecting, mice were sprayed with disinfectant to minimize contamination. LNs were collected in cold BSS/BSA buffer and CD4<sup>+</sup> T lymphocytes were isolated by negative selection procedure. LN cells were incubated with antibodies against CD8 and HSA which are surface markers for CD8<sup>+</sup> T lymphocytes and B lymphocytes, respectively. The antibody coupling to the cell surface receptor of unwanted cells allows the retention of these cells on the glass matrix of the column, whereas CD4<sup>+</sup> T cells pass through the column unhindered.



## *Materials and Methods*

*Preparation of the column:* The column was installed onto the stand and washed with 15-20 ml of cold BSS/BSA buffer. In the meantime, the lyophilized Ab supplied with column was solubilized in 1.5 ml of BSS/BSA buffer, loaded onto the column, and left for one hour at RT.

*Preparation of the lymphnode cells:* All LNs were collected in cold BSS/BSA buffer from sacrificed healthy mice, squeezed on 70 micron cell strainer and collected in 50 ml tube. LN cells were washed twice with BSS/BSA buffer. To the pellet, 2.0 ml of antibodies mixture cocktail (Column Mixture) plus 3.0 ml of BSS/BSA were added and incubated on ice for 30 minutes. After incubation, cells were washed two times with BSS/BSA buffer and finally resuspended in 10 ml of BSS/BSA buffer. LN cells were now ready to load on the column.

*Purification of CD4<sup>+</sup> T lymphocytes:* Before loading cells, each column was washed again with 20 ml of BSS/BSA buffer and flow rate was adjusted to 8-10 drops per minute. Now 10 ml of resuspended cells were loaded onto the column and the flow through was collected in a sterile tube. The flow through contained enriched CD4<sup>+</sup> population which was centrifuged, resuspended the pellet in 10-12 ml of X-VIVO medium supplemented with 5% FBS and kept on ice in cold room O/N.

*Enrichment of CD62L<sup>high</sup> CD4<sup>+</sup> T lymphocytes:* Mouse CD62L (L-selectin) MACS microbeads were used for the positive selection of naïve CD4<sup>+</sup> T cell population. CD62L is expressed on B cells, monocytes, neutrophils, eosinophils, thymocytes and T cells. The level of CD62L expression is high on naive T cells, but low on T cells pre-activated to effector or memory Th cells. The enrichment of naive T cells from CD4<sup>+</sup> T cell population was achieved by removing pre-activated CD62L<sup>low</sup> T cells on MACS column.

*Magnetic Labeling of CD4<sup>+</sup> Cells:* CD4<sup>+</sup> Cells were pelleted down, and for every  $1 \times 10^7$  cells, mixed with 10  $\mu$ l of CD62L MACS beads plus 90  $\mu$ l of BSS/BSA and incubated in dark for 15 minutes at RT/4-8°C. (Optional, for purity analysis in flow cytometry: added CD62L-biotinylated antibody [usually 1:200 dilution] and incubated for an additional 10 minutes at RT/4-8°C in dark. Cells were washed with BSS/BSA, resuspended in 100  $\mu$ l of BSS/BSA, added 1  $\mu$ l of streptavidin-Cytochrome [usually 1:100 dilution] and incubated for further 5-10 minutes.) Now cells were washed with BSS/BSA and resuspended in 1 ml of BSS/BSA. Cells are ready for loading on the MACS column.

*Preparation of LS column:* The midiMACS Separation Unit was attached to the MACS Multistand and placed the LS separation column into the magnet and one sterile tube under the column to collect the flow through. In all further steps special care was taken to prevent the entry of air bubble into the column. In this regard, the buffer was degassed for 3 hours. The column was washed with 5 ml of fresh BSS/BSA and let the buffer run through. Magnetically labeled

cell suspension containing up to  $10^8$  positive cells in  $2 \times 10^9$  total cells was loaded onto the LS column and allowed the cell suspension to run through in a very strong magnetic field and collected the effluent as negative fraction. The column was detached from separator (very strong magnetic field) and placed on a new collection tube under no magnetic field. Now 5 ml of buffer was applied to the column and firmly flushed out cells using the plunger supplied with the column. The flushed out cells belonged to  $CD62L^{high} CD4^+$  T cell population, which was further washed once with BSS/BSA buffer.

***CD4<sup>+</sup> T cell activation and differentiation:***  $CD4^+$  T lymphocytes were induced to proliferate and differentiate *in vitro* by antigen stimulation in the presence of respective cytokines and neutralizing antibodies. The establishment of stable phenotype was achieved after 5-7 days of culture under skewing conditions. The default or undifferentiated Th (Th0) cells were obtained usually by activating naïve  $CD4^+CD62L^{high}$  cells in the presence of IL-2 and neutralizing antibodies to IFN- $\gamma$  and IL-4 (to block Th1 and Th2 differentiation, respectively). The culture of  $CD4^+$  or  $CD4^+CD62L^{high}$  T cell was set up at a density of  $5 \times 10^5$  cells per ml with a maximum volume of 2 ml per well in 24 well plate. The day of activation was considered as day 0.

## 6. BIBLIOGRAPHY

1. Weiss, A. and D.R. Littman, *Signal transduction by lymphocyte antigen receptors*. Cell, 1994. **76**(2): p. 263-74.
2. Cantrell, D., *T cell antigen receptor signal transduction pathways*. Annu Rev Immunol, 1996. **14**: p. 259-74.
3. Crabtree, G.R. and E.N. Olson, *NFAT signaling: choreographing the social lives of cells*. Cell, 2002. **109 Suppl**: p. S67-79.
4. Kelly, K. and U. Siebenlist, *Immediate-early genes induced by antigen receptor stimulation*. Curr Opin Immunol, 1995. **7**(3): p. 327-32.
5. Cockerill, G.W., et al., *Regulation of granulocyte-macrophage colony-stimulating factor and E-selectin expression in endothelial cells by cyclosporin A and the T-cell transcription factor NFAT*. Blood, 1995. **86**(7): p. 2689-98.
6. Schreiber, S.L. and G.R. Crabtree, *The mechanism of action of cyclosporin A and FK506*. Immunol Today, 1992. **13**(4): p. 136-42.
7. Lopez-Rodriguez, C., et al., *NFAT5, a constitutively nuclear NFAT protein that does not cooperate with Fos and Jun*. Proc Natl Acad Sci U S A, 1999. **96**(13): p. 7214-9.
8. Graef, I.A., et al., *Evolutionary relationships among Rel domains indicate functional diversification by recombination*. Proc Natl Acad Sci U S A, 2001. **98**(10): p. 5740-5.
9. Rao, A., C. Luo, and P.G. Hogan, *Transcription factors of the NFAT family: regulation and function*. Annu Rev Immunol, 1997. **15**: p. 707-47.
10. Serfling, E., et al., *The role of NF-AT transcription factors in T cell activation and differentiation*. Biochim Biophys Acta, 2000. **1498**(1): p. 1-18.
11. Ranger, A.M., et al., *Inhibitory function of two NFAT family members in lymphoid homeostasis and Th2 development*. Immunity, 1998. **9**(5): p. 627-35.
12. Chuvpilo, S., et al., *Autoregulation of NFATc1/A expression facilitates effector T cells to escape from rapid apoptosis*. Immunity, 2002. **16**(6): p. 881-95.
13. Chuvpilo, S., et al., *Multiple NF-ATc isoforms with individual transcriptional properties are synthesized in T lymphocytes*. J Immunol, 1999. **162**(12): p. 7294-301.
14. Chuvpilo, S., et al., *Alternative polyadenylation events contribute to the induction of NF-ATc in effector T cells*. Immunity, 1999. **10**(2): p. 261-9.
15. Northrop, J.P., et al., *NF-AT components define a family of transcription factors targeted in T-cell activation*. Nature, 1994. **369**(6480): p. 497-502.

16. Okamura, H., et al., *Concerted dephosphorylation of the transcription factor NFAT1 induces a conformational switch that regulates transcriptional activity*. Mol Cell, 2000. **6**(3): p. 539-50.
17. Crabtree, G.R. and N.A. Clipstone, *Signal transmission between the plasma membrane and nucleus of T lymphocytes*. Annu Rev Biochem, 1994. **63**: p. 1045-83.
18. Choi, M.S., et al., *Induction of NF-AT in normal B lymphocytes by anti-immunoglobulin or CD40 ligand in conjunction with IL-4*. Immunity, 1994. **1**(3): p. 179-87.
19. Hutchinson, L.E. and M.A. McCloskey, *Fc epsilon RI-mediated induction of nuclear factor of activated T-cells*. J Biol Chem, 1995. **270**(27): p. 16333-8.
20. Aramburu, J., et al., *Activation and expression of the nuclear factors of activated T cells, NFATp and NFATc, in human natural killer cells: regulation upon CD16 ligand binding*. J Exp Med, 1995. **182**(3): p. 801-10.
21. Macian, F., et al., *Transcriptional mechanisms underlying lymphocyte tolerance*. Cell, 2002. **109**(6): p. 719-31.
22. Mattila, P.S., et al., *The actions of cyclosporin A and FK506 suggest a novel step in the activation of T lymphocytes*. Embo J, 1990. **9**(13): p. 4425-33.
23. Macian, F., C. Garcia-Rodriguez, and A. Rao, *Gene expression elicited by NFAT in the presence or absence of cooperative recruitment of Fos and Jun*. Embo J, 2000. **19**(17): p. 4783-95.
24. Hogan, P.G., et al., *Transcriptional regulation by calcium, calcineurin, and NFAT*. Genes Dev, 2003. **17**(18): p. 2205-32.
25. Liu, J., et al., *Calcineurin is a common target of cyclophilin-cyclosporin A and FKBP-FK506 complexes*. Cell, 1991. **66**(4): p. 807-15.
26. Schulman, H., *The multifunctional Ca<sup>2+</sup>/calmodulin-dependent protein kinases*. Curr Opin Cell Biol, 1993. **5**(2): p. 247-53.
27. Wang, T., et al., *The immunophilin FKBP12 functions as a common inhibitor of the TGF beta family type I receptors*. Cell, 1996. **86**(3): p. 435-44.
28. Aramburu, J., et al., *Selective inhibition of NFAT activation by a peptide spanning the calcineurin targeting site of NFAT*. Mol Cell, 1998. **1**(5): p. 627-37.
29. Aramburu, J., et al., *Affinity-driven peptide selection of an NFAT inhibitor more selective than cyclosporin A*. Science, 1999. **285**(5436): p. 2129-33.
30. Shibasaki, F., et al., *Role of kinases and the phosphatase calcineurin in the nuclear shuttling of transcription factor NF-AT4*. Nature, 1996. **382**(6589): p. 370-3.

31. Okamura, H., et al., *A conserved docking motif for CK1 binding controls the nuclear localization of NFAT1*. Mol Cell Biol, 2004. **24**(10): p. 4184-95.
32. Zhu, J., et al., *Intramolecular masking of nuclear import signal on NF-AT4 by casein kinase I and MEKK1*. Cell, 1998. **93**(5): p. 851-61.
33. Sheridan, C.M., et al., *Protein kinase A negatively modulates the nuclear accumulation of NF-ATc1 by priming for subsequent phosphorylation by glycogen synthase kinase-3*. J Biol Chem, 2002. **277**(50): p. 48664-76.
34. Roach, P.J., *Multisite and hierarchal protein phosphorylation*. J Biol Chem, 1991. **266**(22): p. 14139-42.
35. Yang, T.T., et al., *Phosphorylation of NFATc4 by p38 mitogen-activated protein kinases*. Mol Cell Biol, 2002. **22**(11): p. 3892-904.
36. Chow, C.W., et al., *c-Jun NH(2)-terminal kinase inhibits targeting of the protein phosphatase calcineurin to NFATc1*. Mol Cell Biol, 2000. **20**(14): p. 5227-34.
37. Crabtree, G.R., *Generic signals and specific outcomes: signaling through Ca<sup>2+</sup>, calcineurin, and NF-AT*. Cell, 1999. **96**(5): p. 611-4.
38. Park, S., M. Uesugi, and G.L. Verdine, *A second calcineurin binding site on the NFAT regulatory domain*. Proc Natl Acad Sci U S A, 2000. **97**(13): p. 7130-5.
39. Zhu, J. and F. McKeon, *NF-AT activation requires suppression of Crm1-dependent export by calcineurin*. Nature, 1999. **398**(6724): p. 256-60.
40. Lenschow, D.J., T.L. Walunas, and J.A. Bluestone, *CD28/B7 system of T cell costimulation*. Annu Rev Immunol, 1996. **14**: p. 233-58.
41. Nishizuka, Y. and S. Nakamura, *Lipid mediators and protein kinase C for intracellular signalling*. Clin Exp Pharmacol Physiol Suppl, 1995. **22**(1): p. S202-3.
42. Ghaffari-Tabrizi, N., et al., *Protein kinase Ctheta, a selective upstream regulator of JNK/SAPK and IL-2 promoter activation in Jurkat T cells*. Eur J Immunol, 1999. **29**(1): p. 132-42.
43. Whitmarsh, A.J. and R.J. Davis, *Transcription factor AP-1 regulation by mitogen-activated protein kinase signal transduction pathways*. J Mol Med, 1996. **74**(10): p. 589-607.
44. Derijard, B., et al., *Independent human MAP-kinase signal transduction pathways defined by MEK and MKK isoforms*. Science, 1995. **267**(5198): p. 682-5.
45. Gupta, S., et al., *Transcription factor ATF2 regulation by the JNK signal transduction pathway*. Science, 1995. **267**(5196): p. 389-93.

46. Kallunki, T., et al., *JNK2 contains a specificity-determining region responsible for efficient c-Jun binding and phosphorylation*. Genes Dev, 1994. **8**(24): p. 2996-3007.
47. Su, B., et al., *JNK is involved in signal integration during costimulation of T lymphocytes*. Cell, 1994. **77**(5): p. 727-36.
48. Derijard, B., et al., *JNK1: a protein kinase stimulated by UV light and Ha-Ras that binds and phosphorylates the c-Jun activation domain*. Cell, 1994. **76**(6): p. 1025-37.
49. Yang, D., et al., *Targeted disruption of the MKK4 gene causes embryonic death, inhibition of c-Jun NH2-terminal kinase activation, and defects in AP-1 transcriptional activity*. Proc Natl Acad Sci U S A, 1997. **94**(7): p. 3004-9.
50. Fraser, J.D., et al., *Regulation of interleukin-2 gene enhancer activity by the T cell accessory molecule CD28*. Science, 1991. **251**(4991): p. 313-6.
51. Verweij, C.L., M. Geerts, and L.A. Aarden, *Activation of interleukin-2 gene transcription via the T-cell surface molecule CD28 is mediated through an NF-kB-like response element*. J Biol Chem, 1991. **266**(22): p. 14179-82.
52. McGuire, K.L. and M. Iacobelli, *Involvement of Rel, Fos, and Jun proteins in binding activity to the IL-2 promoter CD28 response element/AP-1 sequence in human T cells*. J Immunol, 1997. **159**(3): p. 1319-27.
53. Coudronniere, N., et al., *NF-kappa B activation induced by T cell receptor/CD28 costimulation is mediated by protein kinase C-theta*. Proc Natl Acad Sci U S A, 2000. **97**(7): p. 3394-9.
54. Sun, Z., et al., *PKC-theta is required for TCR-induced NF-kappaB activation in mature but not immature T lymphocytes*. Nature, 2000. **404**(6776): p. 402-7.
55. Iacobelli, M., W. Wachsman, and K.L. McGuire, *Repression of IL-2 promoter activity by the novel basic leucine zipper p21SNFT protein*. J Immunol, 2000. **165**(2): p. 860-8.
56. Bower, K.E., et al., *Correlation of transcriptional repression by p21(SNFT) with changes in DNA.NF-AT complex interactions*. J Biol Chem, 2002. **277**(38): p. 34967-77.
57. Ho, I.C., et al., *The proto-oncogene c-maf is responsible for tissue-specific expression of interleukin-4*. Cell, 1996. **85**(7): p. 973-83.
58. Kim, J.I., et al., *The transcription factor c-Maf controls the production of interleukin-4 but not other Th2 cytokines*. Immunity, 1999. **10**(6): p. 745-51.
59. Bodor, J., J. Bodorova, and R.E. Gress, *Suppression of T cell function: a potential role for transcriptional repressor ICER*. J Leukoc Biol, 2000. **67**(6): p. 774-9.

60. Decker, E.L., et al., *Early growth response proteins (EGR) and nuclear factors of activated T cells (NFAT) form heterodimers and regulate proinflammatory cytokine gene expression*. Nucleic Acids Res, 2003. **31**(3): p. 911-21.
61. Avni, O., et al., *T(H) cell differentiation is accompanied by dynamic changes in histone acetylation of cytokine genes*. Nat Immunol, 2002. **3**(7): p. 643-51.
62. Nemer, G. and M. Nemer, *Cooperative interaction between GATA5 and NF-ATc regulates endothelial-endocardial differentiation of cardiogenic cells*. Development, 2002. **129**(17): p. 4045-55.
63. Wada, H., et al., *Calcineurin-GATA-6 pathway is involved in smooth muscle-specific transcription*. J Cell Biol, 2002. **156**(6): p. 983-91.
64. Musaro, A., et al., *IGF-1 induces skeletal myocyte hypertrophy through calcineurin in association with GATA-2 and NF-ATc1*. Nature, 1999. **400**(6744): p. 581-5.
65. Taniguchi, T., et al., *IRF family of transcription factors as regulators of host defense*. Annu Rev Immunol, 2001. **19**: p. 623-55.
66. Rengarajan, J., et al., *Interferon regulatory factor 4 (IRF4) interacts with NFATc2 to modulate interleukin 4 gene expression*. J Exp Med, 2002. **195**(8): p. 1003-12.
67. Lieberson, R., et al., *Tumor necrosis factor receptor-associated factor (TRAF)2 represses the T helper cell type 2 response through interaction with NFAT-interacting protein (NIP45)*. J Exp Med, 2001. **194**(1): p. 89-98.
68. Bert, A.G., et al., *Reconstitution of T cell-specific transcription directed by composite NFAT/Oct elements*. J Immunol, 2000. **165**(10): p. 5646-55.
69. Liu, S., et al., *Cyclosporin A-sensitive induction of the Epstein-Barr virus lytic switch is mediated via a novel pathway involving a MEF2 family member*. Embo J, 1997. **16**(1): p. 143-53.
70. Sommer, H., et al., *Deficiens, a homeotic gene involved in the control of flower morphogenesis in Antirrhinum majus: the protein shows homology to transcription factors*. Embo J, 1990. **9**(3): p. 605-13.
71. Wu, H., et al., *Activation of MEF2 by muscle activity is mediated through a calcineurin-dependent pathway*. Embo J, 2001. **20**(22): p. 6414-23.
72. Blaeser, F., et al., *Ca(2+)-dependent gene expression mediated by MEF2 transcription factors*. J Biol Chem, 2000. **275**(1): p. 197-209.
73. Lu, J., et al., *Signal-dependent activation of the MEF2 transcription factor by dissociation from histone deacetylases*. Proc Natl Acad Sci U S A, 2000. **97**(8): p. 4070-5.

74. Mao, Z., et al., *Neuronal activity-dependent cell survival mediated by transcription factor MEF2*. Science, 1999. **286**(5440): p. 785-90.
75. Youn, H.D., et al., *Apoptosis of T cells mediated by Ca<sup>2+</sup>-induced release of the transcription factor MEF2*. Science, 1999. **286**(5440): p. 790-3.
76. de la Pompa, J.L., et al., *Role of the NF-ATc transcription factor in morphogenesis of cardiac valves and septum*. Nature, 1998. **392**(6672): p. 182-6.
77. Ranger, A.M., et al., *The transcription factor NF-ATc is essential for cardiac valve formation*. Nature, 1998. **392**(6672): p. 186-90.
78. Ranger, A.M., et al., *Delayed lymphoid repopulation with defects in IL-4-driven responses produced by inactivation of NF-ATc*. Immunity, 1998. **8**(1): p. 125-34.
79. Yoshida, H., et al., *The transcription factor NF-ATc1 regulates lymphocyte proliferation and Th2 cytokine production*. Immunity, 1998. **8**(1): p. 115-24.
80. Hodge, M.R., et al., *Hyperproliferation and dysregulation of IL-4 expression in NF-ATp-deficient mice*. Immunity, 1996. **4**(4): p. 397-405.
81. Schuh, K., et al., *Retarded thymic involution and massive germinal center formation in NF-ATp-deficient mice*. Eur J Immunol, 1998. **28**(8): p. 2456-66.
82. Erb, K.J., et al., *Mice deficient in nuclear factor of activated T-cell transcription factor c2 mount increased Th2 responses after infection with Nippostrongylus brasiliensis and decreased Th1 responses after mycobacterial infection*. Infect Immun, 2003. **71**(11): p. 6641-7.
83. Xanthoudakis, S., et al., *An enhanced immune response in mice lacking the transcription factor NFAT1*. Science, 1996. **272**(5263): p. 892-5.
84. Viola, J.P., et al., *Regulation of allergic inflammation and eosinophil recruitment in mice lacking the transcription factor NFAT1: role of interleukin-4 (IL-4) and IL-5*. Blood, 1998. **91**(7): p. 2223-30.
85. Oukka, M., et al., *The transcription factor NFAT4 is involved in the generation and survival of T cells*. Immunity, 1998. **9**(3): p. 295-304.
86. Kegley, K.M., et al., *Altered primary myogenesis in NFATC3(-/-) mice leads to decreased muscle size in the adult*. Dev Biol, 2001. **232**(1): p. 115-26.
87. Graef, I.A., et al., *Signals transduced by Ca(2+)/calcineurin and NFATc3/c4 pattern the developing vasculature*. Cell, 2001. **105**(7): p. 863-75.
88. Peng, S.L., et al., *NFATc1 and NFATc2 together control both T and B cell activation and differentiation*. Immunity, 2001. **14**(1): p. 13-20.



89. Graef, I.A., et al., *Neurotrophins and netrins require calcineurin/NFAT signaling to stimulate outgrowth of embryonic axons*. Cell, 2003. **113**(5): p. 657-70.
90. Phillips, C., et al., *Inducible nuclear factors binding the IgM heavy chain pre-mRNA secretory poly(A) site*. Eur J Immunol, 1996. **26**(12): p. 3144-52.
91. Laemmli, U.K., *Cleavage of structural proteins during the assembly of the head of bacteriophage T4*. Nature, 1970. **227**(259): p. 680-5.
91. Luo, C., et al., *Recombinant NFAT1 (NFATp) is regulated by calcineurin in T cells and mediates transcription of several cytokine genes*. Mol Cell Biol, 1996. **16**(7): p. 3955-66.
92. Schorpp, M., et al., *Characterization of mouse and human nude genes*. Immunogenetics, 1997. **46**(6): p. 509-15.
93. Sorensen, A.B., et al., *Sequence tags of provirus integration sites in DNAs of tumors induced by the murine retrovirus SL3-3*. J Virol, 1996. **70**(6): p. 4063-70.
94. Park, J., A. Takeuchi, and S. Sharma, *Characterization of a new isoform of the NFAT (nuclear factor of activated T cells) gene family member NFATc*. J Biol Chem, 1996. **271**(34): p. 20914-21.
95. Serfling, E., Chuvpilo, S., Liu, J., Hofer, T. & Palmetshofer, A. *NFATc1 autoregulation: a crucial step for cell-fate determination*. Trends Immunol **27**, 461-469 (2006).
96. Macian, F., C. Lopez-Rodriguez, et al. (2001). *"Partners in transcription: NFAT and AP-1."* Oncogene **20**(19): 2476-89.
97. Kel, A., O. Kel-Margoulis, et al. (1999). *"Recognition of NFATp/AP-1 composite elements within genes induced upon the activation of immune cells."* J Mol Biol **288**(3): 353-76.
98. Rhodes, S. J., R. Chen, et al. (1993). *"A tissue-specific enhancer confers Pit-1-dependent morphogen inducibility and autoregulation on the pit-1 gene."* Genes Dev **7**(6): 913-32.
99. Hofer, T., H. Nathansen, et al. (2002). *"GATA-3 transcriptional imprinting in Th2 lymphocytes: a mathematical model."* Proc Natl Acad Sci U S A **99**(14): 9364-8.
100. Lun, Y., M. Sawadogo, et al. (1997). *"Autoactivation of Xenopus MyoD transcription and its inhibition by USF."* Cell Growth Differ **8**(3): 275-82.
101. Ouyang, W., M. Lohning, et al. (2000). *"Stat6-independent GATA-3 autoactivation directs IL-4-independent Th2 development and commitment."* Immunity **12**(1): 27-37.

102. Arron, J. R., M. M. Winslow, et al. (2006). "*NFAT dysregulation by increased dosage of DSCR1 and DYRK1A on chromosome 21.*" *Nature* **441**(7093): 595-600.
103. Wu, C. C., S. C. Hsu, et al. (2003). "*Nuclear factor of activated T cells c is a target of p38 mitogen-activated protein kinase in T cells.*" *Mol Cell Biol* **23**(18): 6442-54.
104. Giffin, M. J., J. C. Stroud, et al. (2003). "*Structure of NFAT1 bound as a dimer to the HIV-1 LTR kappa B element.*" *Nat Struct Biol* **10**(10): 800-6.
105. Avots, A., M. Buttmann, et al. (1999). "*CBP/p300 integrates Raf/Rac-signaling pathways in the transcriptional induction of NF-ATc during T cell activation.*" *Immunity* **10**(5): 515-24.
106. Terui, Y., N. Saad, et al. (2004). "*Dual role of sumoylation in the nuclear localization and transcriptional activation of NFAT1.*" *J Biol Chem* **279**(27): 28257-65.
107. Rothenberg, E. V. (2000). "*Stepwise specification of lymphocyte developmental lineages.*" *Curr Opin Genet Dev* **10**(4): 370-9.
108. Fiering, S., J. P. Northrop, et al. (1990). "*Single cell assay of a transcription factor reveals a threshold in transcription activated by signals emanating from the T-cell antigen receptor.*" *Genes Dev* **4**(10): 1823-34.
109. Swain, S. L. (1991). "*Lymphokines and the immune response: the central role of interleukin-2.*" *Curr Opin Immunol* **3**(3): 304-10.
110. Street, N. E., J. H. Schumacher, et al. (1990). "*Heterogeneity of mouse helper T cells. Evidence from bulk cultures and limiting dilution cloning for precursors of Th1 and Th2 cells.*" *J Immunol* **144**(5): 1629-39.
111. Fontenot, J. D., J. P. Rasmussen, et al. (2005). "*Regulatory T cell lineage specification by the forkhead transcription factor foxp3.*" *Immunity* **22**(3): 329-41.
112. Yousang Gwack, Sonia Sharma, Julie Nardone, Bogdan Tanasa, Alina Iuga, Sonal Srikanth, Heidi Okamura, Diana Bolton, Stefan Feske, Patrick G Hogan & Anjana Rao. (2006). "*A genome-wide Drosophila RNAi screen identifies DYRK-family kinases as regulators of NFAT.*" *Nature* **441**, 646 – 650.
113. Asagiri, M. et al. (2005) "*Autoamplification of NFATc1 expression determines its essential role in bone homeostasis.*" *J. Exp. Med.* **202**, 1261–1269

## 7. CURRICULUM VITAE

### Personal Information

#### **Dmitry Y. Tyrsin (Mr.)**

E-mail : Tyrsin@gmail.com  
Born : May 30, 1977  
Civil Status : Married, no dependants  
Nationality : Citizen of Russia

### Academic Qualification

M.Sc. Microbiology, 1999  
Faculty of Biology  
M.V. Lomonossov Moscow State University  
Moscow, Russia.

### Work Experience

Since Dec. 2004: Business Development Manager, ChemDiv Inc.  
Sep. 2001 – Jul. 2004: Graduate student at the Institut für Pathologie, Universität Würzburg, leading to the qualification Doktor rer.nat. Thesis title "Autoregulation of NFATc1 gene".

### Technical Skills

DNA isolation and sequencing, Southern/Western blotting, RNA isolation, RNase protection assay, RT-PCR, Quantitative real-time RT-PCR, isolation of whole cell and nuclear extracts from cell cultures, cell culture manipulations, DNA-protein interaction assays (EMSA, Chromatin Immunoprecipitation), cloning .

### Publications

1. Chuvpilo S., Jankevics E., **Tyrsin D.**, Akimzhanov A., Moroz D., Jha M.K., Schulze-Luehrmann J., Santner-Nanan B., Feoktistova E., König T., Avots A., Schmitt E., Berberich-Siebelt F., Schimpl A., Serfling E. Autoregulation of NFATc1/A expression facilitates effector T cells to escape from rapid apoptosis. **Immunity**. 2002 Jun;16(6)